METSIM Modelling of Selenium Recovery on Lignin Using Biosorption

A Thesis Submitted to the College of Graduate and Postdoctoral Studies in Partial Fulfillment of the Requirements for the Degree of Master of Science in the Department of Chemical and Biological Engineering
University of Saskatchewan, Saskatoon, SK
Canada

By
Mohammed Ayman Mohamed Aly Abdallah
September 9th, 2021

PERMISSION TO USE

In presenting this thesis in partial fulfillment of the requirements for a postgraduate degree from the University of Saskatchewan, I agree that the libraries of this university may make it freely available for inspection. I further agree that permission for copying of this thesis in any manner, in whole or in part, for scholarly purposes may be granted by the professor or professors who supervised my thesis work or, in their absence, by the Head of the Department or the Dean of the College in which my thesis work was done. It is understood that any copying or publication or use of this thesis or parts thereof for financial gain shall not be allowed without my written permission. It is also understood that due recognition shall be given to me and to the University of Saskatchewan in any scholarly use which may be made of any material in my thesis.

Requests for permission to copy or to make other use of materials in this thesis in whole or in part should be addressed to the Department of Chemical and Biological Engineering or the College of Graduate and Postdoctoral Studies listed below:

Head of the Department
Chemical and Biological Engineering
University of Saskatchewan
57 Campus Drive
Saskatoon, Saskatchewan S7N 5A9
Canada

College of Graduate and Postdoctoral Studies
Room 116
Thorvaldsen Building
110 Science Place
Saskatoon, Saskatchewan S7N 5C9
Canada

ABSTRACT

Selenium is an important mineral for plants and living organisms; trace amounts are needed for our everyday function. However, when large amounts are consumed, it becomes really dangerous with adverse health effects; as a result of this, its removal has been the focus of many studies over the past decades. Selenium is found in most sulfide ores since they both share similar chemical attributes, such as atomic radius.

The mining and refining industries release the most amounts of selenium which are present in their wastewater in most cases. Current conventional methods of recycling selenium include pyrometallurgical and hydrometallurgical processes, which are often costly, environmentally unfriendly and potentially hazardous. Therefore, researchers have turned towards the study of biomass-based adsorbents, also known as biosorbents, for applications in selenium recovery and recycling. Biosorption was the process of choice for reasons such as its operating cost, its recovery rates and reusability

In the research presented in the thesis herein, lignin which is a major component in plants was used to adsorb selenium from selenium monochloride (Se_2Cl_2) using METSIM as the simulation software of choice due to its versatility and flexibility to control numerous parameters, add new components and perform mass and heat balances. Lignin was the only component that was added, and the thermodynamic data was found via some research articles where it was plotted in excel and entered in METSIM.

Further data analysis revealed that the adsorption rate of selenium (Se) on lignin progressed via the pseudo-second order rate model. Adsorption isotherm model studies indicate that the adsorption of Se by lignin followed the Freundlich adsorption isotherm. Calculated energy levels of activation by Se suggest that adsorption progresses due to chemisorption in nature. Thermodynamic studies reveal that lignin adsorption of Se is exothermic in nature and that the increasing temperature reduces the efficiency of the adsorption process.

A recovery rate of 99.4% was achieved for Se_2Cl_2 at 25 °C temperature and 0.39M HCl. To further prove that this model is functional, the two other known chloride forms of selenium, $SeCl_2$ and $SeCl_4$ were tested; selenium recovery rate from $SeCl_2$ and $SeCl_4$ was 45% and 40%, respectively.

ACKNOWLEDGEMENTS

I would like to thank my supervisor, Dr. Shafiq Alam, for his technical advice and support, as well as for providing me an opportunity to work under him and helping me achieve my first step in entering the world of scientific research and academia. The fast progress of my research work and completion of this thesis would not have been possible if it were not for his expert guidance.

I am grateful to my advisory committee members, Dr. Oon-Doo Baik and Dr. Duncan Cree for taking the time to provide me with suggestions that helped me to improve my research scope and analysis of data.

My sincere gratitude goes to the financial support from the Department of Chemical and Biological Engineering and Dr. Alam for awarding me with Teaching Assistant and Mitacs Internship positions

And above all, I would like to wholeheartedly thank my parents, Mr. Ayman Aly, and Ms. Jihan Elbibany, for always believing that I can achieve my dreams, no matter what that may be, and for supporting me financially. I would also like to thank my siblings, especially my brother, Dr. Ahmed for always listening to me during difficult times.

DEDICATION

This thesis is dedicated to my parents Mr. Ayman Aly and Ms. Jihan Elbibany.
It is also dedicated to my siblings, Dr. Ahmed, Dr. Mayar, Merna and Lamar.
Thank you all for always being proud of me, even when I am not proud of myself.

TABLE OF CONTENTS

LIST OF TABLES

LIST OF FIGURES

LIST OF ABBREVIATIONS

Terminology

DTO = Dithiooxamide

PLS = Pregnant leach solution

PM = Precious metals

ppm = Parts per million (mg/L)

rpm = Revolutions per minute

ppb = Parts per billion

Da = Dalton/ unified atomic mass unit

PE = Polyethylene

ORP = Oxidation-Reduction Potential

pm = Picometer

APL = named after the book "A programming language"

S/L ratio = Solid/ liquid ratio

Elements

Ag = Silver

Au = Gold

Co = Cobalt

Cu = Copper

Se = Selenium

Cl = Chlorine

H = Hydrogen

Ni = Nickel

Pt = Platinum

Pd = Palladium

Zn = Zinc

Fe = Iron

NOMENCLATURE

DTO = Dithiooxamide

Se_2Cl_2 = Selenium monochloride

$SeCl_2$ = Selenium chloride

$SeCl_4$ = Selenium tetrachloride

HCl = Hydrochloric acid

H_2O_2 = Hydrogen peroxide

Se^{4+} = Selenite

Se^{6+} = Selenate

$HSeO_3$ = Bi-selenite

MIBK = Methyl isobutyl ketone

PbS = Galena

$CuFeS_2$ = Chalcopyrite

FeAsS = Arsenopyrite

$C_{10}H_8(OH)_4$ = Lignin

$C_{10}H_6O_4$ = Product lignin

CHAPTER 1 Introduction

1.1 Introduction

Selenium (Se) and its oxyanions have become a major health and environmental concern in recent years; environmental contamination by selenium can occur due to various sources like metal ores, mine drainage, water drainage, industrial effluents, and fossil fuels residues. Various studies have focused on selenium removal from water using different techniques [1]. In the periodic table, Se belongs to the chalco-gene group and is mostly present in minerals containing sulphur [2]. Selenium, the essential trace mineral, is vital to human health. Selenium deficiency may have detrimental impacts on the resistance to diseases and overall health maintenance. Several studies show that selenium deficiency affects the immune system, viral infection, cardiovascular disorders, and thyroid function [3]. Another disease associated with selenium deficiency is Clinical Se deficiency also known as white muscle disease, which can cause nutritional myodegeneration, which is a disease that occurs mostly in farm animals like sheep and cows [4]. The only micronutrient regulated by the food and drug administration (FDA) as a feed additive is selenium and that is due to its toxicity. In 1974, the environmental protection agency (EPA), under the safe drinking water act, determined the maximum contaminant level goal (MCLG) of selenium to be 0.05 mg/L or 50 ppb, so selenium removal from surface and ground waters is necessary to meet drinking water standards. The selenium concentration in contaminated wastewater must also be reduced to minimize its impact on natural water resources or to be reused [5]. Electronics, glass, ceramics, glass coloring, steel, pigment manufacturing, and rubber production are only a few of the industries that use selenium. Selenium is used in antidandruff shampoos and as a dietary supplement in medicine [6]. The presence of selenate and selenite, the low discharge limits and the generation of huge amounts of wastewater made the removal of selenium from the aqueous medium complex and expensive [7]. The principal aqueous forms of selenium are selenite (Se^{4+}) and selenate (Se^{6+}); selenate is harder to treat and remove than selenite. Selenate is present in the oxidizing state as SeO_4^{2-} and selenite is present in the reducing state as SeO_3^{2-} or $HSeO_3^-$ [8]. In the pH range of 6 to 8 only elemental selenium [Se, (0)], selenate, selenite and bi-selenite ion ($HSeO_3$) exist in water. Sequestration of selenium occurs when other suspended particles are present in water; for example, the partitioning of selenite on amorphous iron oxyhydroxides and manganese dioxide on particles

[9]. Factors like ultraviolet radiation, high abundance of selenite oxidizing bacteria or redox-active transition metals are all factors that enhance the oxidation of Selenite. Both selenate and selenite are stable in natural water but to facilitate their removal, they can be oxidized or reduced; for example, reducing selenate to Se (0) can remove it quickly from the water. Selenium is located between sulphur and tellurium in the V1B group of the periodic table and has chemical and physical features that are intermediate between metal and non-metal [10]. Selenium can be found in ores containing sulfides along with sulfide minerals, which is due to similar traits such as ionic radii. Sulfide has an ionic radius of 184 ppm, whereas selenium's ionic radius is 196 ppm. Selenium occurs in minerals like galena: PbS, chalcopyrite: $CuFeS_2$, arsenopyrite: FeAsS. It is generally used in various industries such as fertilizers, pigments, electronics, and glass manufacturing because it gives the glass a distinctive red color, also It is a semiconductor hence its use in the manufacturing of solar cells, and it is used as a replacement for the more toxic lead as an alloying element. Part of the direct emission of selenium to water, soil, and air has been occurring due to its involvement in these industries [7]. Other activities like mining, coal combustion, and metal smelting contribute to selenium mobilization [7].

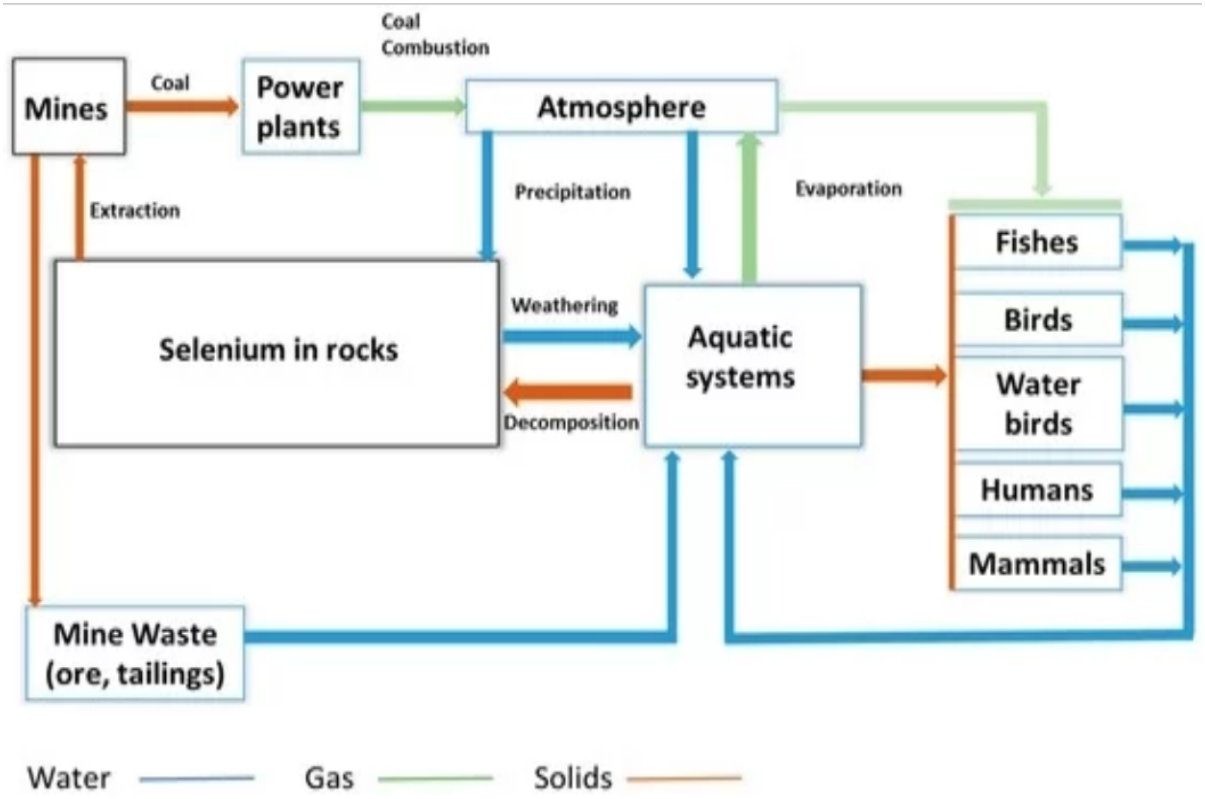

Figure 1. 1 The cycle of selenium in the environment during mining [7]

Selenium contamination is a global problem and is related to various human activities [11]. One of the key contributors to the release of selenium into the atmosphere is the mining industry. Active mining used to reach coal, phosphate, or ore body produces lots of waste rocks. As a result, runoff and other releases produced from tailings and piles of waste rock can release huge amounts of selenium, which can end up in aquatic ecosystems if they are not controlled or mishandled [9] as shown in Figure 1.1. In a research study by Lemly [11] , it was observed that a relationship between selenium concentration and degree fertility rate of sensitive fish species as shown in Figure 1.2 below, a slight increase in waterborne selenium concentration can have a major impact on aquatic life [11].

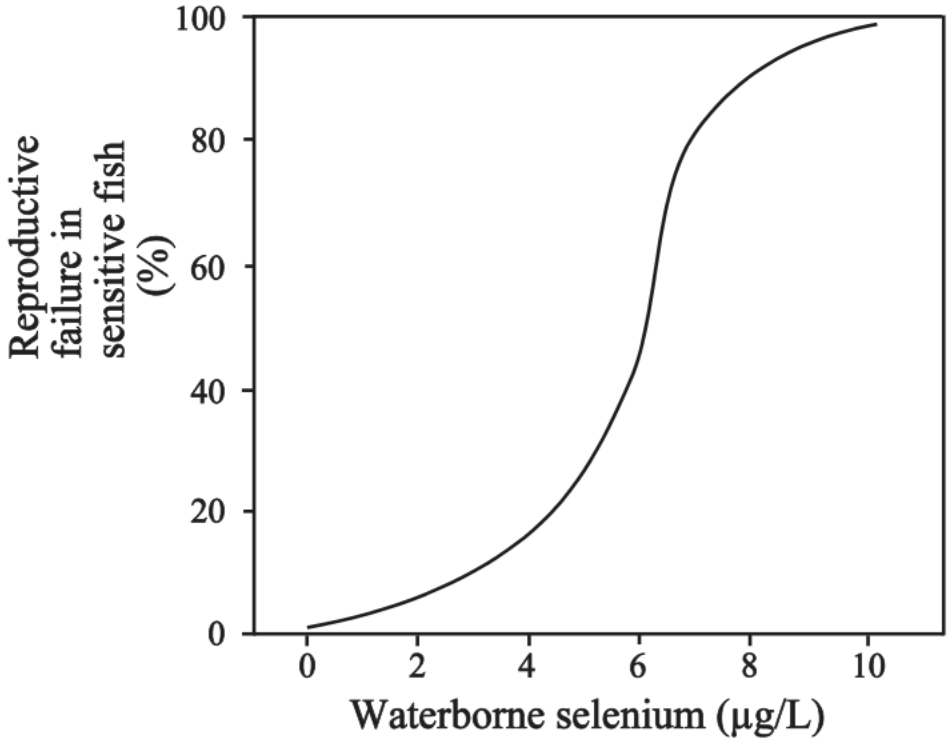

Figure 1. 2 Effect of waterborne selenium concentration on the fertility rate of sensitive fish [11] permission enclosed in Appendix A

Moreover, fossil fuel (coal and oil) combustion releases large amounts of selenium into the atmosphere. Historically, coal-fired power plants released selenium, often in the vapour phase, to the

atmosphere and as aqueous selenate, as selenium dioxide (SeO_2) [9]. The pH in an element's geochemical cycle is collated with selenium in soil; it also correlates to elements solution chemistry. The selenium content of host rocks involves important factors such as redox capacity, pH and the characteristics of the water drained. Selenium concentrations in wastes and minerals are different from one ore to another, a summary of selenium concentrations in different ores is presented in Table 1.1.

Table 1. 1 Selenium concentration in different ores and waste effluents.

Ore or waste	Se Concentration (ppm)	References
Surface waters	0.2	[12]
Agricultural drainage water	140	[11]
Copper ore	20-80	[11]
Mining wastewater	3-12	[11]
Coal mining pond water	8.8-389	[12]
Gold mine wastewater	0.2-33	[11]
Uranium mine wastewater	1600	[11]
Oil shale	1.3-5.2	[12]
Crude shale oils	92-540	[12]
Crude oil	500-2200	[12]
Refined oils	5-258	[11]
Oil refinery wastewater	15-75	[11]
Phosphate ore	2-20	[13]
Coal cleaning solid waste leachate	2–570	[12]
Ash pond effluents	2–260	[11]

From Table 1.1, it can be observed that selenium is a valuable resource to be recovered since it is more beneficial for the environment and health of living organisms, and it can be sold as a by-product.

Different recovery or treatment processes like (Biological) oxidation/reduction, phytoremediation, membrane separation technologies, coagulation or flocculation, and adsorption have been studied

and used by researchers to recover selenium. Although industries might receive economic gain from recovering selenium with these processes, excessive operation costs and obeying environmental regulations may make selenium recovery less likely to be adopted on a massive scale. Researchers have favored biosorption because it produces almost no waste; it is more economical compared to other processes. Finally, it is practical in the sense that each country could use the abundant biomass it has to recover selenium. Roberts et al. [1] used Gracilaria waste biomass as a bioresource for selenium biosorption, where the Gracilaria waste was treated with iron (Fe) and observed that almost 99% of selenium was removed. iron (Fe) has proved to be efficient when it comes to selenium biosorption as shown in Figure 1.3. However, it was discovered by Roberts et al. [1] that one limitation of this approach is that significant amounts of iron can leach from the surface of the adsorbent causing future environmental issues. As the rate of Se uptake is negatively correlated with Fe leaching, the biosorbent capacity should increase if further optimization of the biosorbent is done.

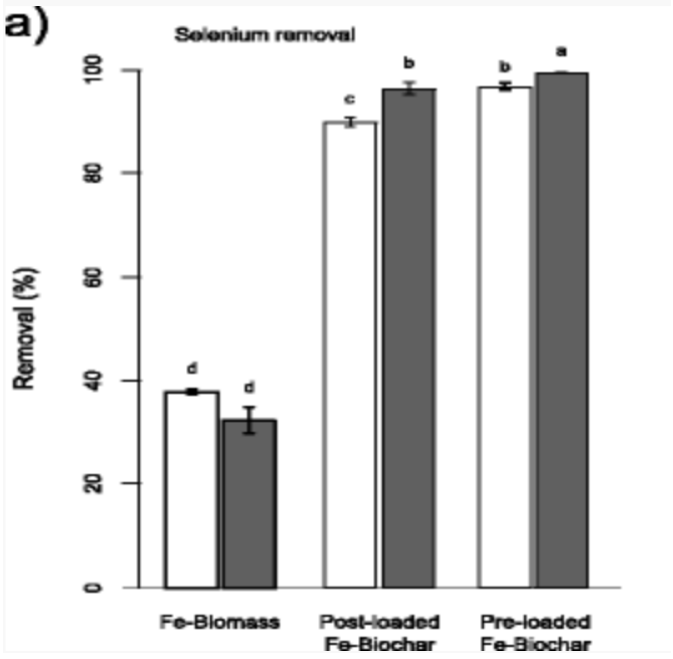

Figure 1. 3 Removal (%) of Se as Se^{4+} (white bars) and Se^{6+} (grey bars) into treated samples with Fe-treated GW biomass and biochar [1]

1.2 Knowledge gaps

From the study of present research proposed in the field of biosorption of selenium, the following main knowledge gaps are identified:

1. Although many processes like oxidation/reduction, membrane separation technologies, co-agulation or flocculation, and adsorption were used by many researchers, the additional waste they produce, and the high cost of operations can limit their use in industries. On the other hand, biosorption produces almost no waste and it is much more economical, which makes it a better option.
2. Research articles focus on the efficiency of biosorbents in recovering more valuable metals such as gold, platinum, and palladium but few focuses on selenium which is important to be removed due to its toxicity.
3. There are few research works done on the recovery of selenium using modeling software such as METSIM or Aspen HYSYS.

1.3 Objectives

The overall purpose of this research work is to develop an efficient biosorption process for recovering selenium from selenium in chloride solutions. Specific objectives are broken down as indicated below:

1. To develop a successful realistic model that shows the adsorption process of selenium on lignin.
2. To evaluate the efficiency of lignin in recovering selenium from industrial effluents.
3. To analyze the effect of various experimental parameters such as pH, temperature, and concentration, etc., on the adsorption of selenium and conduct studies on its kinetic behavior, adsorption isotherm, and thermodynamics.

1.4 Overall outline of the thesis

This thesis details the simulation, testing, results analysis, and conclusion of the complete research and provides the information required for general understanding. An introduction of the importance and demand of the research work presented in the current thesis as well as an outline of the knowledge gaps and objectives are summarized in Chapter 1. Chapter 2 is the literature review

in the field of biosorption, informing concepts that often arise with the research topic. Chapter 3 describes the methodology and simulation building process. Chapter 4 discusses the obtained results and explains their significance in terms of the biosorbent's efficiency. Finally, chapter 5 concludes the thesis by summarizing the main findings of the research, pointing out any difficulties or challenges of the present work, and provides suggestions for future research within the field.

CHAPTER 2 Literature Review

2.1 Conventional methods of recovery

Over the years, two routes were chosen to recover elements or metals; they are pyrometallurgical and hydrometallurgical processes. Pyrometallurgical processes include, but are not limited to, burning, melting, converting, and refining of waste and has been the go-to process to recover elements from secondary sources for the past several decades. In pyrometallurgy, waste is first burned in a furnace opt molten bath to get rid of plastic components; a slag phase is then formed from the remaining refractory oxides [14]. Disadvantages such as long settling times to separate the slag from the metal collector and high operating temperature range (1800-2000 °C) are associated with pyrometallurgical processes. Also, in most cases, partial separation occurs during pyrometallurgy; that's is why hydrometallurgical treatment is required after pyrometallurgy in order to decrease the limitations mentioned above [14].

Researchers and industry experts prefer hydrometallurgical methods for reasons such as low capital cost, operation flexibility, and overall environmental sustainability compared to pyrometallurgy. Leaching of solid wastes and other secondary sources is the first step during hydrometallurgy. During leaching, sources containing valuable minerals are integrated into a reactor tank containing leaching agents [15]. Valuable minerals are then dissolved from the secondary source by forming a pregnant leach solution through complexation. Further processing such as electrowinning or precipitation is then used to further extract the valuable minerals from the pregnant leach solution (PLS).

A popular leaching agent used customarily in the mining industry is cyanide, which is primarily used for gold leaching; despite it being highly effective, cyanides' toxic nature has caused industrial concerns such as environmental disasters and health hazards that occurred over the years [16]. The collapse of a mine tailings dam in Guyana in 1995 is an example of a devastating environmental crisis involving cyanide contamination, where 2.9 million m^3 of cyanide were discharged into the river. This incident created the urgency to find other alternatives.

Thiosulfate and thiourea were discovered to be good alternatives to cyanide-based lixiviants and are easily scalable and applicable as well. In recent years, the utilization of hydrochloric acid in the chlorine gas in a leach solution is more advantageous [16]. A 2-step bioleaching process for gold and copper was developed by A. Işıldar et al.[17]. This process was able to recover 44% of gold and 98.4% copper from scrap metals using microorganisms that naturally contain cyanide. Aqueous precious metals (PM) ions can be extracted from PLS using different hydrometallurgical methods after the leaching process, such as solvent extraction, ion-exchange, or adsorption with activated carbon. Solvent extraction, also known as liquid-liquid extraction, is used to process a wide range of metals and is differentiated by the use of chemical extractants like Methyl isobutyl ketone (MIBK), Cyanex 471X, and others [17].

Several toxic metals and metalloids have been successfully extracted using coagulation/flocculation [18]. However, there is limited literature on the removal of selenium. Staicu et al. [19] contrasted the removal of colloidal Se(0) from wastewater using aluminum sulfate or ferric chloride in centrifugation, filtration, and coagulation/flocculation [19]. According to the scientists, coagulation/flocculation achieved the highest removal rate (92%) as compared to centrifugation (91%) at 4,500 rpm, 73 percent at 3,000 rpm, and 22 percent at 1,500 rpm, filtration through a 0.45m filter (87%), and coagulation/flocculation with ferric chloride (43%). The most common forms of selenium (Se(IV) and Se(VI)) are both highly soluble. As a result, selenium levels can be decreased by converting it to metallic selenium and then precipitating it. This approach has been used previously and can be used to eliminate other undesirable components. The reduction of Se(IV) or Se(VI) to their metallic state, on the other hand, necessitates the use of a powerful reducing agent, which makes the entire process unfavorable. Se-reducing bacteria may be used in place of powerful reducing agents. Cantafio et al. [20] conducted experiments using a selenate-respiring bacterium [20]. Another process for selenium removal is phytoremediation, which is the removal of toxins from polluted soils, water, or air by plants [21]. Toxic elements may be accumulated and/or detoxified by plants. Metals and metalloids, explosives, solvents, pesticides, and other materials can all be used. In contrast to excavation and ex-situ remediation of polluted soil, it is a relatively inexpensive method.

According to the literature review, most of the current study is based on the removal of Se (IV) and Se(VI), but the key concern is the removal of the organic form of selenium. It has a higher

bioavailability than other selenium compounds and bioaccumulates faster. It is created when bacteria reduce selenium compounds, and it's most likely linked to the amount of soluble organic materials used. From the standpoint of cleaner processing, preventive steps to reduce selenium release should be considered, and treatment technologies should be evaluated using green chemistry principles [5]. Adsorption is effective in the treatment of low-pollutant industrial and municipal wastewaters. The key disadvantage of adsorption is the transfer of the contaminated medium, i.e., the toxin, from the water phase to a solid phase on which the contaminant is concentrated, and in most situations, this adsorbent should then be regenerated before reuse or processed before the final disposal [7]. The amount of adsorbate that can be adsorbed on the adsorbent is determined by a material's adsorption capacity. The ultimate adsorbent will be a chemical or substance that allows for the lowest possible discharge limits for selenium by using the least amount of adsorbent material possible. In an ideal case, a desorption procedure that regenerates the adsorbent may be used.

Biosorption methods have the potential to fill a void in the existing PM recycling market by offering a more cost-effective, environmentally sustainable, and, in some instances, better functioning process for removing metal ions from PLS. Dead biomass is favored to reduce toxicity and the need for a growth medium, which would raise operational costs. The use of dead biomass for biosorption also allows for the desorption of adsorbed selenium which helps recover the resource (biosorbent).

2.2 Mechanism of selenium biosorption

The bioaccumulation of heavy metals from wastewater through physio-chemical or metabolically mediated pathways of uptake is known as biosorption [22]. In other words, biosorption is a physicochemical process that allows contaminants to passively bind and concentrate onto the cellular structure of the biomass [23]. The state of biomass (living or nonliving), types of biomaterials, properties of metal solution chemistry, and environmental conditions (pH, temperature) are all factors that influence the biosorption mechanism.

Extensive research has been conducted about biosorption since the 1970s for various reasons [24], such as,

1. Cost: since biosorption is mainly done by biomass, they are found in abundant quantities, which makes scaling up the process more cost-effective as compared to conventional adsorption processes.
2. Metal selectivity: biomass can be selective on different metals, factors such as type of biomass, pre-treatment method and reactions involved influence this selectivity.
3. Possibility of metal recovery: it is relatively easy to recover adsorbed metals
4. Competitive performance: some biosorbents proved to be more effective than conventional adsorbents.

Biosorption can either be a physical adsorption process or a chemical adsorption process, in physical adsorption, the metals bind to the surface of a high surface area sorbent by Vander Waals force, and they generate slightly higher heat than the heat of sublimation of the adsorbate but still relatively low adsorbent heat. Chemisorption, on the other hand, is the occurrence of a chemical reaction between sorbent sites and the target gas to bind through covalent bonds with much greater adsorption heat which is usually equal to reaction heat [25]. The visual representation is shown in Figure 2.1.

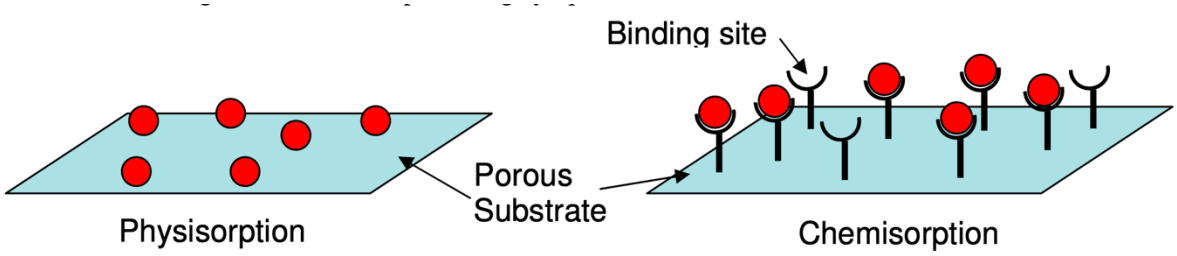

Figure 2. 1 The difference between physisorption and chemisorption during CO_2 adsorption [25] permission enclosed in Appendix B

Biosorption mechanisms can be divided into two parts according to dependency on cell metabolism; they are metabolism dependent and non -metabolism dependent [26]. The main mechanisms involved in biosorption are adsorption, precipitation, surface complexation, ion entrapments in intrafibrillar and interfibrillar capillaries, chelation and ion exchange [7]. Many functional groups are present on the cellular wall of the biomass, the composition differs from one biomass to an-

other, but the most important structures for metal biosorption are hydroxyl, thiol, sulfonate, thioether, amine, secondary amine, amide, imidazole, carboxyl, carbonyl, phosphonate and the phosphodiester group [7].

In the energy industry, biomass refers to the biological materials that were living and which were alive until recently, and which can be used as fuel or in industrial production [27]. Most biomass is plant material used as biofuel, but the term also refers to plant or animal materials used in the production of fibers, chemicals, or heat. Biomass may also include the naturally decomposing waste that can be burned as fuel. An exception is made for organic matter that ground processes have converted into coal or oil. Biofuels include ethanol, biodiesel, biogas, and bio-butanol, all of which are fuels that are used directly in petroleum engines.

Although biomass is a renewable fuel, it still contributes significantly to global warming, which occurs when the natural carbon balance is disrupted, for example, in cases of deforestation or the expansion of cities into green areas. The reason for this is that biomass is part of the carbon cycle. Carbon in the atmosphere is transformed into biomaterial by photosynthesis, and it is released back into the air when plants are decomposed or burned. This usually occurs over a short period of time, and the plant material used as fuel can be replaced by planting a new plant. Therefore, a reasonable air carbon balance, or what is known as carbon neutrality, would arise from the use of biomass as fuel. Other uses of biomass, other than burning it as fuel or as an energy source: in building materials. biodegradable plastic and paper bags (using cellulose fibers).
The abundant polyphenol content in plant structures is what makes them great candidates to act as biosorbents. Chemist Haslam [28] mentioned in an article that, for a phenolic compound to qualify as a polyphenol, it should

1. Be found in plants.
2. Contain between 12 to 16 phenolic hydroxyl groups.
3. Possess 5 to 7 aromatic rings per 1000 Da of molecular mass.

Polyphenolic compounds engage in redox reactions and can reduce Au(III) to Au(0) in their active sites; that is why they can demonstrate effective chelation with metal ions [29]

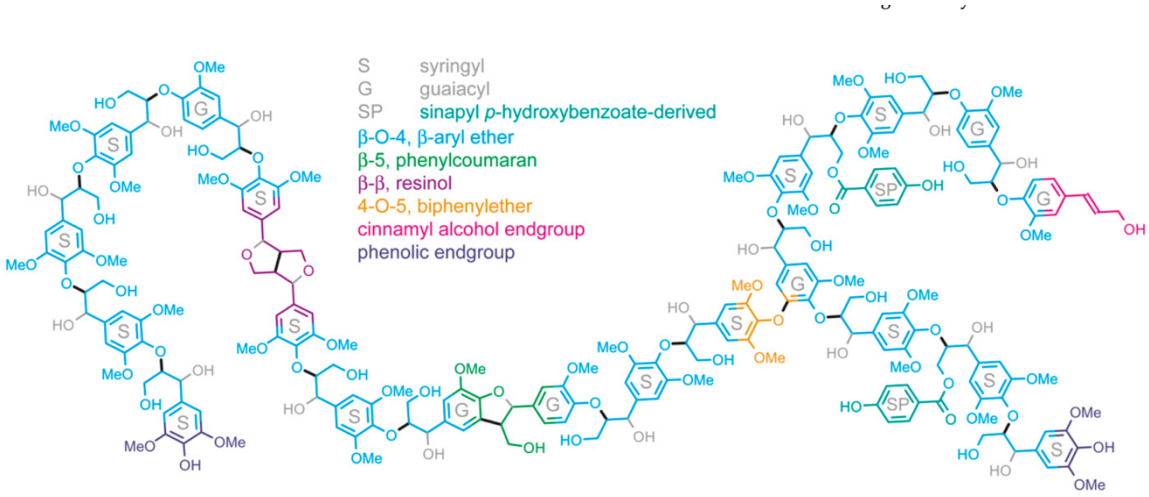

Figure 2. 2 Proposed polymer structure of lignin [30]

Cellulose, lignin and tannin are found in plants and most of them contain polyphenols in certain forms of organic polymers. The chemical structure of lignin is shown in Figure 2.2. Lignin was first mentioned in 1813 by the Swiss botanist Augustan Piram de Kendol, who described it as a fibrous, tasteless substance, insoluble in water and alcohol but soluble in weak alkaline solutions which could precipitate from solution using acid. The material was called "lignin," which is derived from the Latin word lignum, meaning wood [31]. It is one of the most abundant organic polymers on Earth, surpassed only by cellulose. Lignin forms 30% of the non-fossil organic carbon and 20% to 35% of the dry mass of wood [32]. The Carboniferous Age (geology) was determined in part by the evolution of lignin. The composition of lignin differs from one species to another. An example of the composition from an Aspen sample is 63.4% carbon, 5.9% hydrogen, 0.7% ash (mineral components), and 30% oxygen (with variation), almost identical to the formula (C31H34O11) n. As a biopolymer, lignin is atypical due to its heterogeneity and the lack of a specific base structure. Its most common function is to support by strengthening the wood (made up mainly of xylem cells and solid woody fibers) in vascular plants [33]. Crosslinked lignols are of three main types, all of which are derived from phenylpropane: 4-hydroxy-3-methoxy-phenylpropane, 3.5-dimethoxy-4-hydroxyphenylpropane, and 4-hydroxyphenylpropane. The former tends to be more prevalent in conifers and the latter in hardwoods. Lignin is a cross-linked polymer with molecular masses of over 10,000 atomic mass units. It is relatively hydrophobic and rich in aromatic subunits. The degree of polymerization is difficult to measure since the material

is heterogeneous. Depending on the isolation method, different types of lignin have been described [32].

There are three monolignol (precursors), all of which are methoxylates in different degrees: P-coumaryl alcohol, Coniferyl alcohol, and Sinapyl alcohol [34]. These lignols are incorporated into the lignin in the form of phenylpropanoid p-hydroxyphenyl, guaiacyl, and syringyl, respectively. Gymnosperms contain lignin, which is almost entirely guaiacyl, with small amounts of polyethylene (PE). Angiosperms are often dicotyledon a mixture of guaiacyl and syringyl (with very little PE), and monocyclic lignin is a mixture of the three. Most of the weeds contain guaiacyl, while some palm trees contain mainly syringyl. All lignin contain small amounts of incomplete or modified monolignols, and other monomers are prominent in non-woody plants [30]. Lignin fills in the spaces in the cell wall between the components of cellulose, hemicellulose, and pectin, especially in vascular and supportive tissues: the xylem, vascular elements, and solid cells. It binds covalently to hemicellulose and thus binds different plant polysaccharides, giving mechanical strength to the cell wall and thus the plant.

Lignin plays an important role in water conduction in plant stems. Polysaccharide components in plant cell walls are highly hydrophilic and thus water permeable, whereas lignin is more hydrophobic. The crosslinking of polysaccharides by lignin is an obstacle to water absorption of the cell wall. Thus, lignin makes it possible for plant vascular tissues to deliver water efficiently. Lignin is found in all vascular plants but not in algae, which supports the idea that the original function of lignin was limited to transporting water. However, it is present in red algae, indicating that the common ancestor of red plants and algae also makes lignin. This may indicate that its original function was structural, playing this role in the red algae Calliarthron, as it supports the joints between the calcified parts. Another possibility is that the lignin found in red algae and plants results from convergent evolution rather than common ancestry [35].

World commercial production of lignin is the result of the papermaking industry. In 1988, more than 220 million tons of paper were produced worldwide. Much of this paper has been abstracted, lignin comprising about 1/3 of the mass of lignocellulose, presented on paper. Thus, it can be seen that lignin is dealt with on a very wide scale. Lignin is a barrier to papermaking because it is

colored, yellows in the air, and its presence weakens the paper. Once separated from cellulose, it is burned as fuel. Only a portion is used in a wide variety of low volume applications where shape, not quality, is important [36]. The mechanical or high-yield pulp used to make newsprint still contains most of the lignin originally found in wood. This lignin is responsible for the yellowing of newsprint with age. High-quality paper requires the lignin to be removed from the pulp. These lignin processes are the primary technologies for the paper industry as well as a major environmental concern. In the process of sulfite pulping, lignin is removed from wood pulp as lignosulfonates, for which several applications have been suggested [35].

Sulphate process or Kraft digestion (so-called because of the strength of the paper produced in this way, see Kraft paper) is a chemical-industrial process for the production of cellulose from the wood of trees or from annual plants such as reeds, grain (straw), sugar cane (bagasse), Corn or sunflower (stems). The cell walls are opened up and the lignin and polyoses contained in the plant material are separated off. The resulting cellulose can be used as reinforcing fibers. The sulphate process, in which wood chips are cooked in caustic soda for several hours, is the most common process used to make paper pulp. It was invented in 1879 by Carl Ferdinand Dahl (Danzig), who also gave it the name (Kraft), and applied for a US patent in 1884. In 1890 the first factory used the process in Sweden [37].

Wood bark is comprised of cellulose, hemicellulose, and lignin. Different wood cuts or locations contain different lignin compositions; for example, in a paper by Klash et al. [38] E. grandis and E. dunnii (different types of wood) showed that lignin content on the surface is much lower than the suggested lignin by the bulk composition. Also, lignin composition was directly proportional to mean annual temperature (MAT), which is the average of the highest and lowest temperatures recorded in a year, and inversely proportional to mean annual precipitation (MAP) which is the sum of the assumed water equivalent of snow and rainfall [38].

2.3 Selenium chemistry

Several researchers have thoroughly studied the chemistry of Se. It is worth noting the following points. Jakob Berzelius, a Swedish chemist, discovered selenium in 1817. Its name is derived from the Greek word Selene, which means moon. It has an atomic weight of 78.96 and belongs to the

group through metalloids. Sulfur (S) and selenium (Se) have a lot of chemical similarities, but the radius of the Se^{2+} atom is 0.5 A, while the radius of the S^{2+} atom is 0.37 A. Se, like S, has five valence states: selenide, elemental Se (0), thioselenate (2^{+}), selenite (4^{+}), and selenate (6^{+}) [39]. Selenium is assimilated in plants through the sulfur pathways, where selenate is first activated to adenosine phosphoselenate, then reduced to selenite [40].

Selenium speciation is governed by physical, chemical and biological processes, it exists in both organic and inorganic forms, but this thesis will only discuss the inorganic forms, which are of prime concern to the mining industry. Different oxidation states of inorganic selenium exist; the most common are Se^{-2}, Se (0), Se^{4+}, Se^{6+}, each shows different properties and is affected by pH and redox conditions. They play an important role in designing any selenium treatment process; a Pourbaix diagram like the one shown in Figure 2.3 is used to represent different selenium oxidation states in an aqueous phase at different pH and reduction potential conditions. From Figure 2.3, it is observed that in the pH range of 4 to 9, Selenate (SeO_4^{2-}) is more dominant under strongly oxidizing conditions. Moving down the y-axis, selenate is reduced to selenite (SeO_3^{2-}) for alkaline pH and to hydrogen selenite for acidic and neutral pH. Selenide (Se^{2-}) is present in reducing conditions; another factor that affects the occurrence of selenium in different oxidation states is the type of surrounding elements and ions [12].

Volatile species of selenium— H_2Se, CH_3SeH, $(CH_3)_2Se$, and $(CH_3)_2Se_2$— are also known to be formed in selenium-containing water bodies. Aquatic sediments represent a complex medium where the Physical and chemical properties of sediments, along with various biotic factors, control selenium speciation [9]. In freshwater environments, iron- manganese oxyhydroxides adsorb selenium at sediment surfaces. The oxyhydroxides are reduced, which releases the selenium where it is mineralized with organic matter and removed from pore water as Se(0) and as selenopyrites. Selenium solubility is favored by low Oxidation-Reduction Potential (ORP) as iron selenide or Se(0) phases are formed [9].

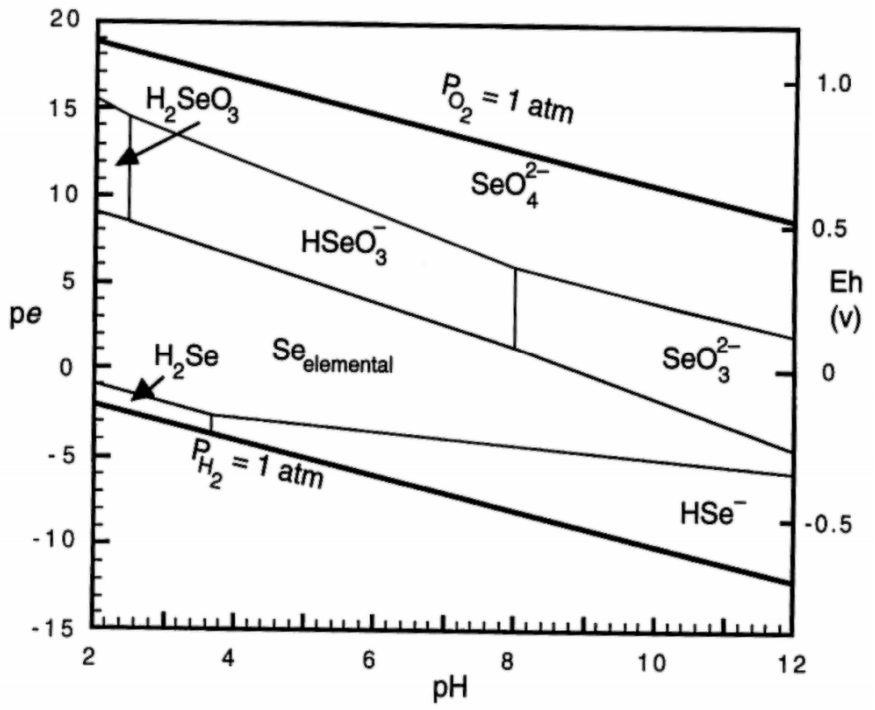

Figure 2. 3 Selenium Pourbaix diagram [12]

Extensive studies have been performed on the chemistry of elemental selenium due to its complexity, polymorphic forms of selenium exist, trigonal and monoclinic. The melting point of trigonal form is higher than that of the monoclinic form, where it is 494.2 K for the former and 413 K for the latter [41]. Selenium, like sulfur, forms many allotropes (different phenotypes with different internal structures of the same element), which transform between them when there are changes in temperature. When selenium is obtained from a chemical reaction, it is often in the form of an amorphous powder with a red-brick color, whose rapid melting at temperatures exceeding 220 °C transforms it into a black glassy form, which is often sold commercially in the form of beaded pellets. The continued heating creates a yellow vapor of selenium. Black selenium is a complex and irregular structure. It is made up of polymeric rings in which the number of atoms reaches about 1000 atoms per ring. Black selenium occurs in the form of fluffy, luminous grains and is soluble in carbon disulfide (CS_2). Heating black selenium softens it at about 50 °C, and then turns gray at 180 °C. The thermal transition threshold may be reduced by the presence of traces of halogens or amines.

The different red shapes alpha (α), beta (β), and gamma were obtained from black selenium solutions by controlling the rate of evaporation of the solvent (often CS_2). These forms are generally considered amorphous materials, with weak irregularities in the structure in the form of monoclinic crystal nuclei, and they contain uneven rings with different arrangements of Se_8, roughly analogous to that of sulfur. The most compact arrangement of atoms in it is alpha (α). The distance between the selenium atoms of Se-Se_8 in the octet rings Se_8 is 233.5 pm, while the angle Se-Se-Se is 105.7 °. Other selenium allotropes can be made of hexagonal Se_6 or hexagonal Se_7 rings [42]. Red selenium is an electrical insulator, and slowly heating it at temperatures above 80 °C turns it gray. Selenium does not exhibit the property of changing the viscosity that sulfur does with a gradual change in temperature [43].

The gray form is the most stable and dense allotrope of selenium. It has a hexagonal crystal structure composed of helical polymeric chains, in which the distance Se-Se is 237.3 μm, and the angle Se-Se-Se is 130.1°. the chains have a minimum distance of 343.6 pm between them. Gray selenium is formed from the gentle heating of other allotropes, from the slow cooling of the molten selenium, or the condensation of the vapor of selenium near its melting point. The gray shape differs from other allotropes by not being able to dissolve into carbon disulfide (CS_2) [42]. The gray shape also differs in that it has semiconducting properties, and it exhibits the phenomenon of optical conductivity as well [42]. The bandgap of gray selenium is 1.74 MeV and lies on the boundary between the energy of visible and infrared light. Exposing gray selenium to light causes a change in its electrical conductivity. This is not due to the presence of electrons in the conduction band. Rather, the optical conductivity occurs due to the presence of electronic holes that are not located and are continuously moving [44].

Selenium can form a number of organic compounds, especially in the state II oxidation, where it forms a stable bond with carbon atoms, similar to the organic sulfur compounds. Common examples are R_2Se (analogous to thioethers) such as selenomethionine or dimethyl selenide, and R_2Se_2 (analogous to disulfide) such as disulfide as well as RSeH (analogous to thiolate), such as selenol benzene (analogous to thiolate), also known as selenophenil. RSeOR compounds of selenoxide can be obtained as intermediate compounds within special organic reactions such as the selenoxide deletion reaction. On the other hand, selino ketones R (C=Se) R and seleno-aldehydes R (C=Se)

H are present [45][46]. However, they are generally difficult to obtain, in accordance with the "double bond rule" [47].

Selenium can be detected quantitatively in an electrochemical method by measuring the polarity at concentrations up to 0.003%, The selenates in a 0.1 M solution of ammonium chloride exhibit a threshold at 1.50 V versus the saturated calomel electrode. The detection of the effects of selenium uses the atomic spectroscopic method, where it can detect small concentrations of selenium in a way atomic absorption spectroscopy reaches the threshold of 0.01 mg/liter [47].
Selenite (Se^{4+}) and selenate (Se^{6+}) are the two most common oxyanions of selenium; this plays an important role in determining the oxidation or reduction state of selenium along with the adsorption efficiency of the selenium species present in the solution. There are 3 chloride forms of selenium, selenium monochloride (Se_2Cl_2), selenium dichloride ($SeCl_2$), and selenium tetrachloride ($SeCl_4$). Elemental selenium Se (0) is the specie present in both Se_2Cl_2 and $SeCl_2$, but different adsorption recovery can be achieved due to the competition between chlorine atoms and selenium atoms. In selenium monochloride, Se-Cl bond is symmetrical, which means there is one selenium atom bonded to one chlorine atom; therefore, the competition between the atom is much less compared to $SeCl_2$, that is why it is very probable that the recovery rate of selenium from Se_2Cl_2 would be double than in $SeCl_2$. Selenite (Se^{4+}) is the selenium specie present in $SeCl_4$; all these chloride forms are present in equilibrium when they are in acetonitrile solution as shown below.

$$3SeCl_2 \rightarrow Se_2Cl_2 + SeCl_4 \quad \text{Eq 2. 1}$$

In a real pregnant leach solution (PLS), it is very hard to pinpoint the selenium species present; variables such as solution pH and selenium concentration play an important role in determining which selenium species is most probable to be present in the solution.

2.4 Significance of immobilization

The immobilization process is divided into two stages: first, the introduction of novel functional groups that aid metal adsorption onto the polyphenolic structure of biomass, followed by cross-linking, or vice versa [48]. The efficiency of biomass can decrease if it is unmodified, it can be

difficult to separate from adsorbed metal on it can have poor strength, which makes successful utilization difficult [49]. Iron (Fe) has proved to be efficient when it comes to selenium biosorption; researchers like Roberts et al. [1] and Rovira et al. [50] used iron to adsorb selenium from wastewater. Seaweeds have a high metal binding capacity which is due to the presence of proteins, polysaccharides or lipids on their cell wall surface, which contains functional groups such as amino, hydroxyl, carboxyl and sulfate, which act as binding sites for metals [51]. It was discovered by Roberts et al. [1] that one limitation of this approach is that significant amounts of iron can leach from the surface of the iron-based sorbent (IBS), causing future environmental issues. As the rate of Se uptake is negatively correlated with Fe leaching, the biosorption capacity should increase if further optimization of the biosorbent is done. In this research work, lignin is unmodified and that is due to the unavailability of thermodynamic data of modified lignin as a simulation work. As a result, raw lignin was entered in METSIM with the thermodynamic data found from the few available research works on lignin.

2.5 Experimental conditions

To test the biosorbent efficiency, biosorption processes are done in batches. In batch tests, parameters like pH, temperature, contact time, etc. are determined, which yield the highest sorption potential. Variations in experimental conditions, including temperature, solution pH, sorbent dosage and initial concentration, can all affect the ability of a biosorbent to uptake Se ions. Many researchers agreed that increasing operating temperatures to a certain extent can result in more efficient adsorption. In the extraction of selenium from water by iron treated Gracilaria, Roberts et al. [1] discovered that 20 °C was the optimum temperature where 99% of selenium was adsorbed. Some of the most successful selenium biosorption experiments were performed at room temperature (20 °C). The pH of the solution is an essential parameter to control for effective ion sorption. The pH affects the properties of selenium forms found in the solution; in the pH range of 4 to 9, selenate (SeO_4^{2-}) is more dominant under strongly oxidizing conditions. For alkaline pH, selenate is reduced to selenite (SeO_3^{2-}); on the other hand, it is reduced to hydrogen selenite for acidic and neutral pH. A pH range of 4 to 9 was used for most of the experiments conducted in the past.

Table 2. 1 Summary of experimental conditions for different types of absorbents for selenium removal.

Biomass type	Selenium species	T (°C)	pH	q_{max} (mg/g)	References
Cladophora hutchinsiae	Se (IV)	20	5.0	74.9	[52]
G. lucidum	Se (IV)	20	5.0	126.99	[53]
Gracilaria modified biochar	Se (IV) Se (VI)	20	4.0	2.72	[1]
S. cerevisiae	Se (IV)	45	5.0-6.0	39.02	[54]
Wheat bran	Se (IV) Se (VI)	30	2.0	72.54 62.51 (μg/g)	[55]
Pseudomonas stutzeri	Se (IV) Se (VI)	25-35	7.0-9.0	–	[56]
Lactobacillus plantarum	Se (IV) Se (VI)	20-50	3.0-9.0	700 (μg/g)	[57]
Enterobacter taylorae	Se (VI)	21	8.2	–	[58]

The extent of biosorption can also be affected by variations in biosorbent and initial concentration. At a given equilibrium concentration, more metal ions are adsorbed by the biomass at low cell densities than at high densities [22]. Electrostatics interaction between the cells also plays an important role in metal uptake. At lower biomass concentrations, the specific uptake of metals is

increased because an increase in biosorbent concentration leads to interference between the bindings sites [22]. At high sorbent dosages, however, there may not be enough available solute to completely cover the available binding sites, resulting in poor solute uptake [48]. To overcome all mass transfer resistance of metal between the aqueous and solid phases, a driving force is provided through initial metal concentration; the optimum percentage of metal removal can be taken at low initial metal concentration. Thus, the metal uptake increases with an increase in initial concentration at a given biomass concentration. In the case of selenium, Tuzen & Sarı [52] compared the effect of concentration on selenium sorption and found that there is an optimum concentration (8 mg/L in their case) as shown in Figure 2.4, where maximum biosorption occurs, then it becomes constant afterward.

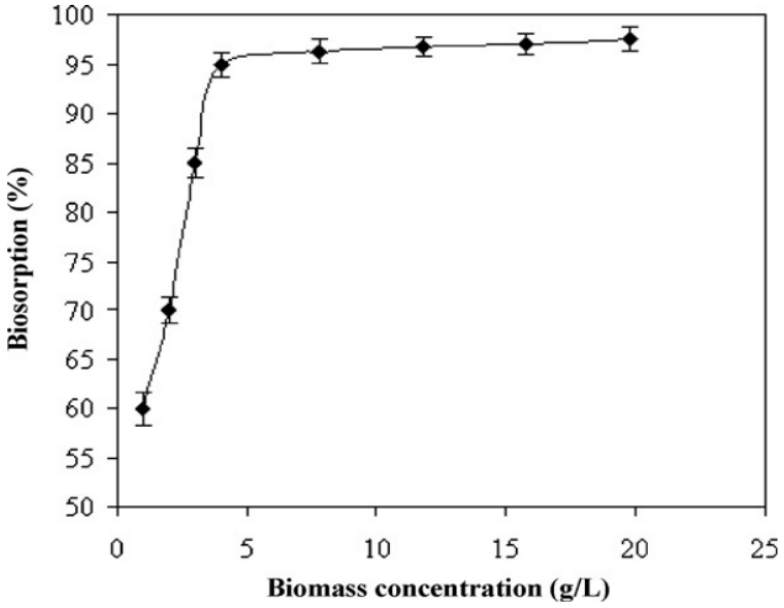

Figure 2. 4 Effect of biomass dosage on the biosorption of Se(IV) by C. hutchinsiae biomass [selenium concentration: 10 mg/L; pH: 5; temperature: 20 (°C) [52] permission enclosed in Appendix C

2.6 Biosorption isotherm models

The mechanism of processes, prediction of reaction outcomes and experimental data analysis can all be understood by Adsorption Isotherm models. The displayed adsorption isotherm is an invaluable non-linear curve describing the adsorption phenomenon at a steady temperature and pH, and the mathematical relationship which is depicted by the modeling analysis is important for operational design and applicable practice of the adsorption systems [59]. On the other hand, linear analysis of isotherm data into isotherm models is an alternative mathematical approach to predict the overall adsorption behavior [60]. In experiments involving solid/ liquid interaction, the Langmuir and Freundlich Isotherms are the most studied isotherms [48].

The Langmuir Isotherm is a non-linear isotherm, it is based on the assumption that adsorption can occur only in a finite number of definite localized sites, interactions among adsorbate molecules are negligible; and the adsorption proceeds with the formation of only one layer of the adsorbate on the adsorbent surface (the so-called: monolayer adsorption) [60].

$$\frac{C_e}{Q_e} = \frac{1}{Q^\circ K_L} + \frac{1}{Q^\circ} C_e \quad \text{Eq 2. 2}$$

Q° describes the quantity of selenium acquired per gram of biosorbent at equilibrium (mg/g), K_L is the Langmuir equilibrium constants between adsorption and desorption. Q_e is the adsorption capacity of the adsorbent (mg/g), C_e is the final concentration of the element (mg/L). The essential characteristics of the Langmuir isotherm can be expressed in terms of a dimensionless equilibrium parameter (R_L). This parameter is defined by Thajeel (2013) [61]

$$R_L = \frac{1}{1+K_L C^\circ} \quad \text{Eq 2. 3}$$

If R_L>1 unfavorable adsorption, R_L=1 linear adsorption, 0<R_L<1 favorable adsorption and R_L= 0 irreversible adsorption. [61]

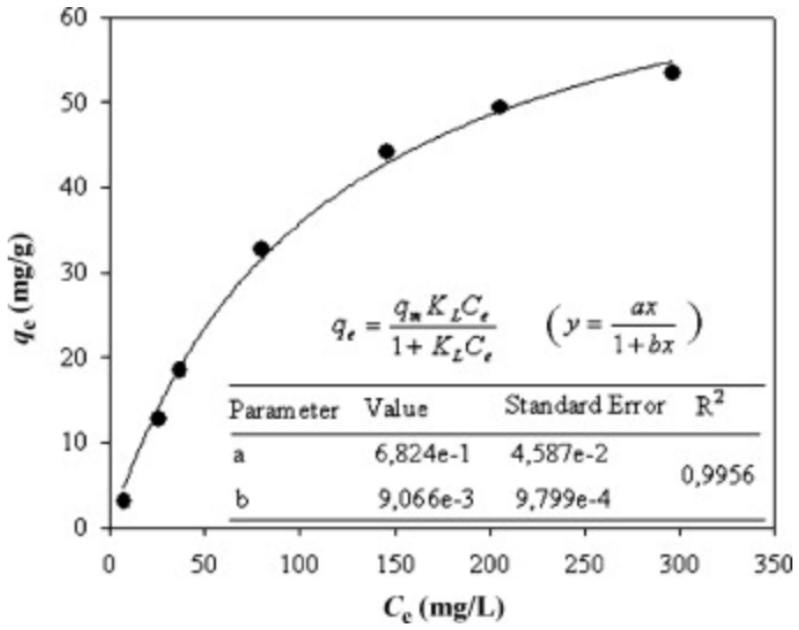

Figure 2. 5 Langmuir isotherm plots for the biosorption of Se(IV) by C. hutchinsiae biomass [52] permission enclosed in Appendix C

Freundlich Isotherm is an empirical model which operates under the assumption that multilayer adsorption, with variable distribution of adsorption affinities and heat over the heterogeneous surface exists [59]

$$C = KP^{\frac{1}{n}} \quad \text{Eq 2. 4}$$

K and *n* are Freundlich constants, *n* gives the indication of how favorable the adsorption process is, whereas *K* is the adsorbent capacity of the adsorbent [61]. A typical Freundlich Isotherm plot has a slope between 0 and 1, which is a measure of adsorption intensity or surface heterogeneity; if its value is closer to zero, then it is more heterogeneous.

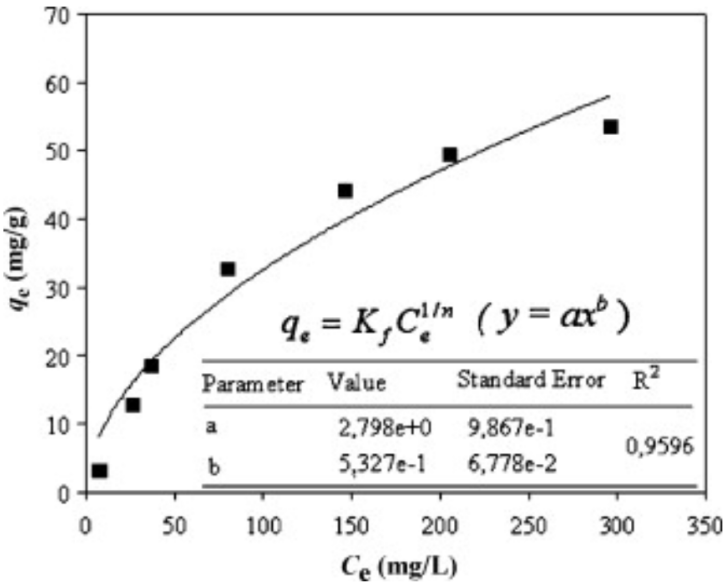

Figure 2. 6 Freundlich isotherm plots for the biosorption of Se(IV) by C. hutchinsiae biomass [52] permission enclosed in Appendix C

Using the findings of Tutzen & Sari [52] as an example, from the plots in Figure 2.6 and 2.7, it is apparent that their C. hutchinsiae biosorbent adheres more to the Langmuir isotherm model than the Freundlich model. This is because the Langmuir plot has a higher R^2 value of 0.9956 when compared to the Freundlich plot's R^2 value of 0.9596, signifying that data points collected from the adsorption of Se(IV) fit better to the Langmuir plot.

Another Isotherm which was used by Khakpour et al. [54] is Sip's isotherm, which is a combined form of Langmuir and Freundlich expressions deduced for predicting the heterogeneous adsorption systems, overcoming the Freundlich Isotherm Limitation which is the rising adsorbate concentration, it applies Freundlich Isotherm at low concentration, but at high concentrations, it assumes a monolayer adsorption capacity which is characteristic of the Langmuir isotherm
The Sip's equation is given as [62]

$$q_e = \frac{K_s C_e{}^{\beta s}}{-a_s C_e{}^{\beta s}} \quad \text{.....Eq 2. 5}$$

Where a_s and K_s are Sip's isotherm model constant, βs is Sips isotherm exponent.

During a study conducted on the use of wheat bran as a biosorbent for selenate and selenite, Hasan et al. [55] used Thomas model. The Langmuir kinetics of adsorption-desorption are assumed in Thomas model; it also assumed that the rate driving force obeys second-order reversible reaction, a constant separation factor which is relevant to either favorable or unfavorable isotherms. The main limitation of the Thomas model is that it's derived from second-order reaction kinetics which means that, sorption is rather controlled by interphase mass transfer, not limited by chemical reaction kinetics which can lead to some error when this method is used to model the adsorption process. The equation representing Thomas Model is given as [55]

$$In\left(\frac{C_o}{C_t}-1\right)=\frac{K_{Th}q_{Th}M}{Q}-\frac{K_{Th}C_o}{Q}V_{eff} \qquad \text{Eq 2. 6}$$

Thomas rate constant is represented by K_{Th} whereas, q_{Th} represents the maximum solid-phase concentration of the solute. By plotting In[(C_o/C_t) − 1] against V_{eff} at a given flow rate, both the kinetic coefficient k_{Th} and the adsorption capacity of the bed q_{Th} can be determined.

Arrhenius equation shown below is used to calculate the activation energy (E_A)

$$In\ K_l = In\ A - \frac{E_A}{R}\left(\frac{1}{T}\right) \qquad \text{Eq 2. 7}$$

Where R represents gas constant (usually 8.314 J/mol K), K_l represents a rate constant and A signifies the Arrhenius constant. Typical values for physisorption can be up to 4.2 kJ/mol, which is quite low as energies required for physical interactions are generally weak due to the nature of intermolecular forces [63]. Chemisorption, however, occurs at higher activation energies between 8.4 to 83.7 kJ/mol or above; these values emphasize that the forces required for chemical bonds to proceed are present in order for the adsorbent to interact with the metallic ions [64].

2.7 Summary of review

In this chapter, the mechanisms, and operational parameters of metal biosorption were discussed, as well as a comparison of biosorption's use and benefits versus traditional recovery methods are given. Plant materials include structural and functional organic polymers with polyphenolic groups, which have been shown to be effective at adsorbing metal ions in solutions in the past. Conventional methods that are being used in the present day for metals recovery include pyrometallurgy and hydrometallurgy. Although pyrometallurgical processes are available commercially, the long processing times and huge requirements of energy to maintain operating temperature tend to be disadvantages associated with it. Also, in most cases, pyrometallurgical processes are accompanied by hydrometallurgical processes in order to further purify the recovered minerals.

Although selenium recovery processes such as oxidation/reduction, phytoremediation, membrane separation technologies, coagulation or flocculation, and adsorption have proven to be effective over the year, excessive operation costs and obeying environmental regulations may make selenium recovery less likely to be adopted on a massive scale. As a result, biosorption has been adapted by researchers over the past decade since it offers many advantages such as cheap operating cost, regeneration, and similar or higher uptake capacities than conventional adsorbents.
Lignin can be found in all plants; it is an important constituent of wood along with cellulose and hemicellulose, where lignin makes up 30%, cellulose content is 45%, and hemicellulose is 20%. The presence of the polyphenol group (OH) in lignin, is what makes lignin bind to valuable minerals.

Inorganic selenium has 4 different oxidation states selenium exist; the most common are Se^{-2}, Se (0), Se^{4+}, Se^{6+}, each shows different properties and is affected by pH and redox conditions. The extent of selenium biosorption is affected by different variables such as

- Biosorbent dosage
- Initial concentration of selenium
- Residence time
- pH
- Temperature

- Reaction rate

Evidence shows that biomass treatment may improve uptake, but since such treatments may alter the thermodynamic data and chemical structure of the biomass, there is very little literature on these data and as a result, organic lignin is used instead.

CHAPTER 3 Model Procedure

3.1 Software and data

METSIM was only used as a metallurgical simulation program, with the aim to perform mass balances around the unit operations available in the complex flowsheets. Due to its success, the program was expanded to include detailed heat balances, chemistry, process controls, equipment sizing, cost estimation, and process analysis. The program is so versatile, which means that with the least effort, it can be modified or expanded the system, which is due to its unique programming language (APL). The ability to deal with heterogenous solutions (containing solids and liquids) and modify thermodynamic properties makes METSIM stand out when compared to Aspen. Moreover, a few research have been conducted on hydrometallurgical processes simulation; as a result, using METSIM provides an alternative perspective of the process with a different set of results.

Selenium monochloride (Se_2Cl_2) was the chloride form of selenium used in this model since it is one of the most soluble crystalline structure in water, so it is very probable that it would be available in pregnant leach solution or industrial waste effluents. The components needed in this model were Se_2Cl_2, hydrochloric acid, water, and lignin. The main purpose of HCl and water is to control the pH of the solution entering the reactor tank where a chemical reaction is specified.

To add components, it is needed to choose elements from the periodic table available in METSIM and it will show all the available components with the chosen elements, as shown in Figure 3.1. Thermodynamic data of biomass such as plants containing lignin is not available on METSIM and as a result, it was found using a different approach, which is discussed in Section 3.2.

As in the case of any simulation model, some assumptions must be made for the model to work properly. One of these assumptions was the rate of reaction. For the model to run in METSIM, the reaction rate must either be entered as a function of temperature and time such as "1-xRT/t", where x is the initial rate of reaction (e.g. 0.4), R is the gas constant, T is temperature in K and t is time in minutes. This helps study the effect of residence time on the rate of reaction. Or by assuming the reaction rate as a number such as 0.55 which means that reaction rate is assumed as 55%. The

first approach was used here as it is more accurate and time is an important factor in this simulation. Another assumption made in this simulation was the room temperature, according to different researchers, the room temperature in the laboratory was between 20 °C and 25 °C, so a room temperature of 25 °C was assumed in this model. The final assumption made in this simulation was the revolutions per minutes (rpm) in the reactor, most researchers were stirring their solution at 200 to 300 rpms, therefore, a 300 rpm agitation was used for this simulation.

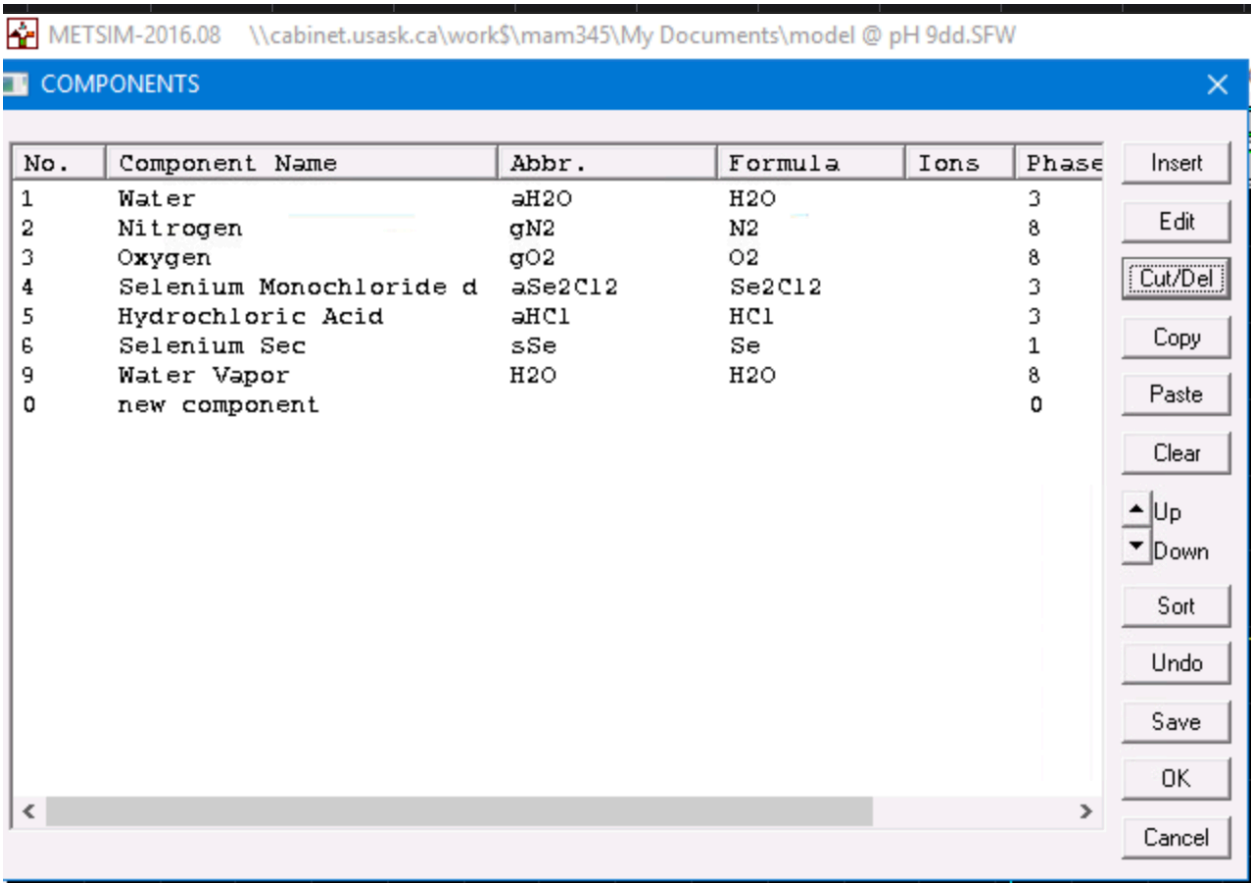

Figure 3. 1 List of components chosen on METSIM before adding lignin

3.2 Thermodynamic data of lignin

Lignin is an aromatic hydrophobic polymer, which along with cellulose and hemicellulose, is one of the major components of plant cell walls, particularly wood cell walls. As mentioned in Section 2.2, there are two types of wood, hard wood, and soft wood. the former has of 45% cellulose, 30% lignin and 20% hemicellulose, the latter has 20% lignin, 30% hemicellulose, and 45% cellulose

[65]. While it was known that only higher land plants (vascular plants) had lignin, some studies confirmed that some algae contain lignin as well [66]. Since the last century, lignin has been expected to be one of the essential organic products because it is the most abundant biomass on this planet alongside cellulose [67]. Lignin has to be separated from wood in order for it to be usable, this can be done in different ways but chemical pulping processes such as sulfite pulping are the most commonly used. Lignin has a wide variety of uses, for example. Lignosulfonate is used as a dispersing agent for concrete.

Before finding the thermodynamic data of lignin it was needed to a find a suitable lignin monomer for this simulation, a proposed lignin chemical structure by Funaoka et al. [65] is shown in Figure 3.2 and is one of three proposed monomers of lignin.

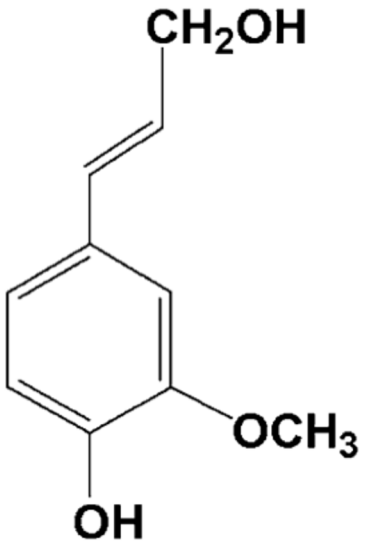

Figure 3. 2 Structure of lignin proposed for the simulation [65] permission enclosed in Appendix D

Thermodynamic properties of lignin were studied by Voikevich et al. [34], and the enthalpy, entropy, heat capacity and Gibbs free energy were calculated for a temperature range of 0 K to 380 K, which covers the temperature range needed to perform this study. They are displayed in Table 3.1 [34].

Table 3. 1 Thermodynamic data of lignin [34]

T/K	$C_{p,m}$ J·K^{-1}·mol^{-1}	$\Delta_0^T H_m^o/T$ J·K^{-1}·mol^{-1}	$\Delta_0^T S_m^o$ J·K^{-1}·mol^{-1}	$-(G_m^o(T)-H_m^o(0))/T$ J·K^{-1}·mol^{-1}	$-\Delta_f H_m^o$ kJ·mol^{-1}	$-\Delta_f G_m^o$ kJ·mol^{-1}
			Amorphous			
0	0.0	0.0	0.0	0.0	673.9	673.9
20	11.87	4.081	5.831	1.749	675.6	669.7
40	32.90	13.16	20.41	7.248	680.3	657.2
60	53.68	23.25	37.73	14.48	685.7	641.1
80	72.74	33.29	55.84	22.55	689.4	625.7
100	89.55	42.88	73.90	31.02	693.1	608.1
120	105.4	51.99	91.64	39.65	695.9	591.4
140	120.5	60.70	109.0	48.32	698.3	573.5
160	135.5	69.11	126.1	56.98	700.6	555.3
180	150.5	77.32	142.9	65.60	702.8	537.1
200	165.6	85.39	159.6	74.16	704.7	518.2
220	180.8	93.36	176.0	82.67	706.7	499.9
240	196.5	101.3	192.4	91.14	708.5	481.1
260	212.3	109.2	208.8	99.56	710.2	461.9
273.15	222.5	114.4	219.5	105.1	711.1	448.9
280	227.7	117.1	225.1	107.9	711.6	442.4
298.15	242.0	124.3	239.8	115.5	712.9	424.8
300	243.5	125.0	241.3	116.3	713.0	423.0
320	260.0	133.0	257.6	124.6	714.2	404.1
340	274.1	140.9	273.8	132.9	715.3	384.9
360	288.8	148.6	289.8	141.2	716.2	365.4
380[b]	307.3	156.5	305.9	149.4	716.9	345.6
			Liquid			
420[b]	413.3	174.5	340.4	165.9	709.9	306.2
440[b]	428.0	185.8	360.1	174.3	708.4	287.0

The above data facilitate the calculations of parameters such as reaction heat or mixing heat which in turn helps determine heat transfer, which is crucial when designing, sizing, or selecting equipment; METSIM requires thermodynamic data to be entered in the form shown in Eq 3.1 as follows,

$$H = A + 0.001BT + 100000CT^{-2} + 0.000001DT^{2} \quad \text{.....Eq. 3. 1}$$

Where *H* is enthalpy. As a result, the thermodynamic data of lignin were plotted as shown in Sections 3.2.1, 3.2.2 and 3.2.3, to obtain a polynomial function and enter values of *A*, *B*, *C*, and *D*.

3.2.1 Enthalpy

A curve of the enthalpy of lignin vs temperature is displayed in Figure 3.3, and the values of A, B, C and D entered in METSIM are shown in Table 3.2.

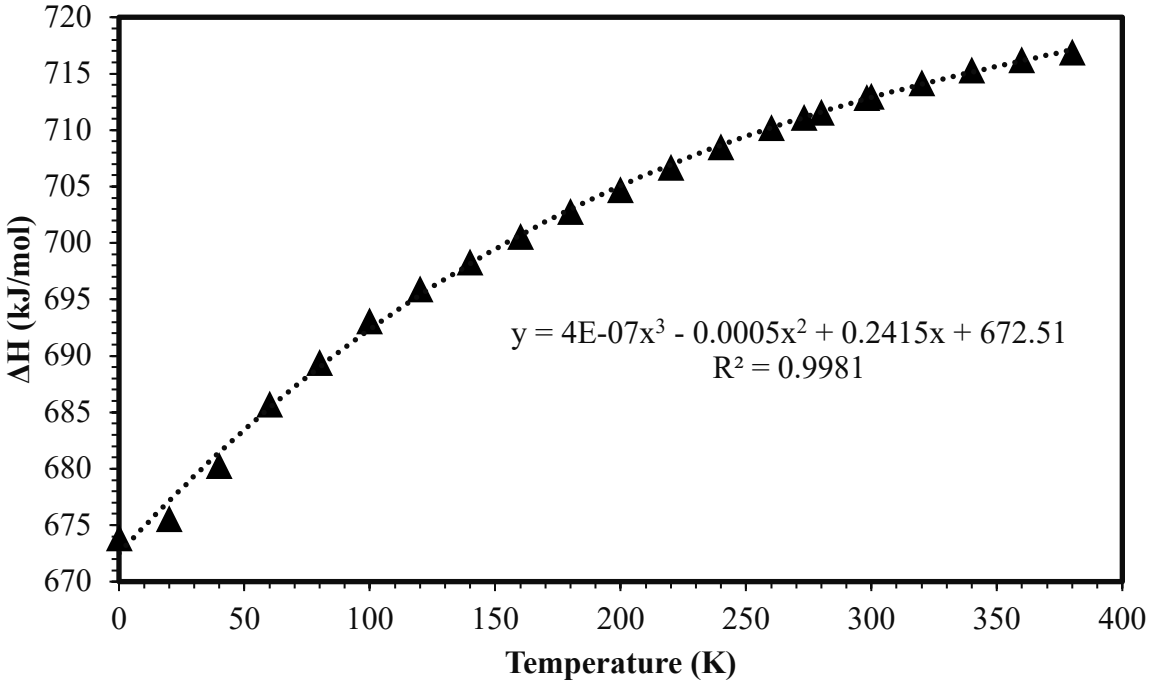

Figure 3. 3 Plotting of enthalpy of lignin vs. temperature

Table 3. 2 A, B, C, and D values of the polynomial function generated for the enthalpy of lignin

A	B	C	D
672.51	0.2415	-0.0005	0.0000004

3.2.2 Gibbs free energy

As shown in Figure 3.4, the Gibbs free energy of lignin is plotted against the temperature, and the values of A, B, C and D are entered in Table 3.3.

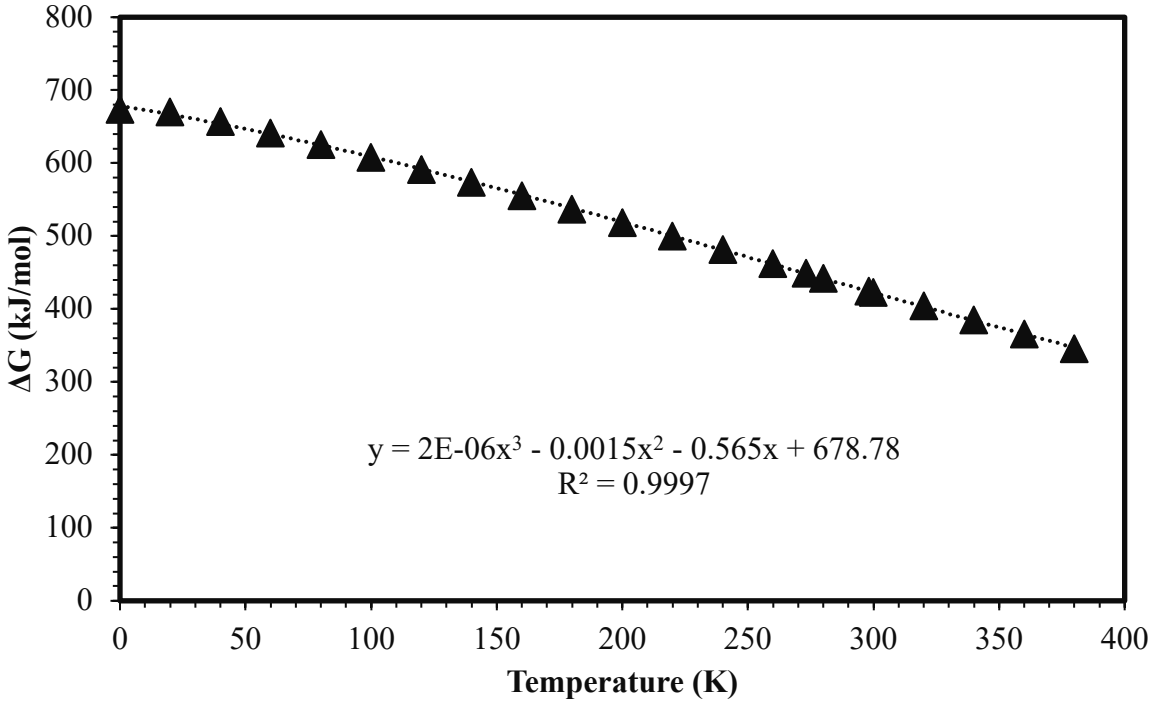

Figure 3. 4 Gibbs free energy of lignin vs. temperature

Table 3. 3 A, B, C, and D values of the polynomial function generated for Gibbs free energy of lignin

A	B	C	D
678.78	-0.565	-0.0015	0.000002

3.2.3 Heat capacity

As shown in Figure 3.5, the heat capacity of lignin is plotted against the temperature, and the values of A, B, C, and D are entered in Table 3.4.

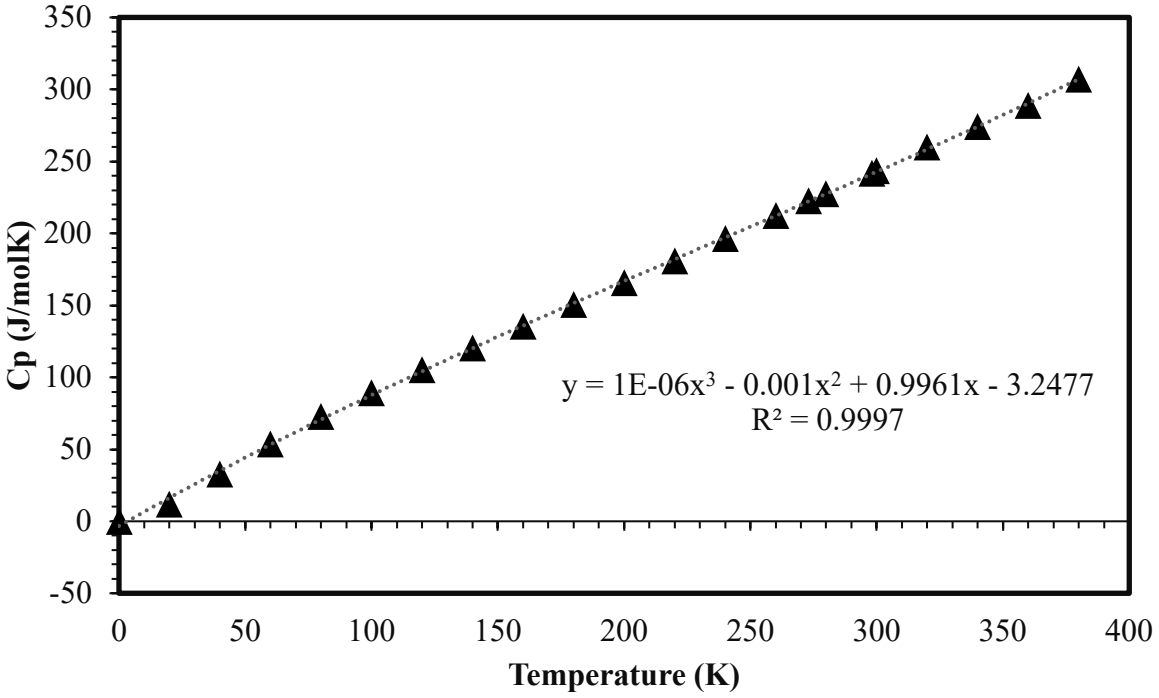

Figure 3. 5 Heat capacity of lignin vs. Temperature

Table 3. 4 A, B, C, and D values of the polynomial function generated for the heat capacity of lignin

A	B	C	D
-3.2477	0.9961	-0.001	0.000001

3.3 Data entry in METSIM

Since the values of A, B, C, and D for all the thermodynamic data have been found, lignin can be added as a component in METSIM as follows,

1- The molecular weight of lignin is entered as 196 g/mol, as shown in Figure 3.6.

2- Values of A, B, C and D can be entered in the thermo data tap as shown in Figure 3.7.

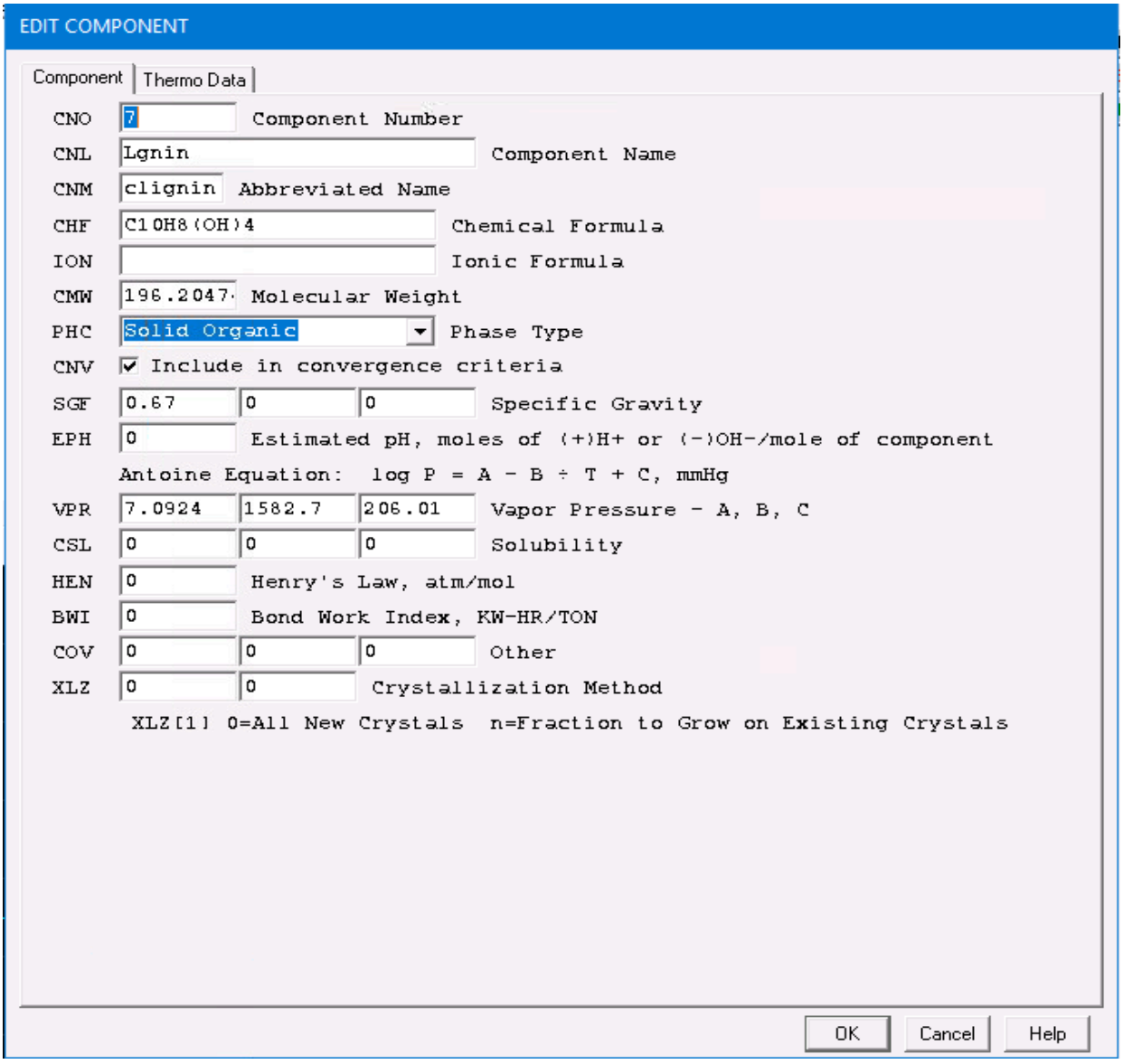

Figure 3. 6 Molecular weight and vapor pressure entering in METSIM

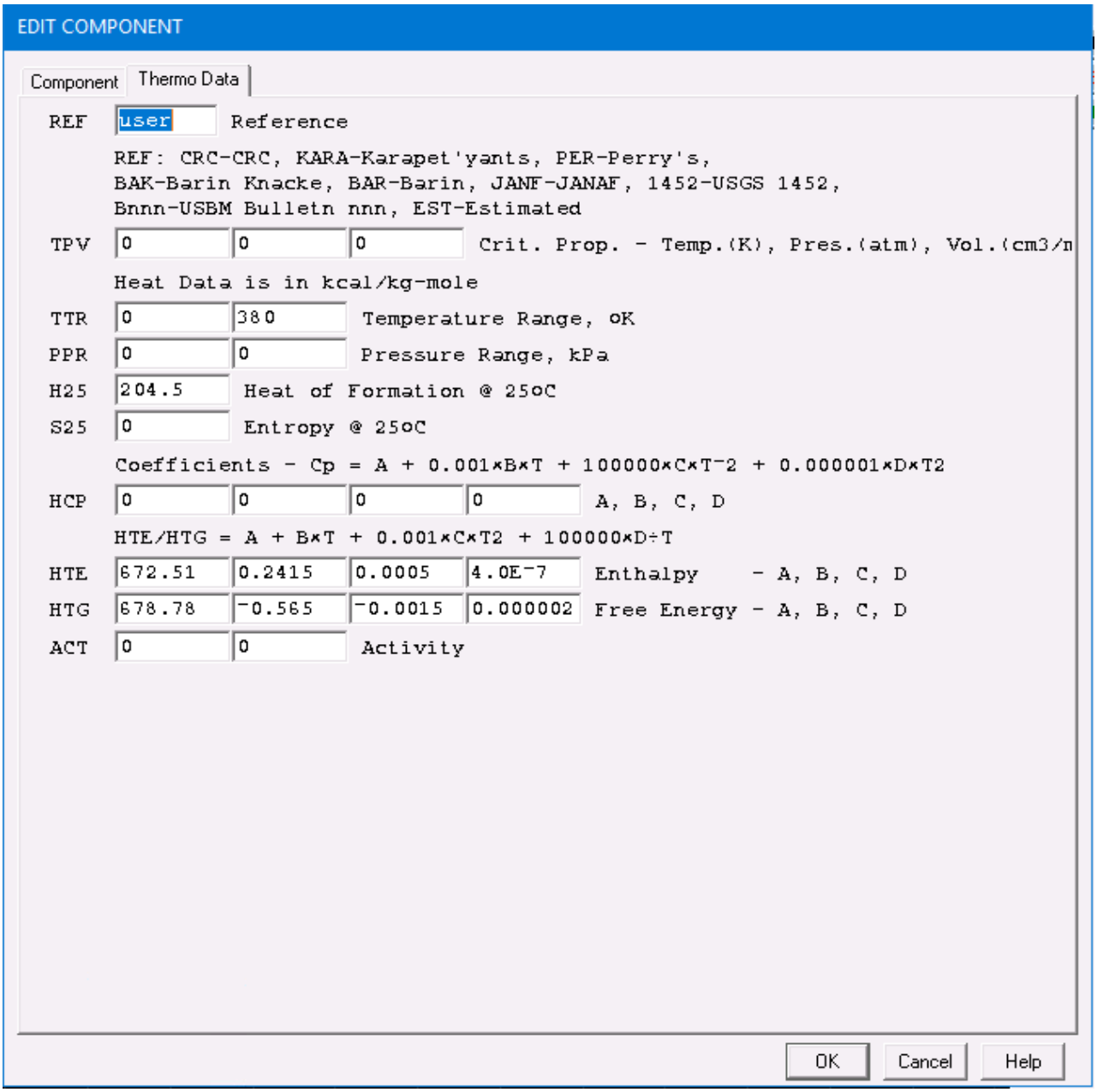

Figure 3. 7 Enthalpy, Gibbs free energy data entry in the "thermo data tap" in METSIM

3.4. Chemical reaction involved

The reaction entered in METSIM is an adsorption reaction where Se_2Cl_2 reacts with lignin to produce selenium, hydrochloric acid, and product-lignin as shown below,

$$3Se_2Cl_2 + C_{10}H_8(OH)_4 \rightarrow 6Se + C_{10}H_6O_4 + 6HCl \quad \text{Eq 3. 1}$$

Both selenium dichloride ($SeCl_2$) and Selenium tetrachloride ($SeCl_4$) were entered as follows,

$$3SeCl_4 + 2\ C_{10}H_8(OH)_4 \rightarrow 6Se + 2\ C_{10}H_6O_4 + 12HCl \quad \text{Eq 3. 2}$$

$$3SeCl_2 + C_{10}H_8(OH)_4 \rightarrow 6Se + C_{10}H_6O_4 + 6HCl \quad \text{Eq 3. 3}$$

Selenium monochloride was the chloride form of choice because chlorine ions compete with the adsorption of other anions such as selenate and selenite, especially when present at higher concentrations; therefore, choosing a chloride form that has equal number of selenium and chloride ions would be more beneficial than $SeCl_2$ and $SeCl_4$ as the chlorine concentration would be much higher in these species which would lead to less percent recovery [68]. Elemental selenium [Se (0)] is the selenium species present in both Se_2Cl_2 and $SeCl_2$. On the other hand, selenite (Se^{4+}) is present in $SeCl_4$.

3.5. Simulation development

A mixer, a heat exchanger and an agitated reactor tank were the three-unit operation utilized in this simulation; the main purpose of the mixer is to adjust the flow rates and concentrations of HCl and Se_2Cl_2, which in turn controls the theoretical pH of the solution entering the heat exchanger which heats the solution to a set temperature before entering the reactor where the main reaction takes place. The process flow diagram is shown in Figure 3.8, Also Table 3.5 details the components present in each stream.

The simulation is designed as follows, selenium monochloride, water and hydrochloric acid enter a mixer at a set hydrochloric acid concentration of 0.39 M (which is the concentration of the pregnant leach solution being simulated in this model). The selenium chloride/water solution then enters a heat exchanger where temperature is controlled, the solution then enters an agitated reactor where it is mixed with lignin (from stream 5) at 300 rpm. The product selenium in stream 9 is found in 2 states, solid and liquid. The solid selenium simulates the amount of selenium that binds to the lignin in a laboratory, the liquid selenium however, is the amount of selenium that remains in the pregnant leach solution after the process is run.

Three-unit operations were used in this simulation. The mixer labeled as MXI was used to mix the selenium monochloride with HCl and water to simulate a real PLS. A shell and tube heat exchanger labeled as HTX was used to heat the Se_2Cl_2 before entering the agitated reactor labeled as TAK, where the main adsorption reaction will happen with lignin.

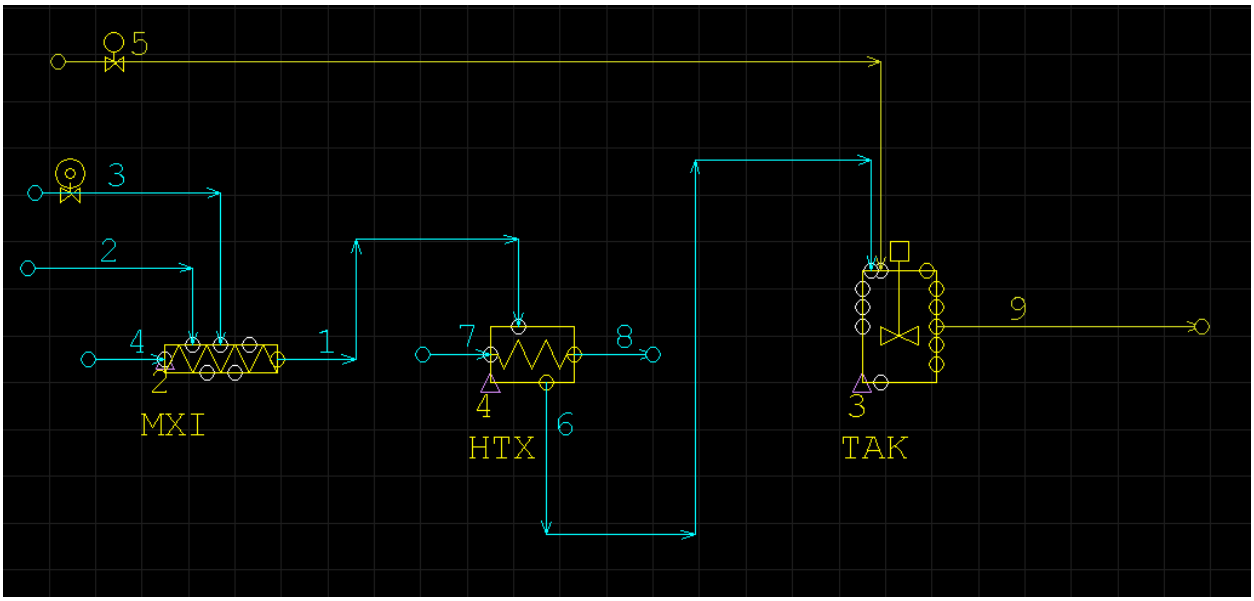

Figure 3. 8 METSIM model developed with all components and unit operations needed

Table 3. 5 Components present in each stream.

Stream Number	Component(s)
1	Heat exchanger feed (Se_2Cl_2, HCl and H_2O)
2	HCl
3	H_2O
4	Se_2Cl_2
5	Lignin
6	Hot feed into reactor (Se_2Cl_2, HCl and H_2O)
7	Cold water in
8	Hot water out
9	Reactor outlet (Se, product lignin, and HCl)

Parameters such as temperature, initial concentration of selenium, pH and residence time were treated as variables to reach the highest percent recovery (% recovery) of selenium in this simulation. As shown in Figure 3.8, there is a feed flow controller on stream 5 (lignin), which is meant to control the mass of lignin per litre of solution, another process control is installed on stream 3

(water), which is meant to control the pH of selenium chloride. The chemical reaction was specified in the agitated reactor as shown in the Figure 3.9.

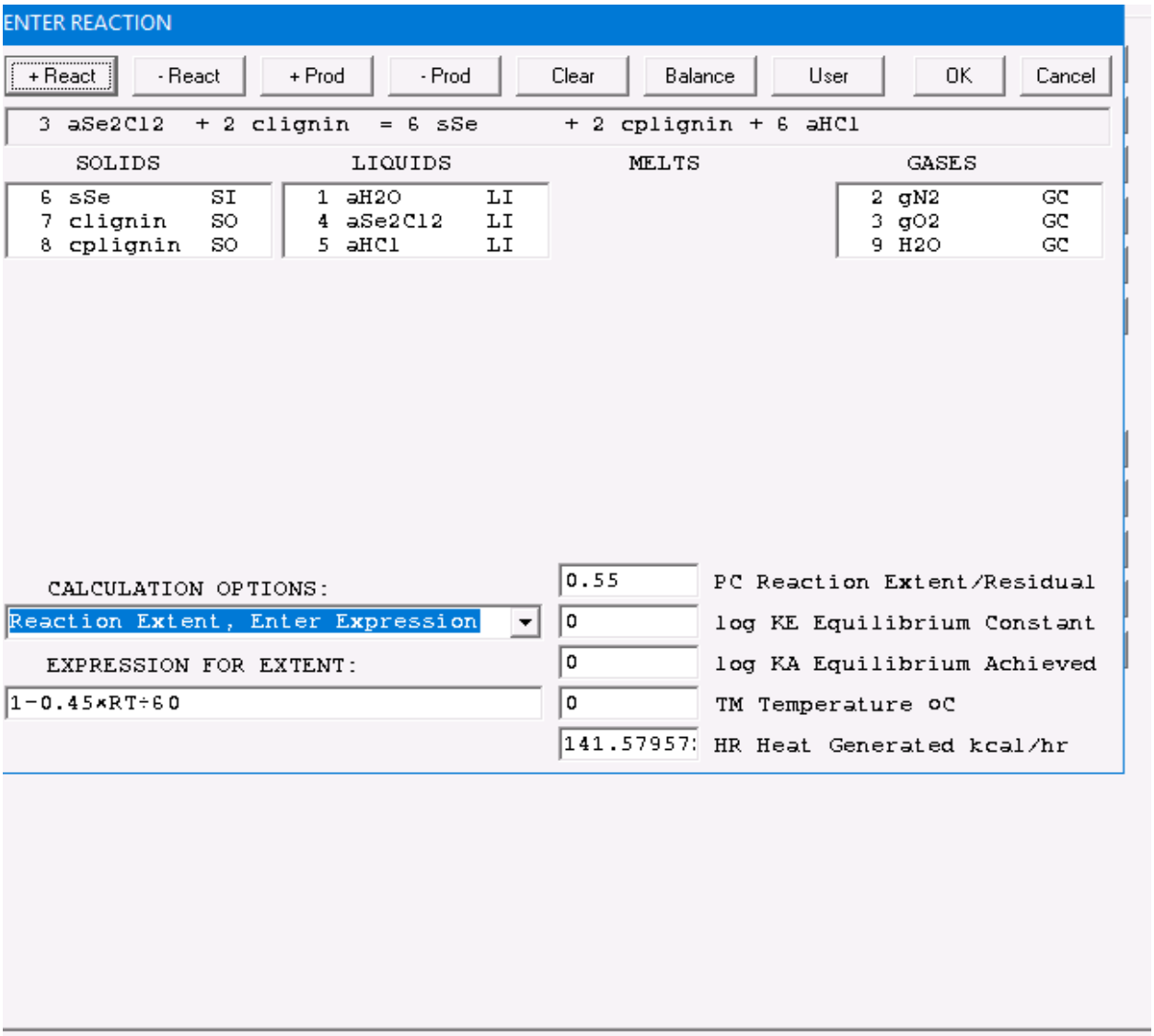

Figure 3. 9 Specific chemical reaction involved during adsorption entered in METSIM

CHAPTER 4 Results and Discussion

4.1 Effect of temperature

The heat exchanger used in this simulation was a shell and tube heat exchanger and the temperature ranges of 25 °C, 35 °C, 45 °C and 55 °C were tested. At 25 °C, the simulation ran without any errors and an initial selenium recovery of 55% was obtained, but at higher temperatures, the simulation did not run and turned completely red, as shown in the Figure 4.1.

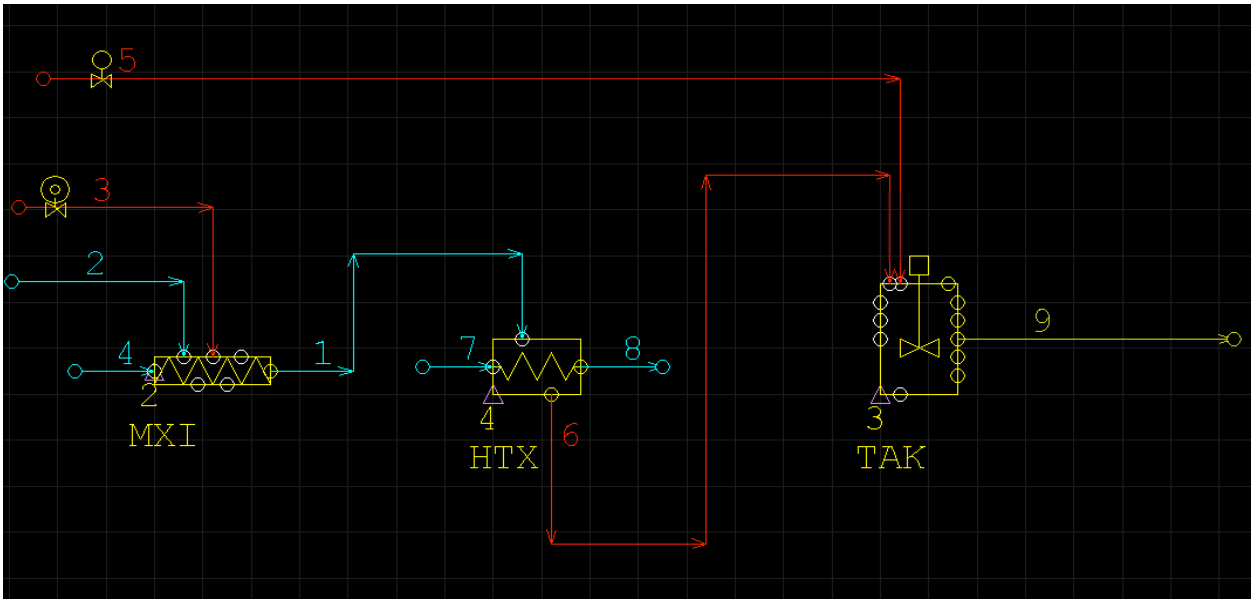

Figure 4. 1 Effect of temperature on the adsorption process and the inefficiency indicated by the red streams (which means they are not running properly)

METSIM modelling equations are not accessible to the public and as a result, a person cannot view what equations/formulas were used during the simulation model and change or modify them. As shown in Figure 4.1, both stream 3 (water) and stream 5 (lignin) did not converge, which suggests that the simulation is only runnable at 25°. Stream 6 (reactor inlet) is marked in red which automatically makes the selenium concentration in the product stream (stream 9) very low as shown in Figure 4.2,

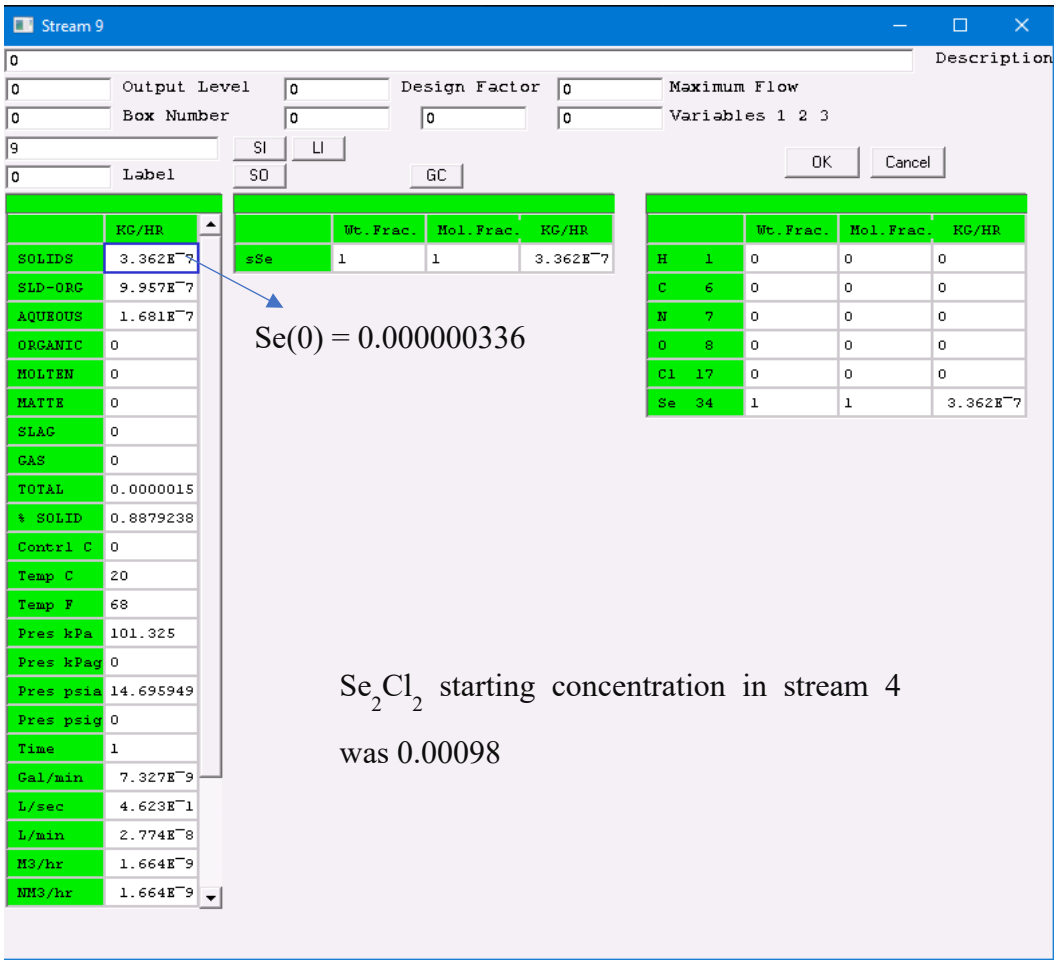

Figure 4. 2 Shows stream 9 (product stream) after it was run at 35 °C and how the selenium recovered was close to 0%, which means that temperature has a negative effect on this particular adsorption reaction

From Figure 4.2, it can be seen that selenium flow rate was 0.98 g/h in the feed stream; then it became almost 0 in the product stream, which means that the adsorption reaction is not running at a higher temperature.

This observation is backed up by a study by Yen Ning lee [69]. In that study, dithiooxamide immobilized wood bark was used to adsorb platinum and palladium from the pregnant leach solution. After it was successful, it was used to co-adsorb other trace elements such as silver, selenium, lead and zinc at temperatures 25 °C, 30 °C, and 40 °C. Adsorption was successful at the

3 temperatures for all the metals except selenium as shown in Figure 4.3. This might mean that selenium dissociates at higher temperatures and as a result, it does not bind to the sorbent material.

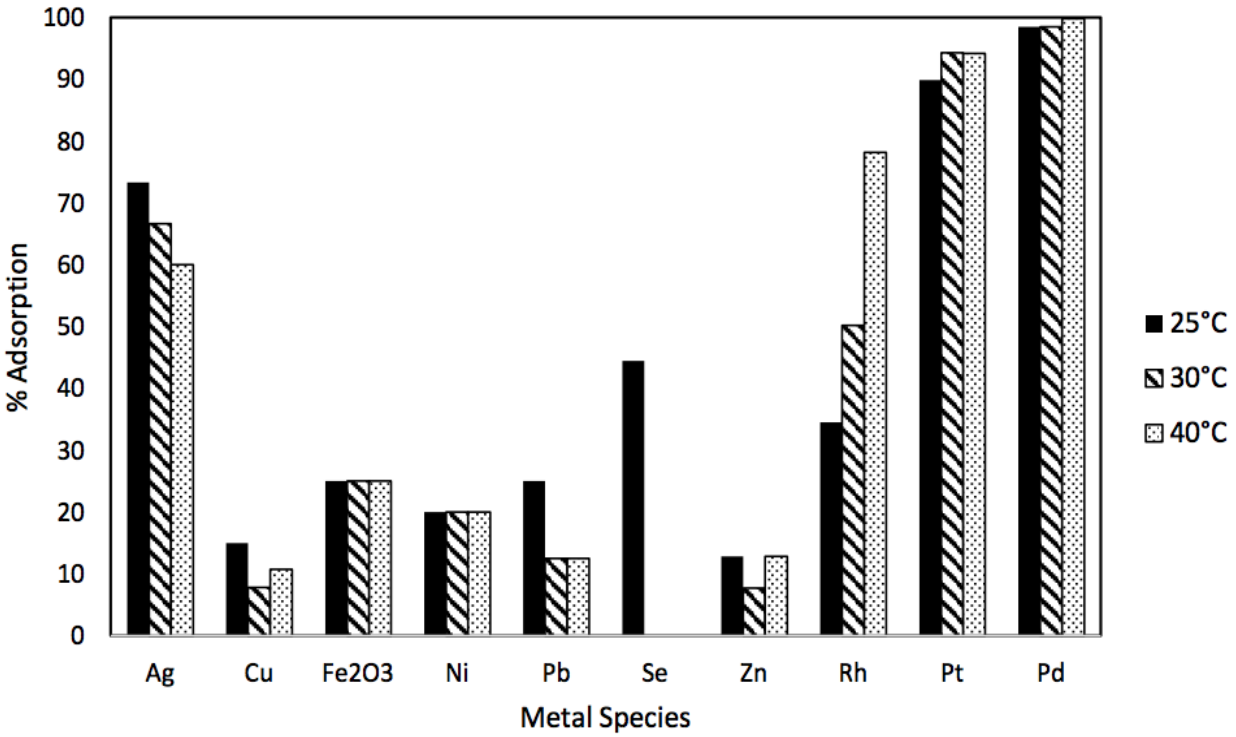

Figure 4. 3 Comparison of effectiveness in co-adsorption of all detectable metal species in received pregnant leach solution by dithiooxamide-immobilized wood bark at various temperatures. Operating conditions: Initial platinum and palladium concentrations = 20 and 44 ppm, solution volume = 200 mL, sorbent dosage = 200 mg, stirring speed = 200 rpm [69]

Since temperature would not be utilized as a parameter, a new model was introduced, where the heat exchanger was removed and two different process controls were introduced; more details will be discussed in Section 4.2.

4.2 Finalized METSIM model

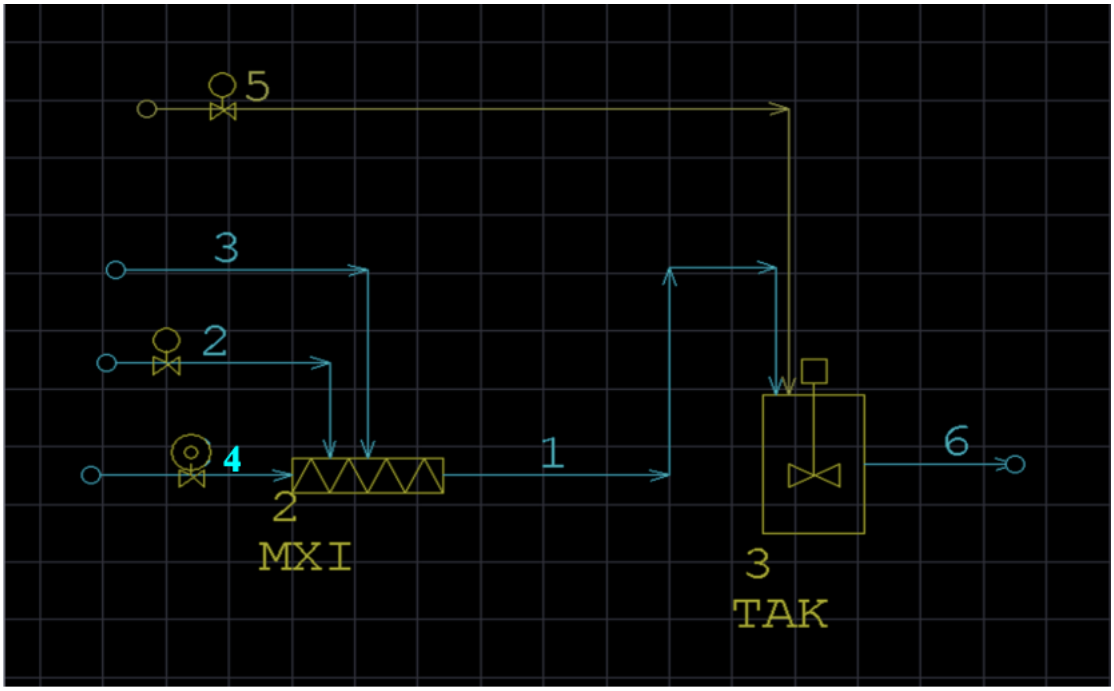

Figure 4. 4 Finalized METSIM model after removing the heat exchanger since the effect of temperature was proved to be negative for this reaction

In the revised flowsheet (Figure 4.4), The feedback controller installed earlier on stream 3 was removed since it was not accurate and different results were found every time the simulation was run; it was rather moved to stream 4 (Se_2Cl_2) and a value function was entered to control the selenium concertation in the solution in g/L, which would be more accurate when calculating uptake values. The other process control is a feed flow controller installed on stream 2 (HCl) and it is to control the ratio between HCl and water which can somehow control the % HCl or flow rate of HCl and water in the simulation.

4.3 Effect of residence time

To control parameters, METSIM offers a wide variety of valuable functions which are beneficial and accurate when one knows how to use them; process controls do not function without introducing value functions into them, the effect of residence time was introduced by controlling the time (minutes) in the reactor tank as shown in Figure 4.5.

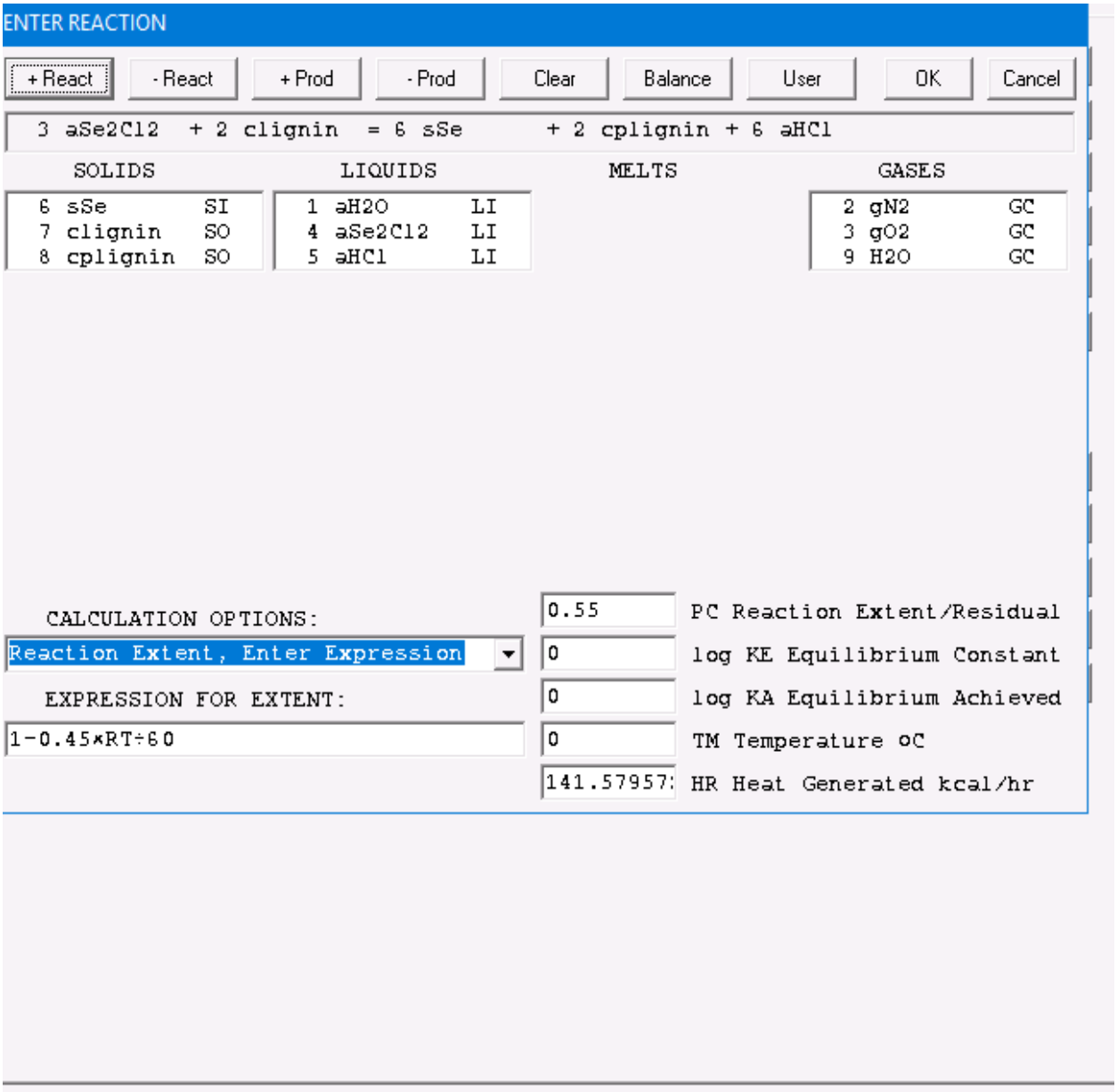

Figure 4. 5 Expression of extent equation for controlling residence time on METSIM

It is observed that the reaction rate at 60 minutes is 55%. When time is increased, the reaction rate also increases, as shown in Figure 4.6.

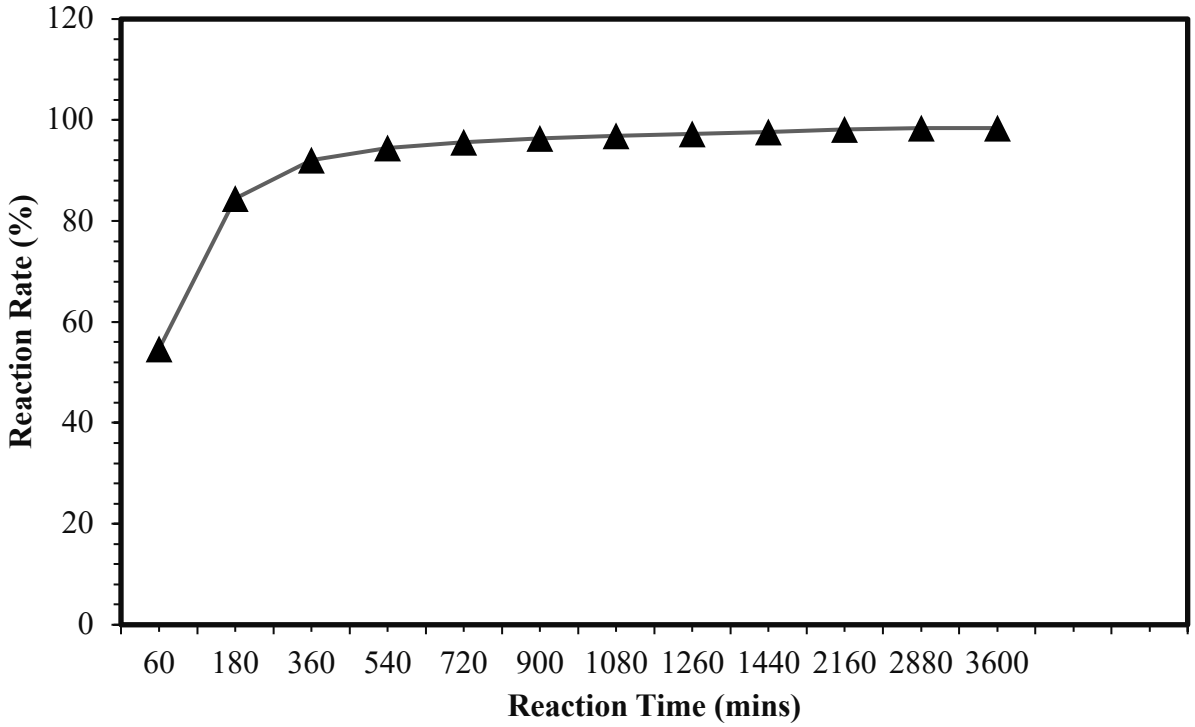

Figure 4. 6 Graphical plot showing the effect of residence time on the percent recovery of Se from Se_2Cl_2 on lignin

As seen in the graph, the rate of reaction rises rapidly to 92%, then it slowly increases to a maximum reaction rate of 99% at the 48-hour mark. As a result, the residence time in the agitated reactor was kept at 48 hours (2880 minutes) as shown in Figure 4.7.

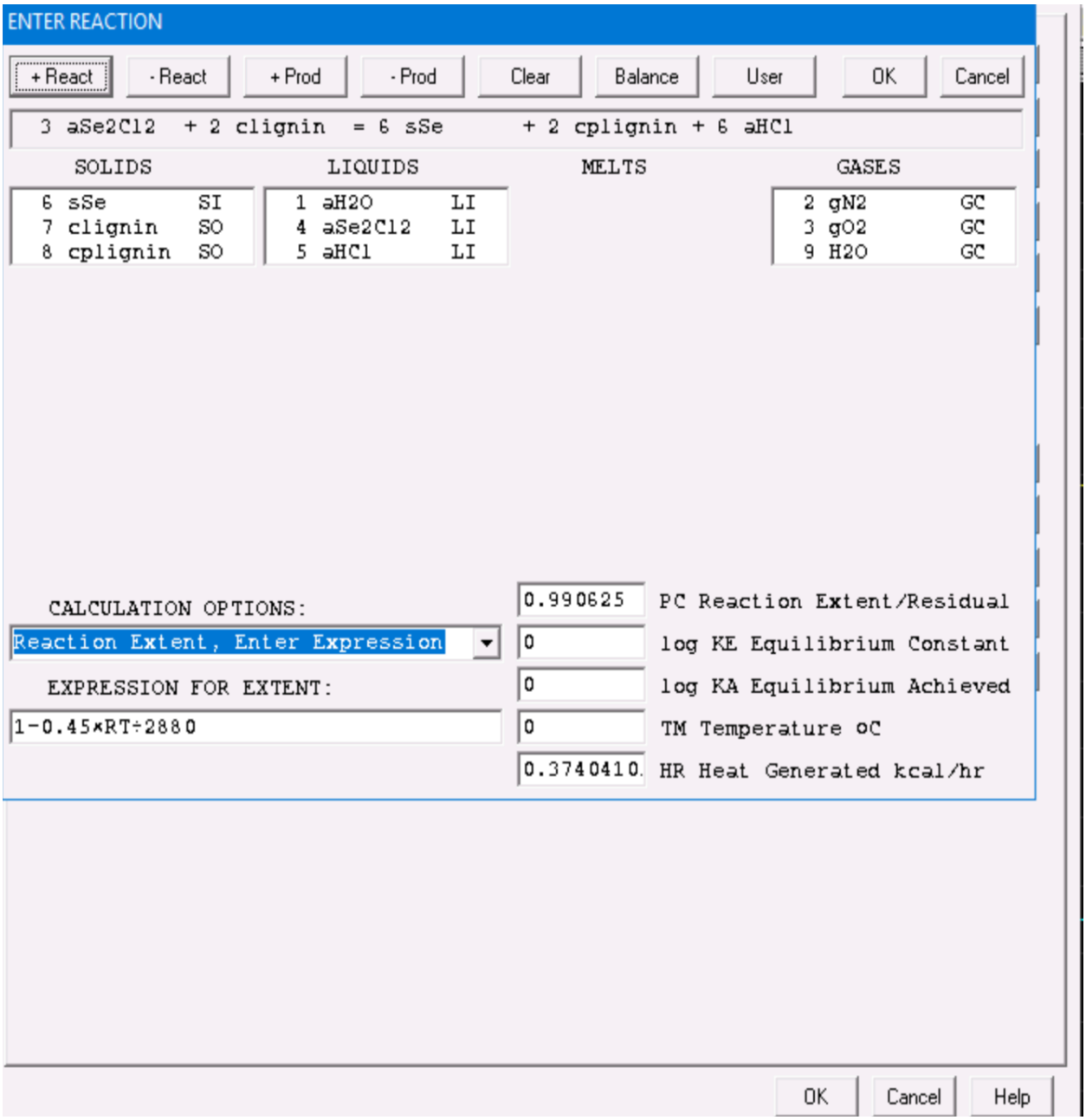

Figure 4. 7 The reaction rate shown at 99.0625% after 48 hours

4.3 Adsorbent dosage

Lignin S/L ratio was controlled by installing a feedforward controller on stream 5 (lignin); the main function of this controller is to set the flow rate of lignin entering the reactor as shown in Figure 4.8.

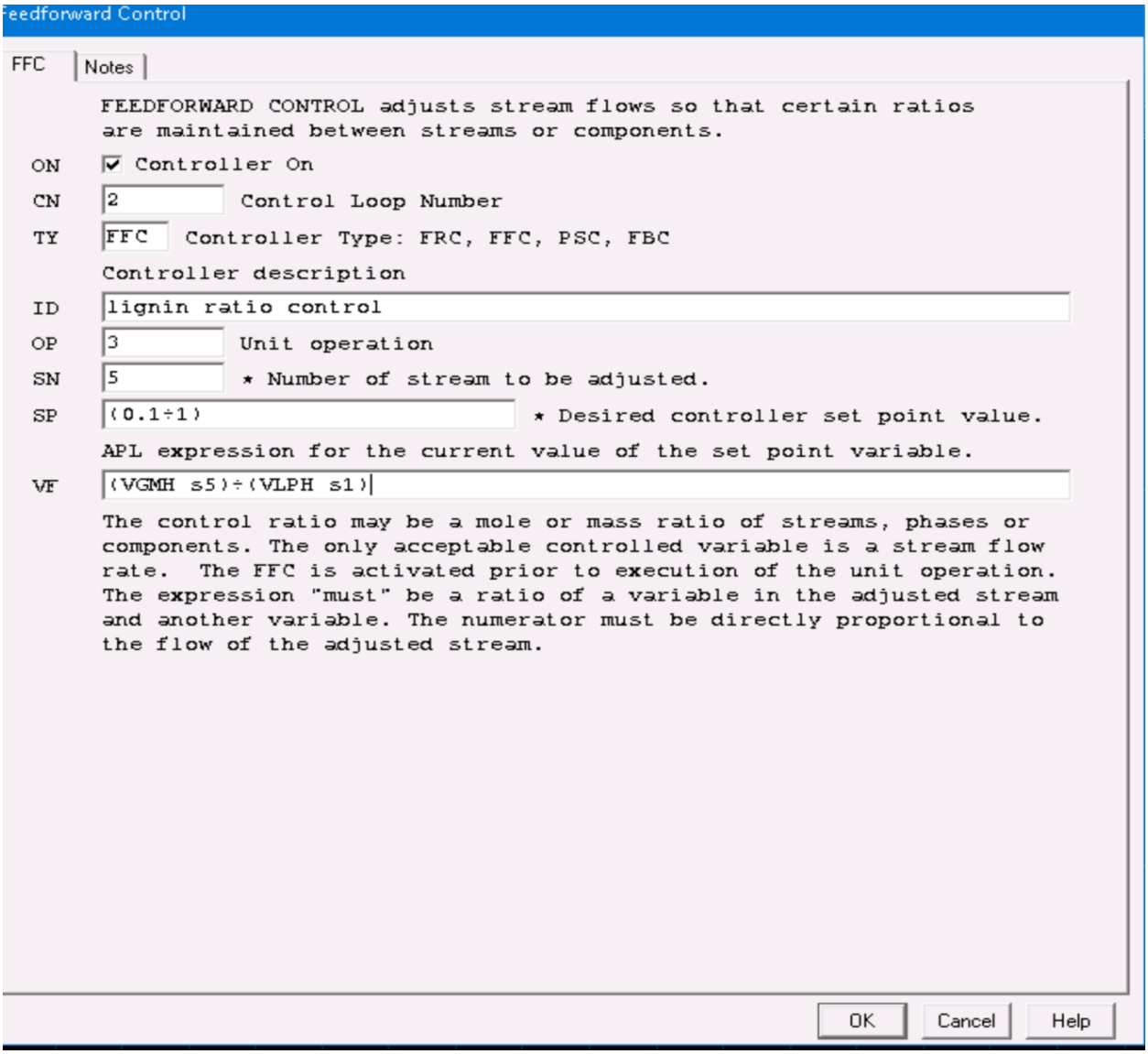

Figure 4. 8 Value function entered in the feedforward controller in order to control lignin dosage by controlling the flow rate ratios between selenium chloride and lignin

From Figure 4.8, it is noticed that to control the lignin dosage, a value function had to be entered, which sets a ratio between the mass of lignin per volume of stream 1 components (reactor feed). The volume stream 1 was set at 1L and the mass of lignin was treated as a variable,

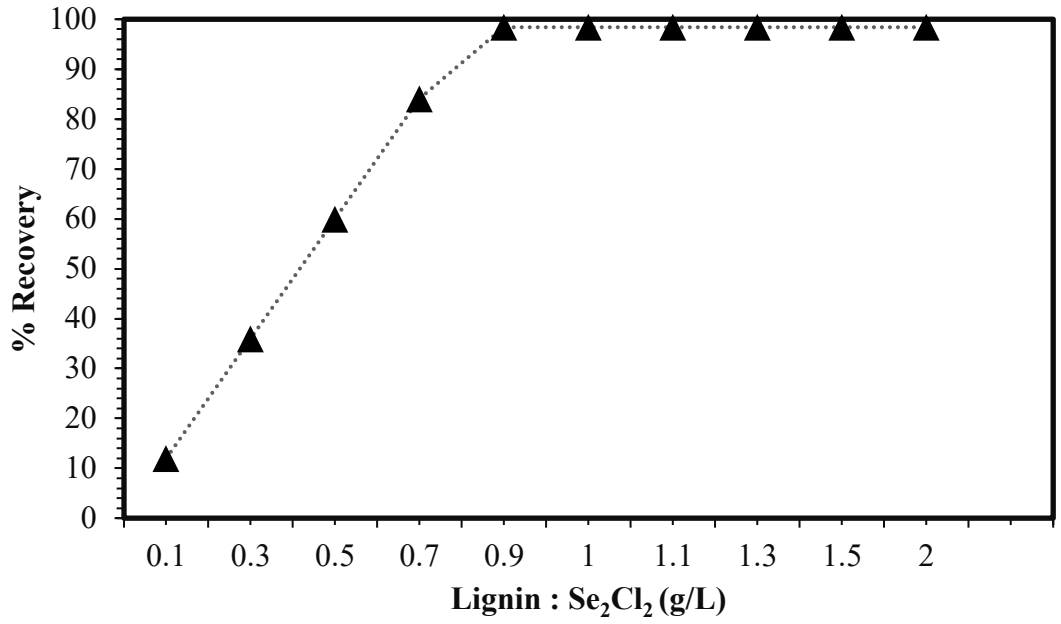

Figure 4. 9 Showing the effect of lignin dosage by plotting the percent recovery of selenium against the S/L ratio

Figure 4.9 shows that selenium % recovery was slightly increasing with increasing lignin dosage, then it reached a maximum recovery at 0.9 g/L of lignin, therefore, a 0.9 g lignin dosage was chosen for this simulation.

4.4. Initial concentration of selenium

To compare the % recovery of selenium accurately, the concentration of selenium in selenium chloride was adjusted in g/L by entering a value function in the feedback controller installed on stream 4 (Se_2Cl_2). This way, it is much easier to compare the final concentration of selenium in stream 9 and calculate uptake and the percent recovery. The data entry is shown in Figure 4.10.

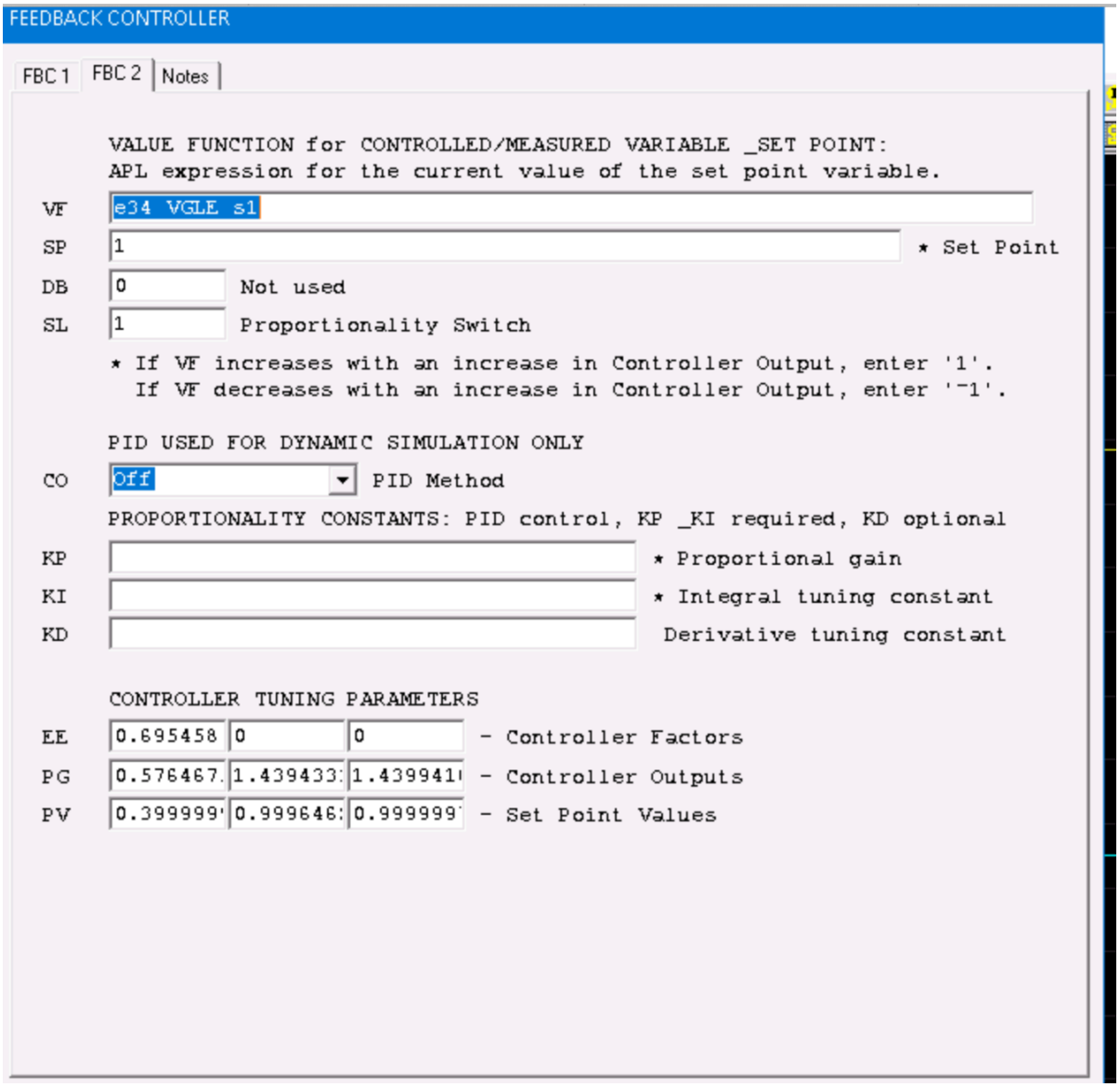

Figure 4. 10 Value function entered in the feedback controller on METSIM in order to control the concentration of selenium present in selenium chloride before entering the reactor

The value function “e34 VGLE s1” means concentration in gram per litre (g/L) of element 34 (which is selenium) in stream 1(the stream entering the reactor to mix with lignin), the range of initial concentration of selenium was set between 50 mg/L and 1000 mg/L as shown in Table 4.1.

Table 4. 1Concentration of selenium recovered in the product stream compared to selenium concentration in the feed stream (C_i).

Ci (mg/L)	**Ce (mg/L)**	**Ci-Ce (mg/L)**
50	0.7	49.3
100	1.44	98.56
150	2.2	147.8
200	2.89	197.11
250	3.589	246.411
300	4.4	295.6
350	5.2	344.8
400	6	394
1000	200	800

The concentration of selenium recovered was plotted against the initial selenium concertation and the results are shown in Figure 4.11.

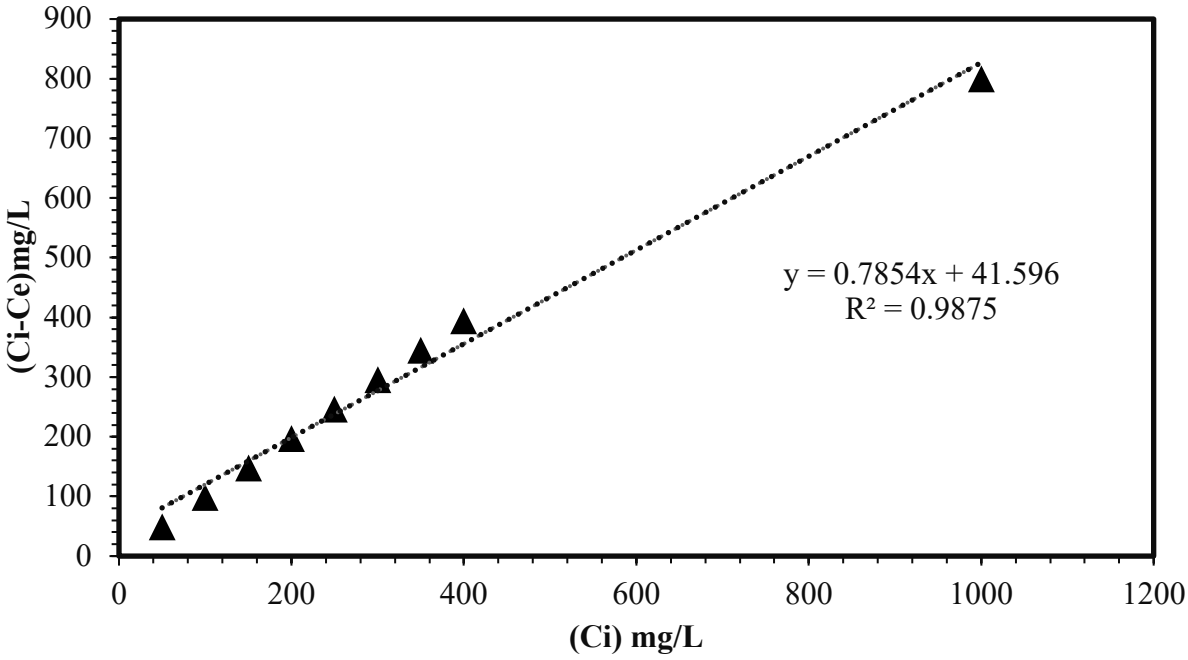

Figure 4. 11 The plotting of selenium concentration recovered against starting selenium concentration

4.5 Solution pH

Controlling pH on METSIM is not very easy because of accuracy issues. One of the process controls in METSIM is a pH set value; one issue with it is, HCl concertation does not change when pH increases or decreases which is not realistic as it should vary. As a result, a feedforward controller was installed on stream 2 (HCl) instead; the main function of that feed flow controller was to adjust the flow rate ratio of HCl and water, this way a change can be seen. The value function entered is shown in Figure 4.12.

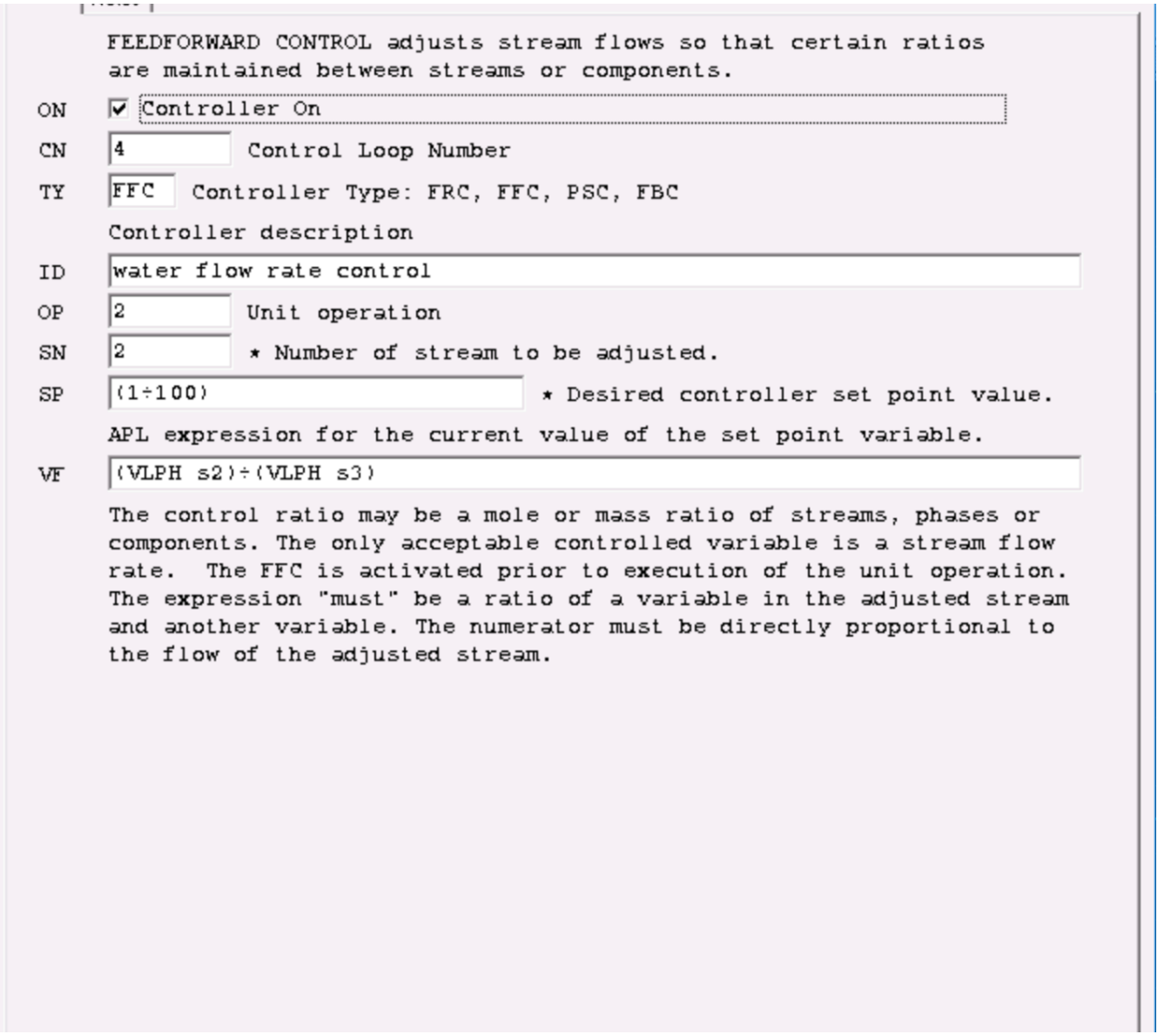

Figure 4. 12 The manipulation of HCl % concentration through controlling the HCl/water ratio in a feedforward controller

No major change was seen in selenium % recovery; the change was rather in the selenium chloride flow rate, at HCl:Water ratio of 1:100, the concertation of Se_2Cl_2 is at 0.99 g/L. On the other hand, at HCl: Water ratio of 100:1, the Se_2Cl_2 concertation is 0.65 g/L, but again the % recovery of the selenium at the end was the same, that might be due to several factors such as,

- Reaction rate: since a reaction rate of 99% is reached in the reactor, the pH effect on selenium recovery might not be noticeable in the simulation but will 100% be seen in a lab.
- Lignin dose: since an optimum lignin dosage of 0.9 g/L is set in the simulation, again, it contributes to the high selenium recovery.

The reasons mentioned above might explain why selenium recovery was not affected drastically when the pH was controlled, which might contradict the findings of researchers such as Roberts et al. (2015), where Gracililaria was used to adsorb selenite at 20 °C and a pH value of 4 was found to be the best for a recovery rate of 98% [1].

4.6 Biosorption kinetics

The obtained results from the kinetic studies performed on lignin for selenium adsorption are presented in Figure 4.13.

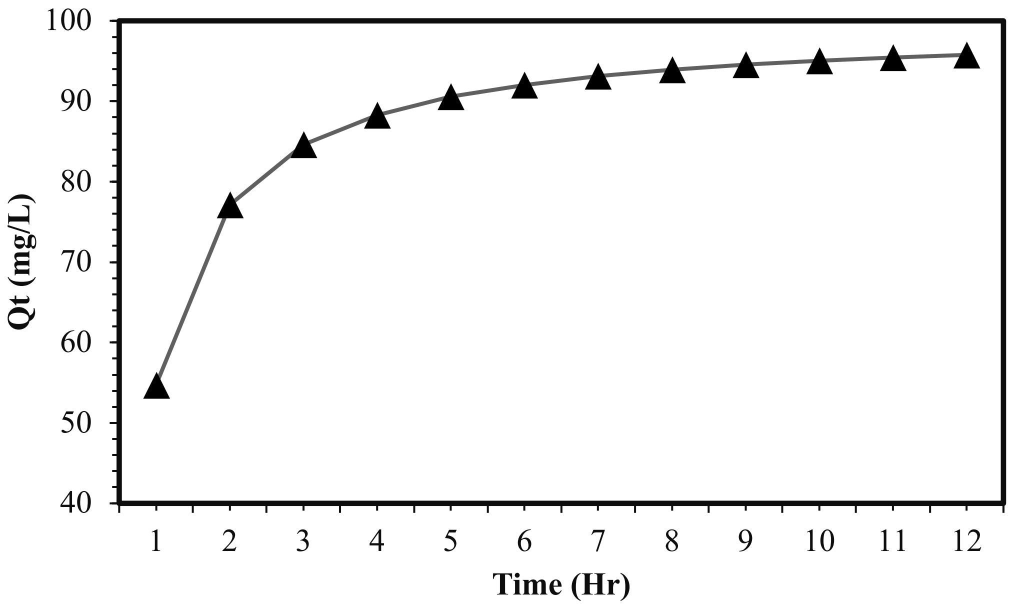

Figure 4. 13 The plotting of uptake versus time at Se starting concentration of 100 mg/L

It is clearly indicated that at 25 °C, the adsorption reaction is very good, where 99% of (100mg/L) selenium available in selenium monochloride solution are adsorbed in 12 hours.

Pseudo first order and Pseudo second order models were fitted and calculated on the results for selenium biosorption on lignin. According to pseudo first and second order kinetic models, Eqs. 4.1 and 4.2 are used for data analysis, respectively. By setting t=0 and t=t as boundary conditions for the equations along with $q_t=q_e$ and integrating the linear forms of Eqs. 4.1 and 4.2, Eqs. 4.3 and 4.4 are obtained respectively.

$$\frac{dq_t}{dt} = k_1(q_e - q_t) \qquad \textit{Eq 4. 1}$$

$$\frac{dq_t}{dt} = k_2(q_e - q_t)^2 \qquad \textit{Eq 4. 2}$$

$$log(q_e - q_t) = logq_e \frac{k_1}{2.303} t \ldots\ldots\ldots\ldots\ldots\ldots\ldots\ldots\ldots\ldots\ldots \textit{Eq 4. 3}$$

$$\frac{t}{q_t} = \frac{1}{k_2 {q_e}^2} + \frac{1}{q_e} t \ldots\ldots\ldots\ldots\ldots\ldots\ldots\ldots\ldots\ldots\ldots \textit{Eq 4. 4}$$

In these equations, the rate constants of pseudo fist order and second orders are represented by k_1 and k_2, and their unit is mg $ppm^{-1}h^{-1}$. By subjecting the experimental data to Eqs. 10 and 11, the different parameters for pseudo first and second order kinetic models were obtained and are summarized in Table 4.2. A sorption process operates via physisorption if the data fit pseudo first order kinetics which means that diffusion is the rate limiting step instead of the reactant concentration as with chemical reactions, if the data fit the pseudo second-order kinetics, on the other hand, then that means that the rate controlling factor is the chemical reaction which means that this is chemisorption. As mentioned earlier in Section 4.1, the only temperature that worked for this model was 25 °C. Also, the R^2 value of the pseudo second order reaction was closer to 1, which suggests that this is a chemisorption process.

Table 4. 2 Summary of pseudo-first order and pseudo-second-order kinetic parameters calculated for this reaction.

	Pseudo-first order kinetic model			**Pseudo-second order kinetic model**		
Temperature (K)	q_e^a	K_1 (h^{-1})	R^2	K_2 (mg ppm^{-1} h^{-1}) x 10^4	R^2	q_e^b
298	98.4	0.2229	0.9169	0.0217	0.998	99

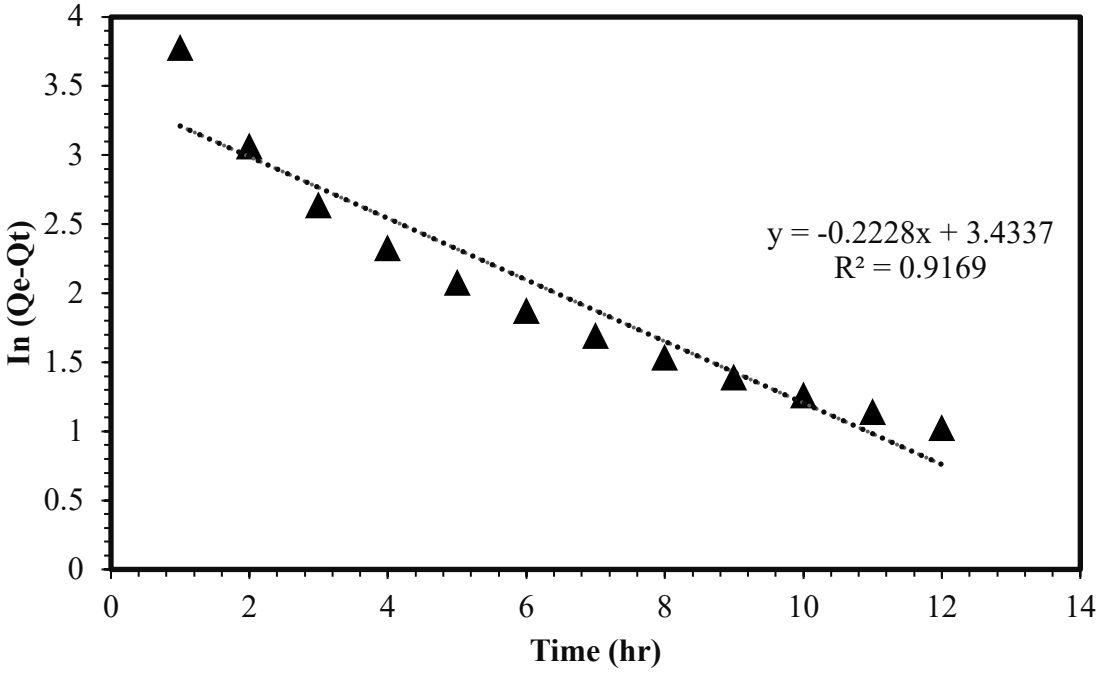

Figure 4. 14 Pseudo first order plot of selenium adsorption on lignin using METSIM

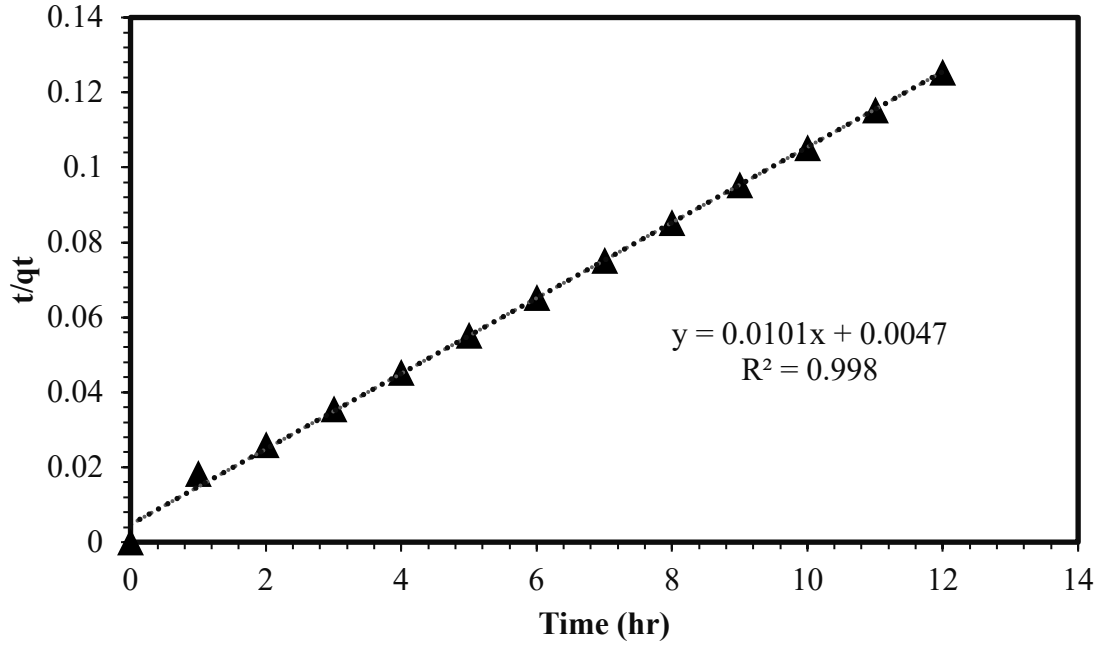

Figure 4. 15 Pseudo-second-order kinetics plots of selenium adsorption on lignin using METSIM. Initial selenium concentration of 100mg/L

Graphical data showing the pseudo-first-order linear fittings of Se adsorption by lignin can be observed in Figures 4.14 and 4.15, respectively. R^2 correlation coefficient fitting of the plots obtained from the trendline was examined to gain insight into whether kinetic behavior of lignin followed the pseudo-first or pseudo-second-order reaction. From Table 4.2, it can be observed that pseudo-first-order fitting R^2 value for the adsorption of Se was in the range of 0.9169 for the various temperatures, while Se adsorption fitting values on pseudo-second-order reaction kinetics was 0.998. These R^2 values signify that in comparison to the behavior exhibited towards Se adsorption on lignin is a better fit with the pseudo-second-order kinetic model. This information assumes that the rate-limiting step of adsorption is due to chemisorption from valency forces via electron exchange between lignin and selenium, which results in the best data correlation [53]. As summarized in Table 4.3, the calculated and experimentally observed adsorption capacity at equilibrium were very similar. Therefore, it can be concluded that the methods used to fit obtained experimental data to the pseudo-second-order model are reliable.

4.7 Activation energies of Se adsorption

Using rate constant K_2 calculated from the pseudo-second-order kinetic model, the energy of activation (E_A) for the adsorption of Se by lignin could be obtained using the Arrhenius equation described in Section 2.6. By evaluating the pseudo-second-order rate constant K_2 against temperature in kelvins (K), an Arrhenius plot was created, as displayed in Figure 4.16.

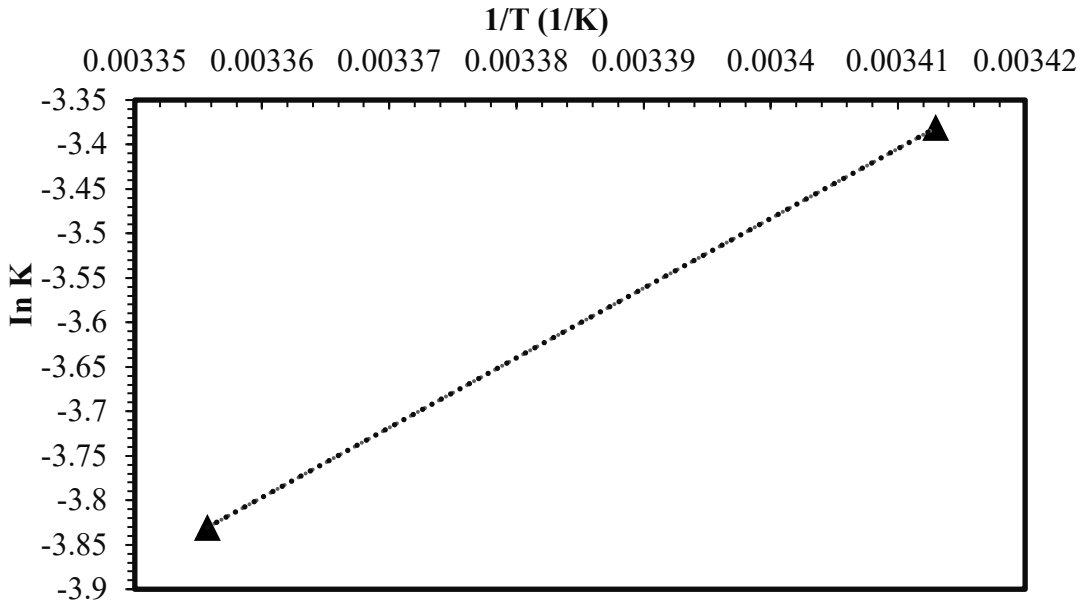

Figure 4. 16 Activation energy plot of K_2 value obtained from pseudo second order reaction against 1/T in kelvin

From the calculations, it was determined that the corresponding E_A for Se adsorption was 9.45 kJ/mol, and the calculated E_A value was 9.49 kJ/mol. As the E_A required to indicate physisorption is usually less than or equal to 4.3 kJ/mol, it can be deduced that the high activation energies expressed by lignin for selenium adsorption is due to chemisorption and that the adsorption is merely governed by chemical bonds and interactions beyond van der Waals forces

4.8 Biosorption isotherm models

This section details the application of both the Langmuir and Freundlich adsorption isotherms to the obtained simulation data of Se adsorption on lignin. The experimental adsorption data for the recovery of Se are displayed in Figure 4.17. From the information in the experimental plot, we can apply the linear forms of the Langmuir and Freundlich isotherm models which were expressed in Section 2.6 as Eqs 2.2 and 2.4', respectively. In doing so, we obtain the corresponding Eqs 4.5 and 4.6 for the linear Langmuir and Freundlich isotherm equations:

$$\frac{C_e}{q_e} = \frac{1}{q_{max}K_L} + \frac{1}{q_{max}} C_e \ldots\ldots\ldots\ldots\ldots\ldots\ldots\ldots\ldots\ldots\ldots\ldots\ldots\ldots \textit{Eq 4. 5}$$

$$log\ Q_e = log\ K_f + \frac{1}{n} log\ C_e \ \ldots\ldots\ldots\ldots\ldots\ldots\ldots\ldots\ldots\ldots\ldots\ldots\ldots \textit{Eq 4. 6}$$

by applying results from figure 4.17 to Eqs 4.5 and 4.6, experimental results can be fitted to the Langmuir and Freundlich models to create Figure 4.18 and Figure 4.19. A summary of calculated Langmuir parameters is also shown in Table 4.3.

Table 4. 3 Langmuir linear parameters calculated using excel and R^2 value.

Temperature (K)	**Langmuir equation**	**$q_{max}{}^a$**	**$q_{max}{}^b$**	**R^2**
298	y = 0.0143-2e-06x	98.4	50000	0.7217

Table 4.3 confirmed that the experimental and calculated values of q_{max} were very different; therefore, one can assume that the method applied to experimental data with the linear Langmuir equation is not reliable, as the deviation between the theoretical $q_{max}{}^a$ and the experimental $q_{max}{}^b$ is very high.

Similarly, as in the case of the fitting of kinetic rate equations, the adsorption behaviour of lignin in terms of adsorption isotherm can be predicted with the obtained R^2 correlation coefficients. The R^2 values found from the trendlines of both Langmuir and Freundlich isotherm are shown in Table 4.4.

Table 4. 4 R^2 coefficient of both the Langmuir and Freundlich isotherms.

Temperature (K)	**R^2 coefficient values**	
	Langmuir	Freundlich
298	0.727	0.9997

Based on the data obtained, R^2 coefficient of the Freundlich model was higher for Se adsorption than for the Langmuir model. This information suggests that Se adsorbs on the surface of lignin in a heterogeneous multilayer fashion.

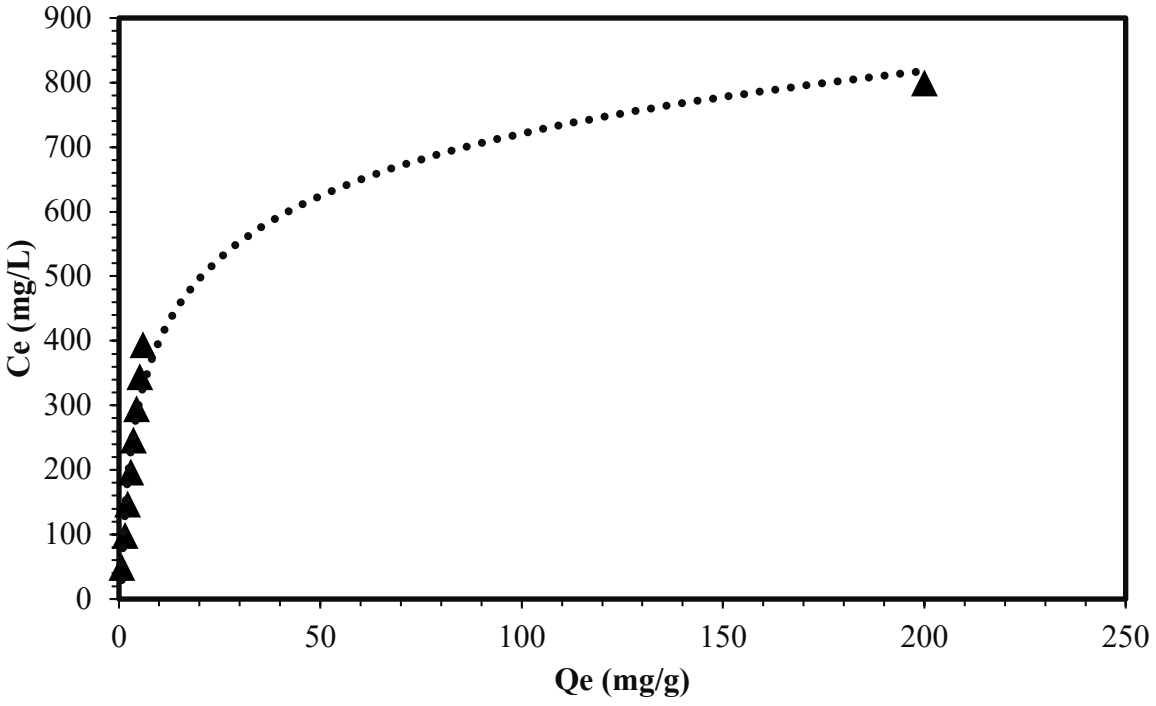

Figure 4. 17 Plot of uptake vs. initial selenium concentration of a range between 50 mg/L and 1000 mg/L

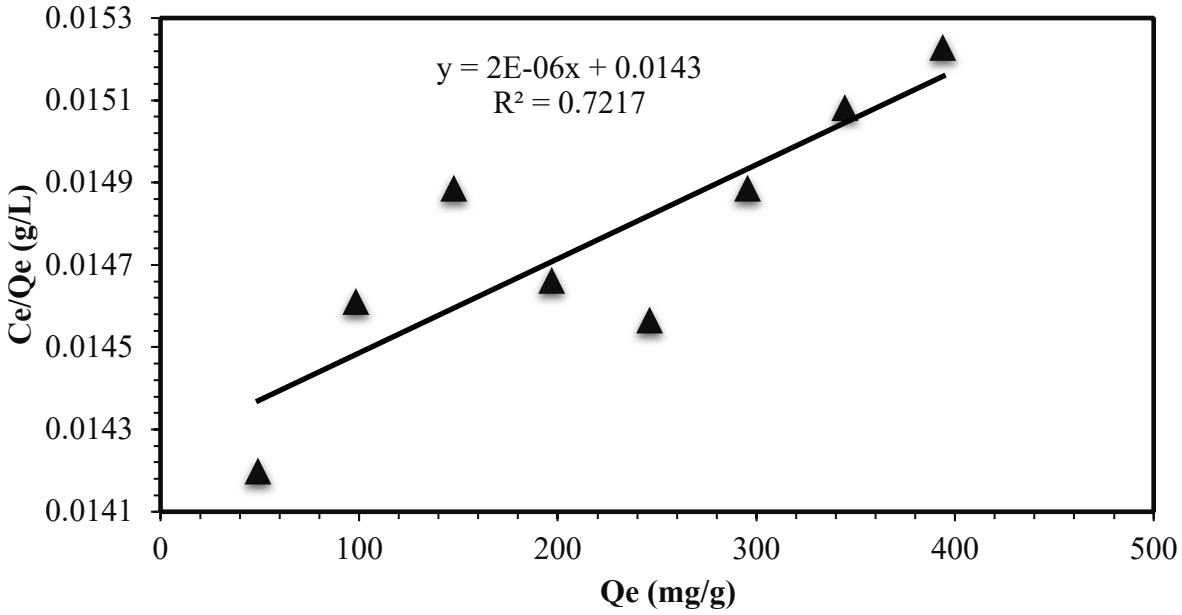

Figure 4. 18 Langmuir Isotherm plot of selenium adsorption on lignin along with the linear equations developed using Excel

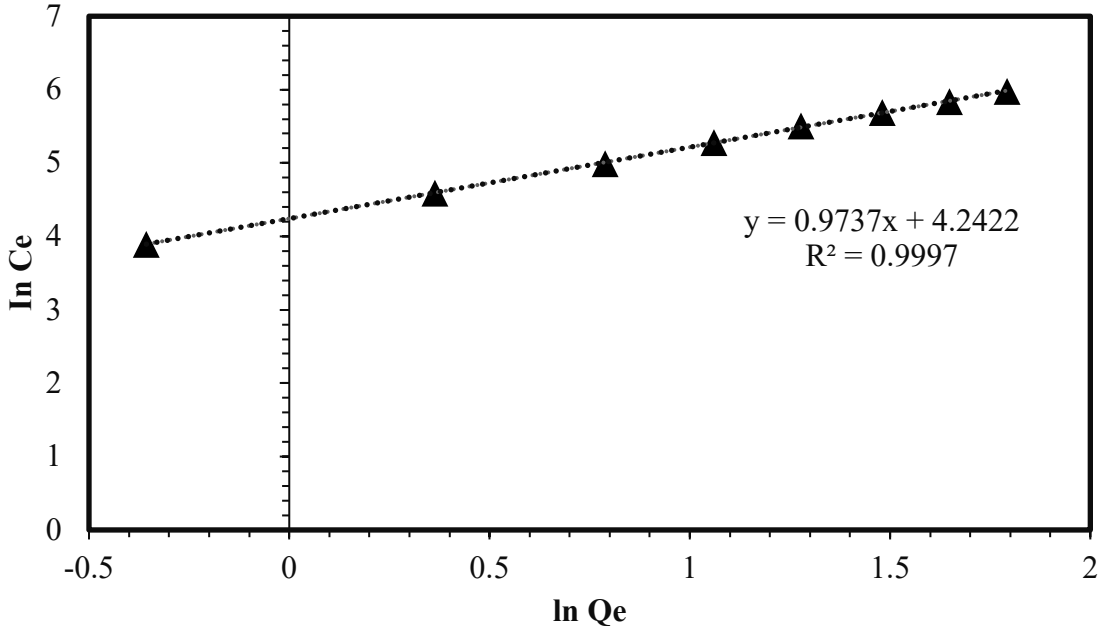

Figure 4. 19 Freundlich Isotherm plot of selenium adsorption on lignin along with the linear equations developed using Excel

4.9 Thermodynamic analysis of adsorption

During this research, it has been evident that the optimum and only operating temperature for this simulation is 25 °C, and other parameters such as residence time and lignin dosage were the main contributing factors to get 98.5% recovery. This phenomenon was further studied by conducting a study on the thermodynamic behaviours of the biosorbent. In this section, the changes in Gibb's free energy (ΔG°), enthalpy (ΔH°) and entropy (ΔS°) were calculated using Eq. 2.6 mentioned in Section 2.6. In addition, the following Eq. 4.7 was also used [63].

$$K_L = \frac{C_{Ae}}{C_e} \quad \text{Eq 4. 7}$$

Where K_L represents the equilibrium constant C_{Ae} is the metal ions concentration on adsorbent at equilibrium and C_e is the metal concentration remaining in solution at equilibrium. As both C_{Ae} and C_e are measuring in mg/L, K_L is unitless. It should be noted that calculations made in this thermodynamic analysis are based on assumptions that experimental conditions are in reference to the standard state. By plotting ln K_L against $1/T$ (where T represents temperature in kelvins) in what is known as a Van't Hoff plot, it is possible to calculate ΔH° and ΔS° by using Eq. 2.6 The obtained Van't Hoff linear plot and corresponding trendline equations are demonstrated in Fig 4.20.

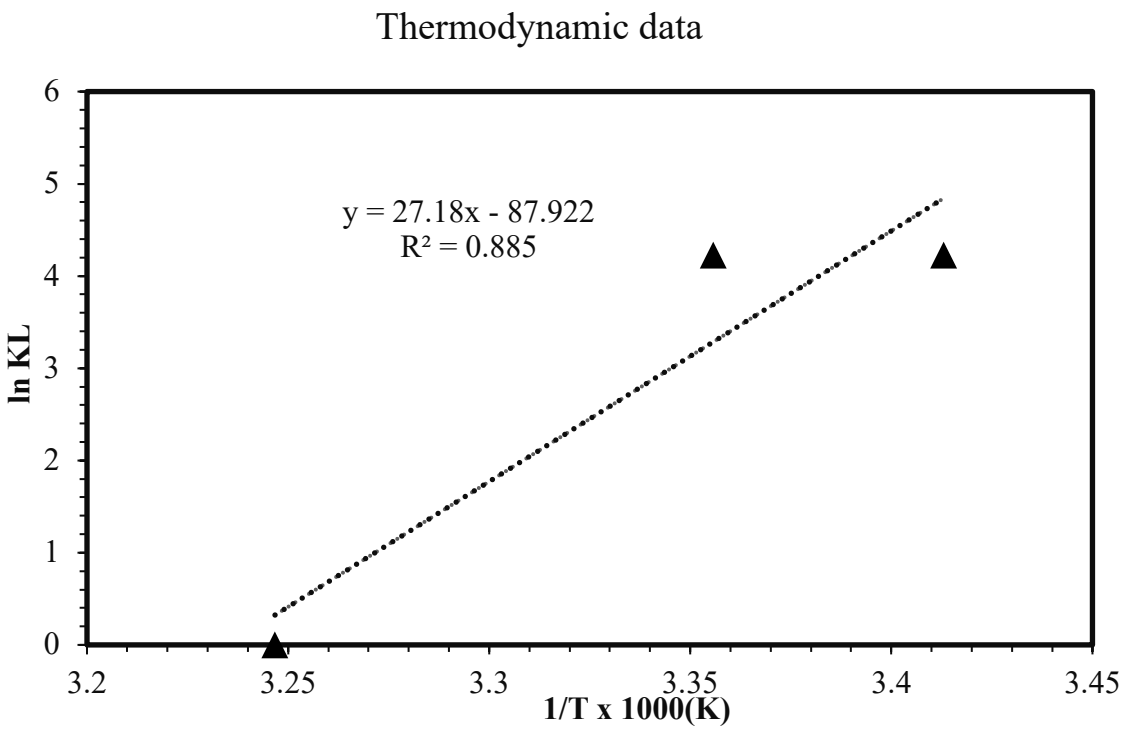

Figure 4. 20 Van't Hoff plot of temperature

Using the trendline generated from the plot for Se, thermodynamic parameters were calculated and summarized in Table 4.5. The obtained ΔG° was revealed to be negative for Se adsorption, indicating that the adsorption process is spontaneous in nature. Negative ΔS° signifies that the randomness of the system during the adsorption process decreases. This decrease in entropy may be due to the less amount of open space in solution as adsorption proceeds, thereby decreasing the number of configurations that residual metal ions can exist in the space. Finally, the negative ΔH° confirms the trend previously observed that increasing temperatures decreases adsorption efficiency, explaining that the adsorption for Se by lignin is an exothermic process.

Table 4. 5 Enthalpy, Entropy and Gibbs free energy of the adsorption reaction.

T (K)	K_L	ΔG° (kJ mol^{-1})	ΔS° (kJ mol^{-1} K^{-1})	ΔH° (J mol^{-1})	R^2
298	68.4	-10.48	-730.98	-225.97	0.885

4.10 Adsorption of other chloride forms

As mentioned in Section 3.9, there are 3 chloride forms of selenium; they are Se_2Cl_2, $SeCl_2$ and $SeCl_4$. In order to test if this model works or not, all three chloride forms have to be entered in the simulation separately.

Yen Ning Lee (2018) developed a novel biosorbent from wood bark by immobilizing it with di-thiooxamide. This biosorbent was able to recover platinum and palladium with a recovery rate of 99% and 97%, respectively. As a result, a metal coadsorption test was performed where 50% of selenium was recovered at 25 °C as shown in Figure 4.3 in Section 4.1. The concentration of all the elements present in the PLS are shown in Table 4.6 [69].

Table 4. 6 Elemental concentrations present in PLS solution [69]

Element	Concentration (ppm)	Element	Concentration (ppm)
Ag	25.7	Hg	0.7
Au	6.5	Ni	147
Pt	706.8	Pb	220
Pd	1816.5	Rh	4
Cd	21	Se	1976
Co	3	Sn	4
Cu	10405	Te	25
Fe	8221	Zn	573

As demonstrated in Table 4.6, the concentration of palladium and selenium are 1816.5 ppm and 1976 ppm, respectively, although the final selenium concentration present in the PLS after dilution is not mentioned, the platinum concentration is mentioned as 44 ppm after dilution, the selenium concentration can be assumed to be 47.8 ppm. By entering this concentration in the feedback controller available in METSIM, the selenium species available in the PLS can be found.

4.11 Selenium dichloride ($SeCl_2$)

To thoroughly compare the different forms of selenium, parameters like HCl concentration and lignin dosage were kept at 0.39M and 1g/L respectively, similar to the numbers that Se_2Cl_2 simulation was run at. Figures 4.21 and 4.22 show the set concentration of selenium (0.048 g/L). Recovery could be calculated by two methods, either by the solid selenium concentration present in the product stream as shown in Figures 4.23, which represents the amount of selenium that are adsorbed on the lignin or by the aqueous selenium concentration (g/L) in the product stream which represents the amount of selenium left in the solution after the adsorption reaction, as shown in Figure 4.24.

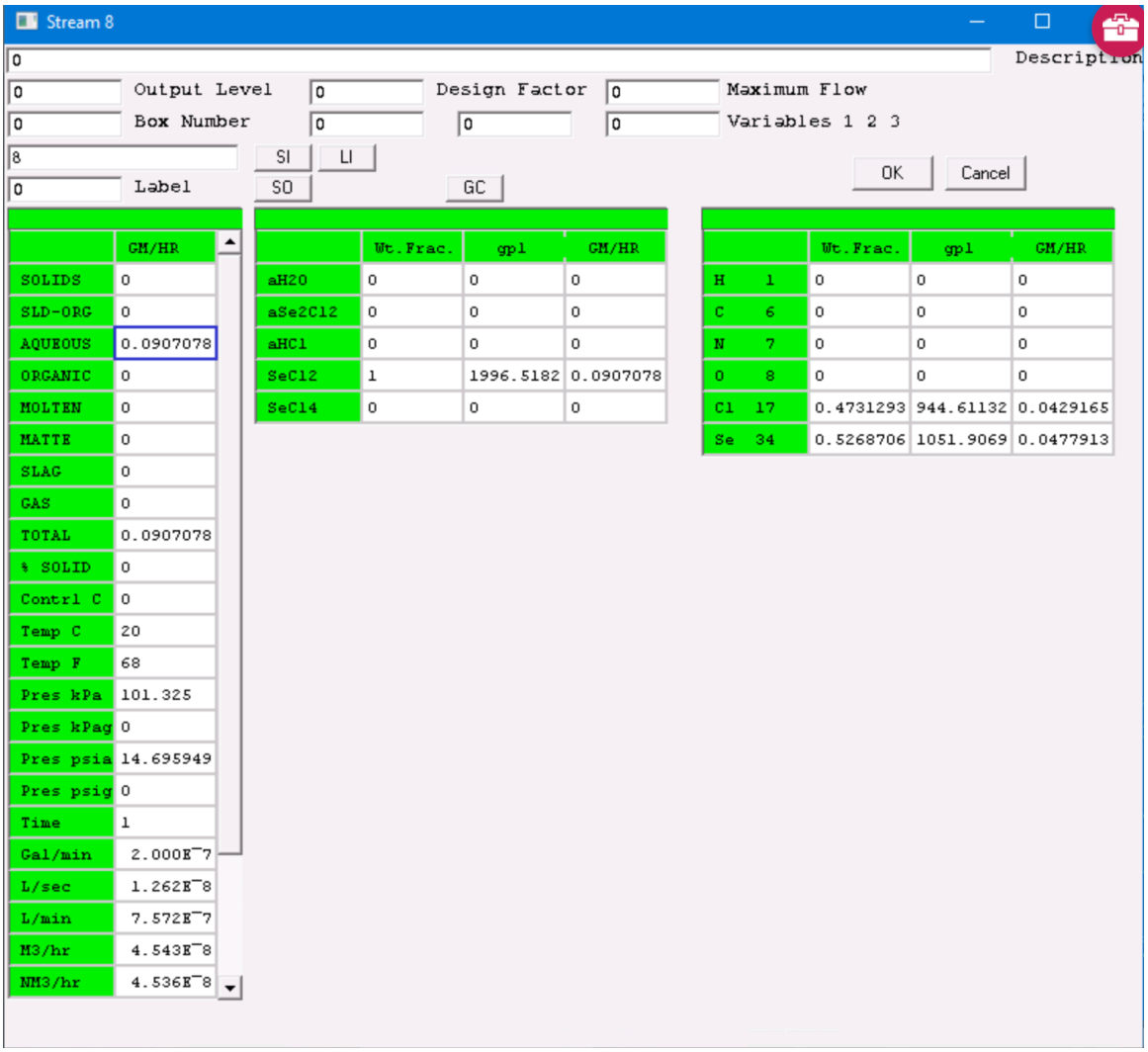

Figure 4. 21 Feed stream of $SeCl_2$ with a set concentration of 0.048, lignin concentration 1g/L

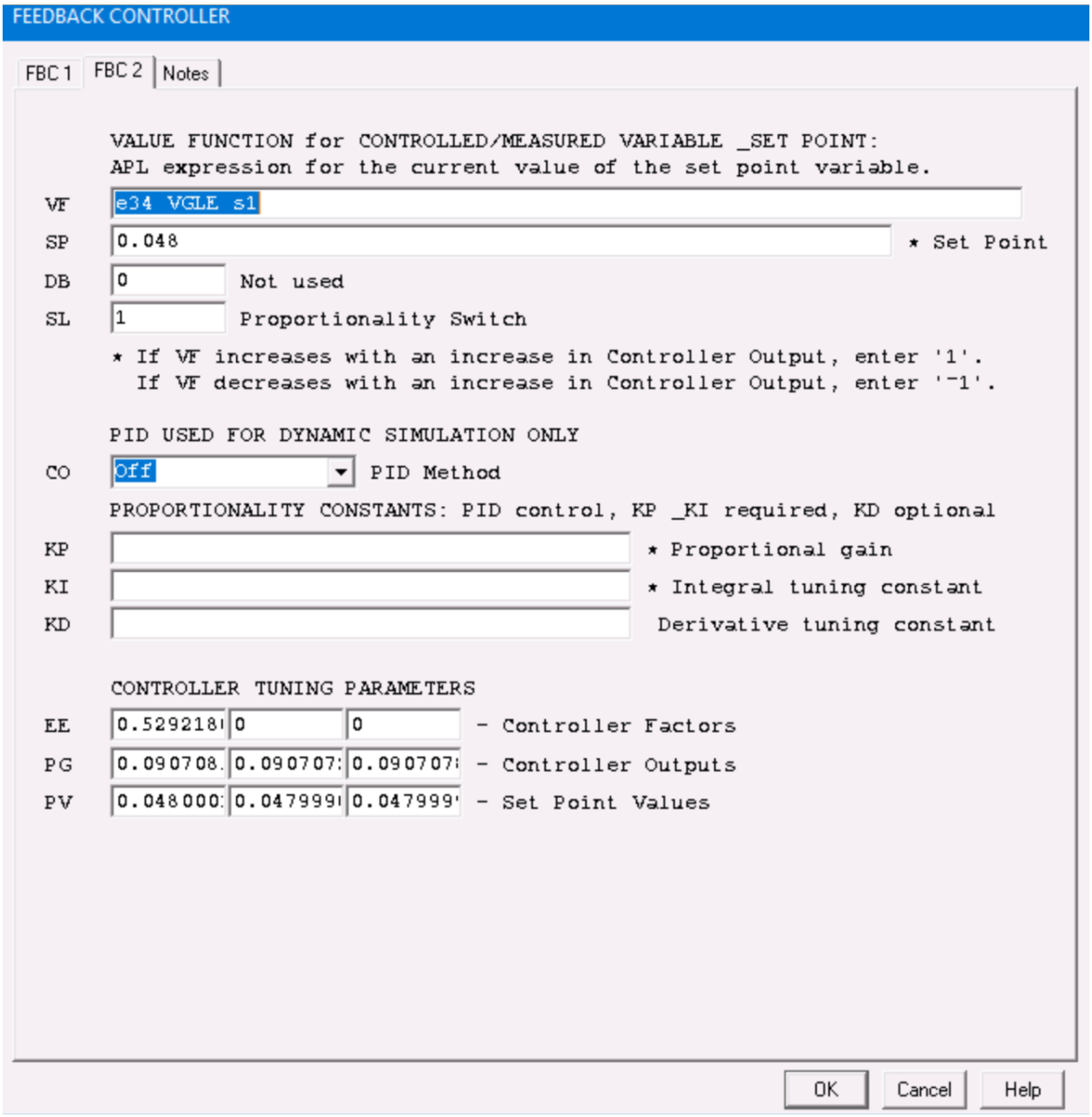

Figure 4. 22 Value function entered in feedback controller installed on stream 8 (feed stream) set point value at 0.048g/L

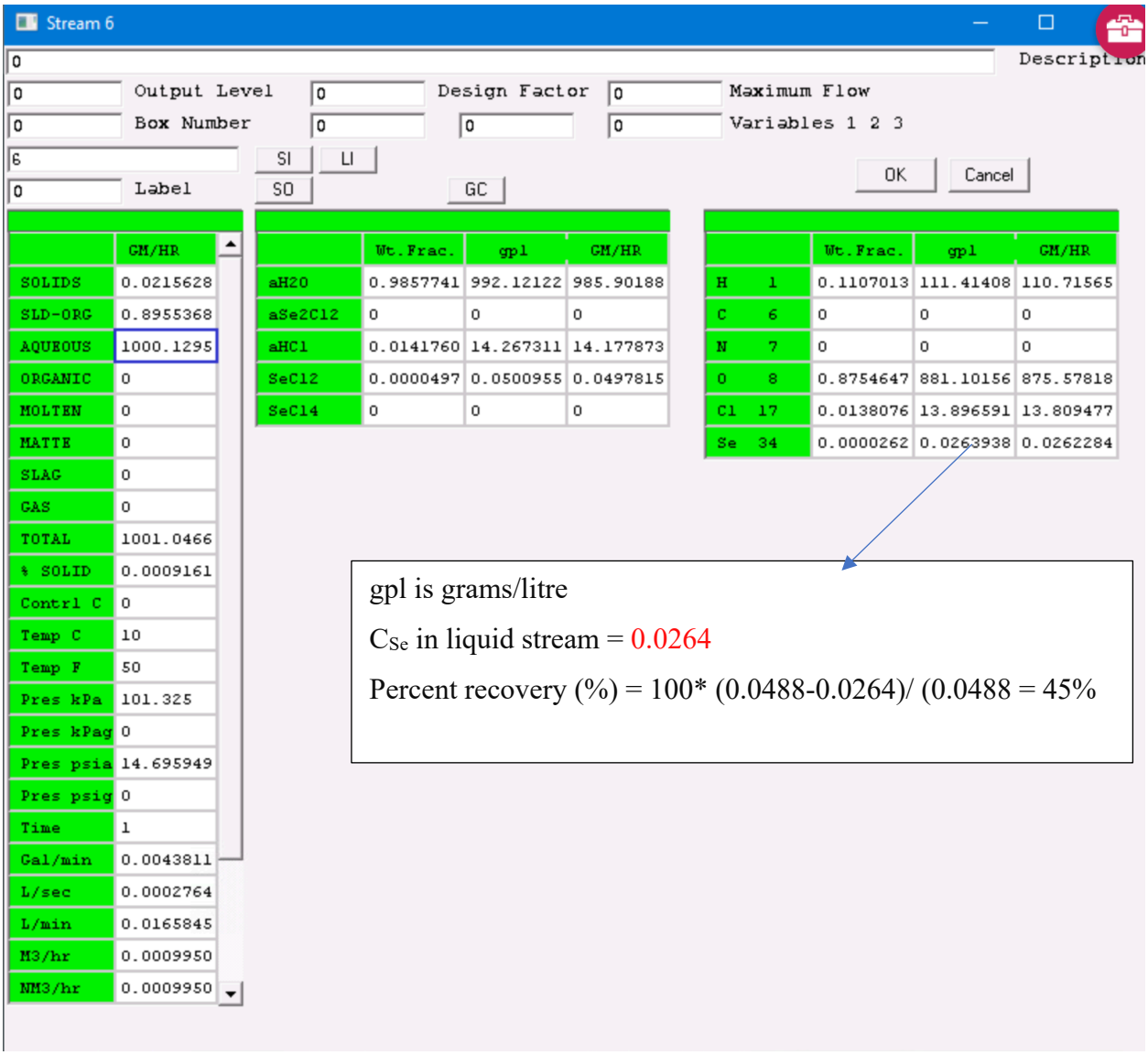

Figure 4. 23 Aqueous components in the product stream, where selenium left in the solution can be found in g/L

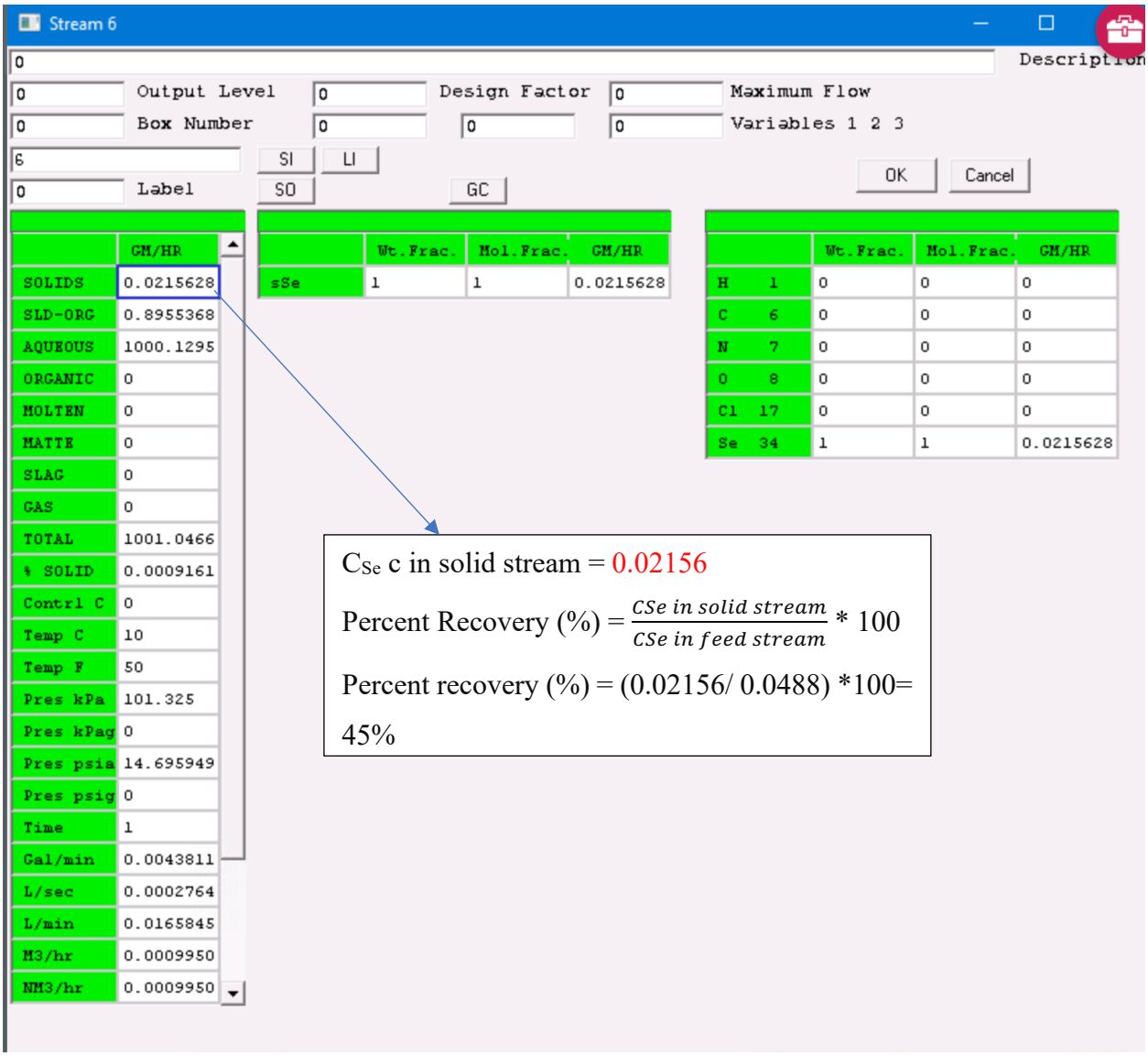

Figure 4. 24 Solid selenium recovered from the solution in the product stream (in a laboratory, it would be bonded to the lignin)

Since the selenium concentration in the product stream was 0.02156 g/L, the selenium recovery rate is 45% as shown in both Figures 4.23 and 4.24.

4.12 Selenium tetrachloride ($SeCl_4$)

Similar to the case of $SeCl_2$, the simulation was run at 0.048g/L of selenium as shown in Figure 4.27, while parameters such as HCl concentration and lignin dosage were unchanged. The chemical reaction between the selenium tetrachloride and lignin was entered as shown in Fig 4.25. Again, recovery could be calculated by either, dividing the solid selenium concentration present in the product stream by the original selenium concertation in the feed stream (0.048 g/L) as shown in Figures 4.28, which represents the amount of selenium that are adsorbed on the lignin, or, subtracting the original selenium concertation in the feed stream (0.048 g/L) by the aqueous selenium concentration (g/L) in the product stream which represents the amount of selenium left in the solution after the adsorption reaction and dividing the answer by the original selenium concertation in the feed stream (0.048 g/L), as shown in Figure 4.26.

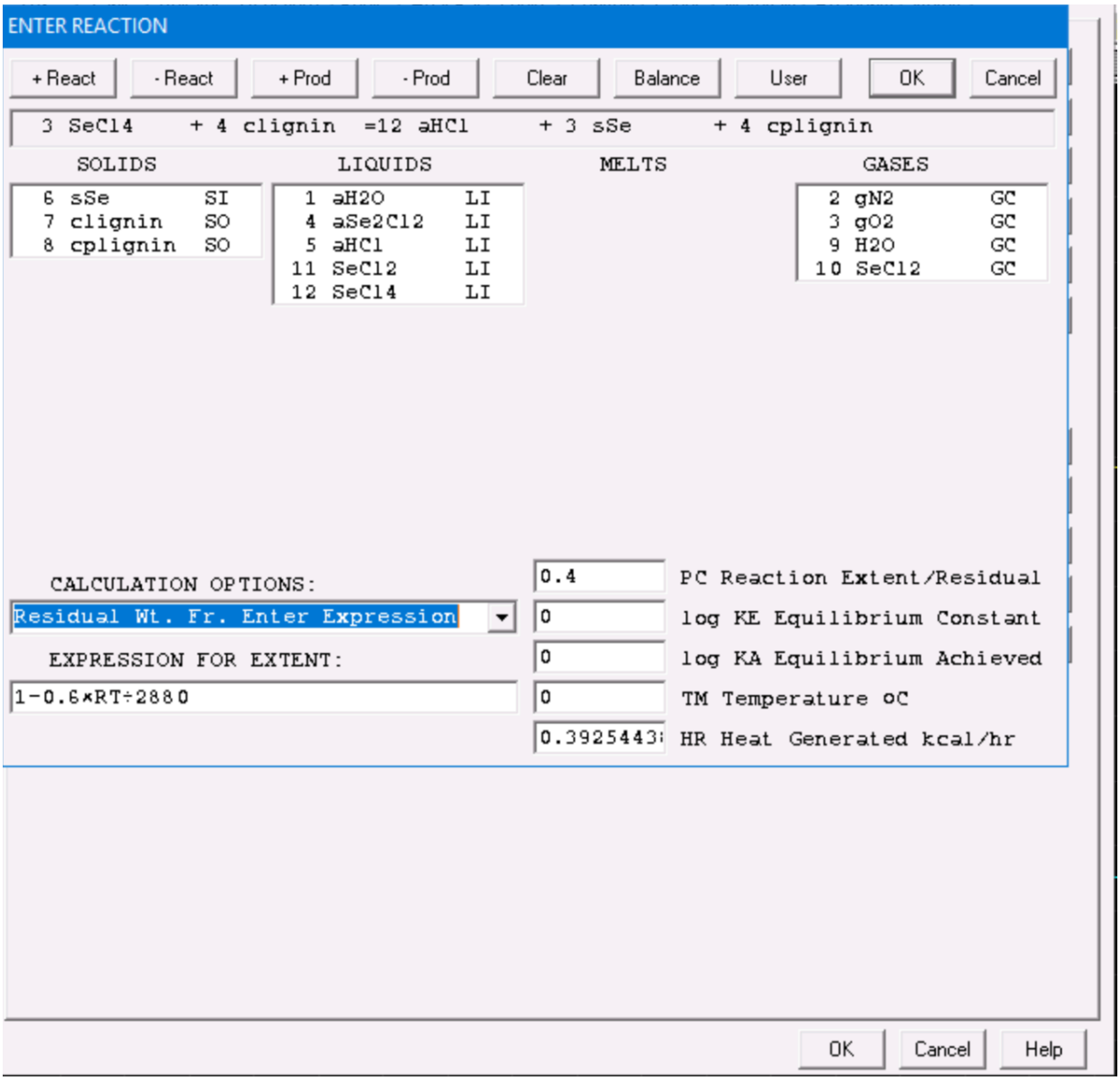

Figure 4. 25: Reaction and reaction rate entered in reactor

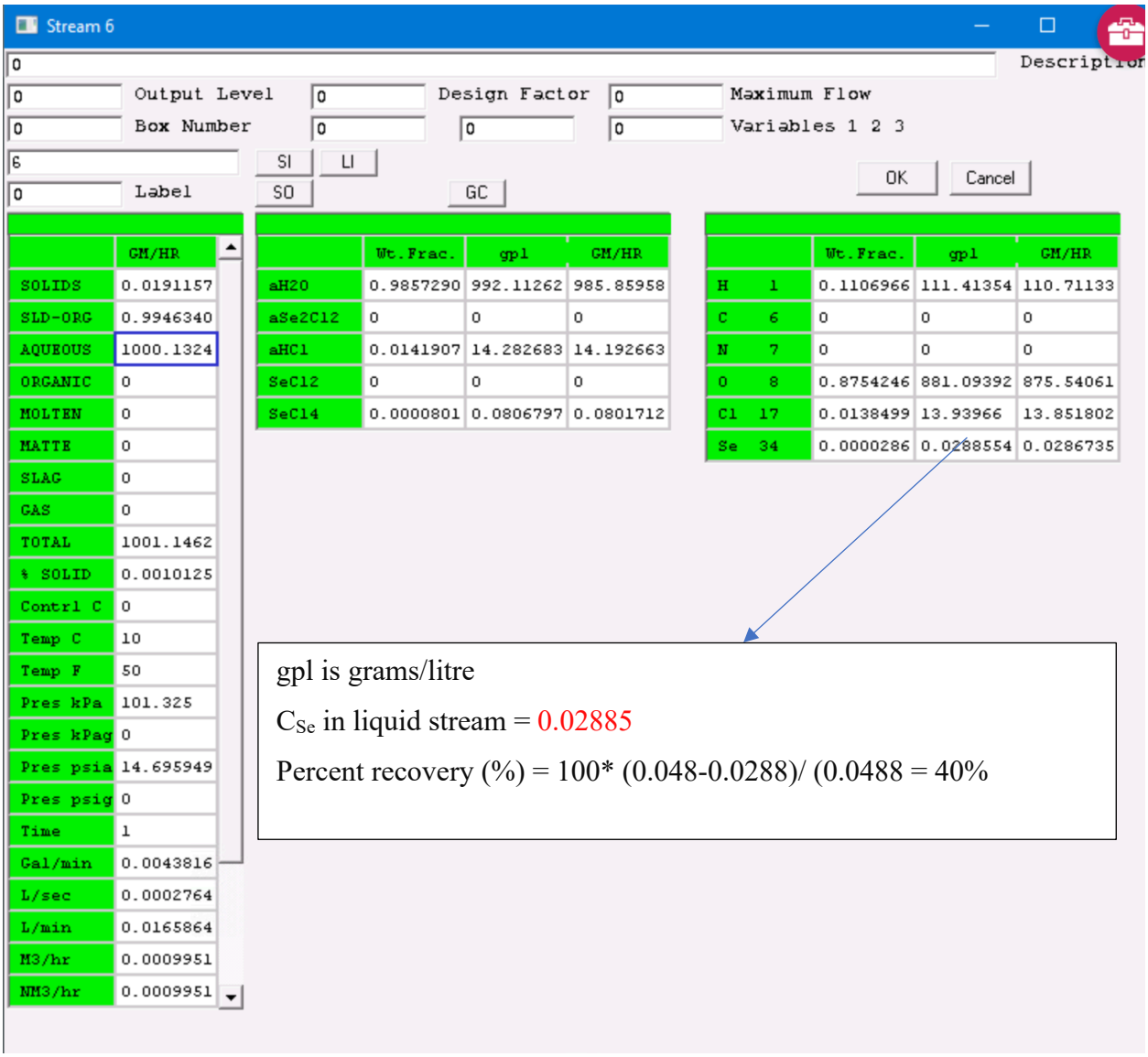

Figure 4. 26 Aqueous components in the product stream, where selenium left in the solution can be found in g/L

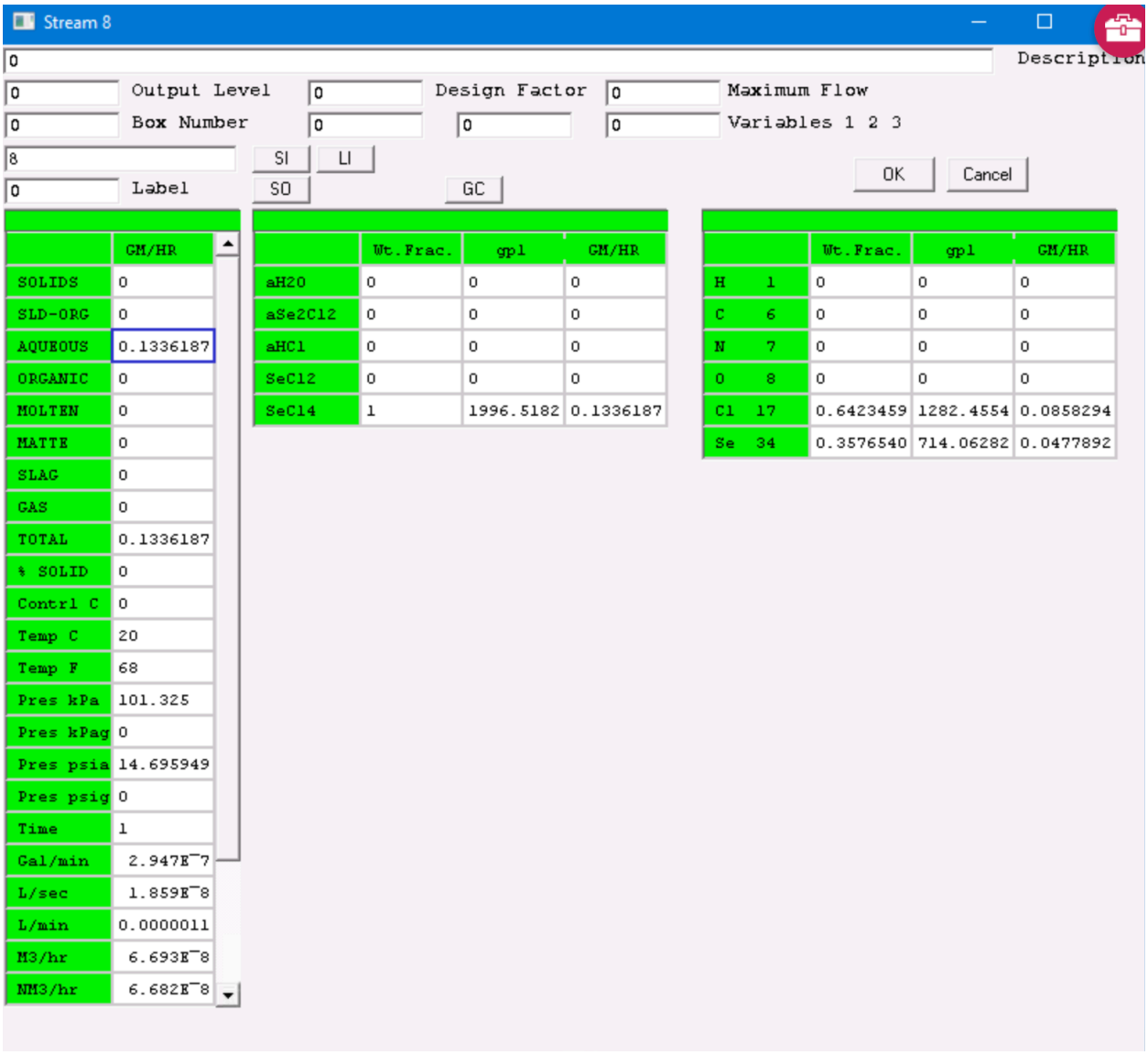

Figure 4. 27 Feed stream of $SeCl_4$ with a set concentration of 0.048, lignin concentration 1g/L

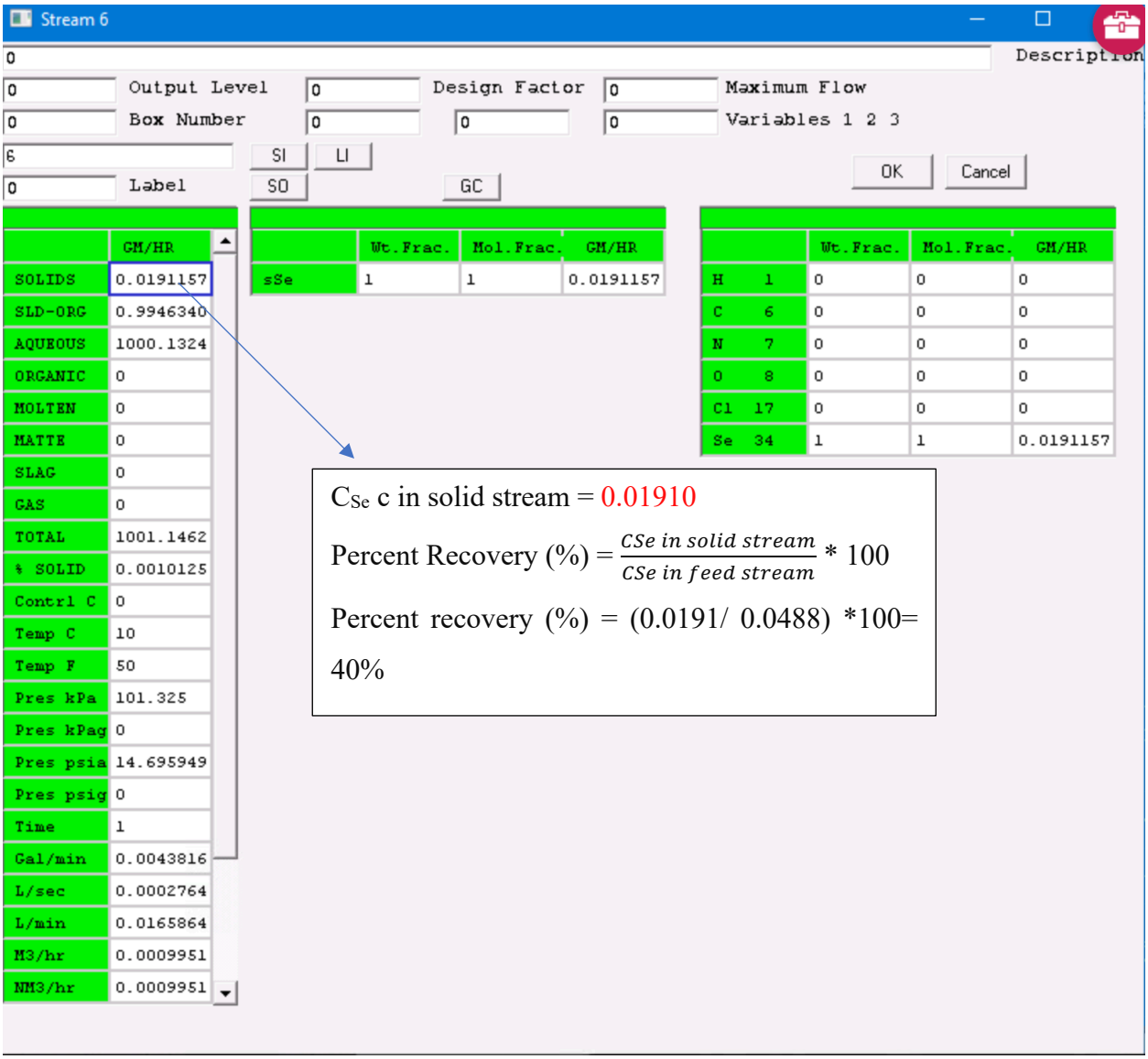

Figure 4. 28 Solid selenium recovered from the solution in the product stream (in a laboratory, it would be bonded to the lignin)

As shown in Figure 4.28, the final solid selenium concentration in the product stream is 0.0191157, which means that 1g/L of lignin can recover 40% of selenium from $SeCl_4$. From the data shown above in both Sections 4.11 and 4.12, we can conclude that the chloride from which was present in Yan Ning Lee's (2018) research work is $SeCl_2$ as it had a similar recovery rate under the same conditions.

CHAPTER 5: Conclusions and Recommendations

5.1 Summary of research and obtained results

The research work herein examined the adsorption process of selenium (Se) using lignin; METSIM was used as a simulation software due to its versatility and its ability to add new components with ease. The chloride species chosen for this research was selenium monochloride (Se_2Cl_2), the reason being that this is the form of selenium found in pregnant leach solution with the highest probability; also, since the ratio of selenium ions and chloride ions is 1:1, then the competition between the two ions would not be as high as in the case of $SeCl_2$ and $SeCl_4$.

Lignin was the only component not available on METSIM; to be able to add it, the thermodynamic data of lignin are crucial for METSIM to perform the mass and heat balances of this adsorption reaction. The enthalpy, Gibbs free energy and heat capacity were plotted in excel; a polynomial function was then created and then entered into the software.

Solid-liquid ratio experiments concluded that the optimal dosage for lignin was revealed to be at a 0.9 S/L ratio. Adsorption kinetic studies explained that the rate of adsorption followed a pseudo-second order model in the adsorption of Se. Adsorption isotherm studies also suggest that adsorption of Se follows a multilayer Freundlich model. The activation energy for the adsorption process of Se was calculated to be 9.49 kj/mol, signifying that the adsorption process progressed via chemisorption.

In terms of thermodynamics, the negative enthalpy change that lignin exhibits confirm that the adsorption process in the adsorption reaction is exothermic. Meaning that the increasing temperature reduces the efficiency of the adsorption process.

A negative change in Gibbs free energy suggests that the Se adsorption is spontaneous in nature. In accordance with the objectives established at the beginning of this thesis in Section 1.3, the present work achieved in the creation, experimentation, and the analysis of biosorbents and their effects in adsorbing Se from Se_2Cl_2:

1. A successful simulation was developed on METSIM for the adsorption of selenium on lignin
2. By altering different factors such as temperature, pH or adsorbent dosage, the efficiency of lignin was examined, and optimal conditions were found.
3. The fitting of lignin adsorption results in pseudo-first and pseudo-second order kinetic models, Langmuir and Freundlich adsorption isotherm models, and the subsequent determination of EA, $\Delta G°$, $\Delta H°$, and $\Delta S°$.
4. The model was proven to be efficient as it was able to achieve similar results to laboratory results.

Overall, this research work successfully developed an alternative clean method for the recovery of selenium which is potentially more cost-effective and environmentally friendly. The implications of the obtained results suggest that lignin coming from biomass, which is considered a waste product, may generate financial gain recuperated in the extraction of metal recycling industry by cost-effectively and efficiently extracting Se from Se_2Cl_2 using a studied component found in almost all plants; therefore, most biomass.

To prove that the simulation is comparable to real-life data, the simulation was run using the 3 different chloride forms of selenium Se_2Cl_2, $SeCl_2$, and $SeCl_4$. It was proven that the selenium chloride species that was present in Yen Ning Lees thesis was selenium dichloride ($SeCl_2$) since the recovery rate in her research work was 50% and the recovery rate using METSIM was 45% as opposed to 98.07% in the case of Se_2Cl_2, and 40% in the case of $SeCl_4$.

5.2 Challenges encountered in the present research

Although useful results were obtained from the research and an effective method was successfully developed, the present research work was not without difficulties. In this section, some challenges which were encountered during this research will be discussed.

The corona virus has impacted everyone. Governments all over the world have taken safety measures to prevent its spread; due to this current situation, the University of Saskatchewan has transitioned to online learning since March of 2020 and as a result, research work that requires to

be done in a laboratory was suspended. Simulation and computer modelling were the best option for most graduate students to be able to progress in their research work remotely.

The original proposal was about the biosorption of selenium from pregnant leach solution using different types of biomasses such as wood bark, wheat straw or canola mill. The idea was to treat those different biomasses with different chemical compounds such as ethylenimine and dithiooxamide and observe how efficient they would be on adsorbing elemental selenium. The pregnant leach solution was going to be provided by Asahi refining company, a mining company located in Ontario, but due to the heavy corona virus measures implemented by the Ontario government, it was very difficult to receive the solutions any time soon. For these reasons, the use of simulation software was the best option to proceed with this research work.

Also, the few research work done on thermodynamic data on different biomass made it very difficult to find the thermodynamic data of other chemical structures found in biomass such as cellulose or hemicellulose or even modify the already available structure with other chemicals.

The model building took the most time as there was almost no extensive simulation work done on metal recovery using biosorption which required more time to get everything right and be able to compare it to other studies done in the laboratory.

It has been acknowledged that the obtained adsorption efficiency for Se adsorption might not be 100% accurate since METSIM takes reaction rate into account, manipulating it to get the highest recovery might have affected the accuracy of other factors, as a result, higher or lower dosage of lignin might be needed in a real-life depiction of this study.

Due to the novel nature of the current research work in which Se were extracted from Se_2Cl_2, there were very few studies that were similar enough to make a direct comparison of results with. Additionally, lignin composition is different from one plant species to another. The lignin used in METSIM was theoretical. It was assumed to be pure, meaning the impurity profile of real plant species might affect the recovery due to interference between impurities or other components.

5.3 Recommendations for future works

For further studies regarding lignin, the exact lignin content present in the biomass should be observed and recorded in terms of percentage. This testing will help understand whether lignin is the only significant component in adsorption or not.

To determine whether the biosorbent will have real potential application on an industrial scale, physical research should be done on the desorption and recycling of lignin should be performed. Furthermore, the study of selenium yield obtained from start to finish of the adsorption process should be conducted.

Studies on different selenium species could be conducted to understand the real effect of other ions on lignin efficiency during adsorption; also, the two most common liquids found in pregnant leach solution (from metal refineries) are chlorides and nitrites, an extensive study on nitrite forms could help understand how effective lignin would be as an adsorbent. In addition to the suggested work, it is advisable that a feasibility study and techno-economic analysis could be conducted to gain insight on whether the novel adsorbent is economically sound or not.

Finally, scale-up tests should be conducted on this process to understand whether lignin would be suitable as an adsorbent at an industrial scale or not.

REFERENCES

[1] D. A. Roberts, N. A. Paul, S. A. Dworjanyn, Y. Hu, M. I. Bird, and R. Denys, "Gracilaria waste biomass (sampah rumput laut) as a bioresource for selenium biosorption," J. Appl. Phycol., vol. 27, no. 1, pp. 611–620, Feb. 2015, doi: 10.1007/s10811-014-0346-y.

[2] S. Etteieb, S. Magdouli, M. Zolfaghari, and S. Brar, "Monitoring and analysis of selenium as an emerging contaminant in mining industry: A critical review," Sci. Total Environ., vol. 698, p. 134339, Jan. 2020, doi: 10.1016/j.scitotenv.2019.134339.

[3] D. Plano, E. Lizarraga, M. Font, J. A. Palop, and C. Sanmartín, "Thermal stability and decomposition of sulphur and selenium compounds," J. Therm. Anal. Calorim., vol. 98, no. 2, pp. 559–566, Nov. 2009, doi: 10.1007/s10973-009-0291-1.

[4] Brummer, Fara A., Laura Gow-Hogge, Chad Mueller, Gene Pirelli, and Gerd Bobe. "Short Communication: Mineral Assessment of Rangeland-Managed Beef Cows in the High Desert Region of Oregon." *Applied Animal Science* 35, no. 6 (December 2019): 577–85. https://doi.org/10.15232/aas.2019-01871.

[5] S. Santos, G. Ungureanu, R. Boaventura, and C. Botelho, "Selenium contaminated waters: An overview of analytical methods, treatment options and recent advances in sorption methods," Sci. Total Environ., vol. 521–522, pp. 246–260, Jul. 2015, doi: 10.1016/j.scitotenv.2015.03.107.

[6] S. C. Gad and T. Pham, "Selenium," in Encyclopedia of Toxicology, Elsevier, 2014, pp. 232–235. doi: 10.1016/B978-0-12-386454-3.00926-X.

[7] J. Stefaniak, A. Dutta, B. Verbinnen, M. Shakya, and E. R. Rene, "Selenium removal from mining and process wastewater: a systematic review of available technologies," J. Water Supply Res. Technol.-Aqua, vol. 67, no. 8, pp. 903–918, Dec. 2018, doi: 10.2166/aqua.2018.109.

[8] M. Reinsel, "Selenium removal technologies: A Review," 2016. Availabe at: https://www.wateronline.com/doc/industrial-water-treatment-for-inorganic-contaminants-emerging-technologies-0001

[9] North American Metals Council, “Review of Available Technologies for the Removal of Selenium from Water,” Jun. 2010. https://www.namc.org/docs/00062756.PDF

[10] L. Fishbein, “Environmental selenium and its significance,” Fundam. Appl. Toxicol., vol. 3, no. 5, pp. 411–419, Sep. 1983, doi: 10.1016/S0272-0590(83)80014-1.

[11] A. D. Lemly, “Aquatic selenium pollution is a global environmental safety issue,” Ecotoxicol. Environ. Saf., vol. 59, no. 1, pp. 44–56, Sep. 2004, doi: 10.1016/S0147-6513(03)00095-2.

[12] A. Khamkhash, V. Srivastava, T. Ghosh, G. Akdogan, R. Ganguli, and S. Aggarwal, “Mining-Related Selenium Contamination in Alaska, and the State of Current Knowledge,” Minerals, vol. 7, no. 3, p. 46, Mar. 2017, doi: 10.3390/min7030046.

[13] George Desborough1, Ed DeWitt1, Jeff Jones2, Alan Meier1and Gregory Meeker1, “Preliminary mineralogical and chemical studies related to the potential mobility of selenium and associated elements in phosphoria formation strata, southeastern Idaho.,” Open-File Rep. 99-129, p. 11, 1999.

[14] J. Cui and L. Zhang, “Metallurgical recovery of metals from electronic waste: A review,” J. Hazard. Mater., vol. 158, no. 2–3, pp. 228–256, Oct. 2008, doi: 10.1016/j.jhazmat.2008.02.001.

[15] S. W. Won, P. Kotte, W. Wei, A. Lim, and Y.-S. Yun, “Biosorbents for recovery of precious metals,” Bioresour.Technology., vol. 160, pp. 203–212, May 2014, doi: 10.1016/j.biortech.2014.01.121.

[16] G. Hilson and A. J. Monhemius, “Alternatives to cyanide in the gold mining industry: what prospects for the future?,” J. Clean. Prod., vol. 14, no. 12–13, pp. 1158–1167, Jan. 2006, doi: 10.1016/j.jclepro.2004.09.005.

[17] A. Işıldar, J. van de Vossenberg, E. R. Rene, E. D. van Hullebusch, and P. N. L. Lens, “Two-step bioleaching of copper and gold from discarded printed circuit boards (PCB),” Waste Manag., vol. 57, pp. 149–157, Nov. 2016, doi: 10.1016/j.wasman.2015.11.033.

[18] F. Fu and Q. Wang, “Removal of heavy metal ions from wastewaters: A review,” J. Environ. Manage., vol. 92, no. 3, pp. 407–418, Mar. 2011, doi: 10.1016/j.jenvman.2010.11.011.

[19] L. C. Staicu, E. D. van Hullebusch, M. A. Oturan, C. J. Ackerson, and P. N. L. Lens, "Removal of colloidal biogenic selenium from wastewater," Chemosphere, vol. 125, pp. 130–138, Apr. 2015, doi: 10.1016/j.chemosphere.2014.12.018.

[20] A. W. Cantafio, K. D. Hagen, G. E. Lewis, T. L. Bledsoe, K. M. Nunan, and J. M. Macy, "Pilot-Scale Selenium Bioremediation of San Joaquin Drainage Water with Thauera selenatis," Appl. Environ. Microbiol., vol. 62, no. 9, pp. 3298–3303, Sep. 1996, doi: 10.1128/AEM.62.9.3298-3303.1996.

[21] J. H. Lee, "An overview of phytoremediation as a potentially promising technology for environmental pollution control," Biotechnology. Bioprocess Eng., vol. 18, no. 3, pp. 431–439, Jun. 2013, doi: 10.1007/s12257-013-0193-8.

[22] Ismail, Ibrahim & Moustafa, Tarek & Sulaymon, Abbas & Abbas, Salman, "Biosorption of Heavy Metals: A Review," journal of Chemical Science and Technology, vol. 3. 74., 2014.

[23] T. V. Silas, "Biosorption Kinetics of Heavy Metals from Fertilizer Industrial Wastewater Using Groundnut Husk Powder as an Adsorbent," J. Appl. Biotechnology. Bioengineering., vol. 2, no. 6, Apr. 2017, doi: 10.15406/jabb.2017.02.00049.

[24] T. V. Ramachandra, A. N, and K. RD, "Biosorption: Techniques and Mechanisms," CES Tech. Rep. 110, Jan. 2005.

[25] A. H. Berger and A. S. Bhown, "Comparing physisorption and chemisorption solid sorbents for use separating CO2 from flue gas using temperature swing adsorption," Energy Procedia, vol. 4, pp. 562–567, 2011, doi: 10.1016/j.egypro.2011.01.089.

[26] Ahalya, N & Ramachandra, T V & Kanamadi, R, "Biosorption of Heavy Metals," esearch Journal Of Chemistry And Environment., no. 7, 2003.

[27] J. Heinimö and M. Junginger, "Production and trading of biomass for energy – An overview of the global status," Biomass Bioenergy, vol. 33, no. 9, pp. 1310–1320, Sep. 2009, doi: 10.1016/j.biombioe.2009.05.017.

[28] S. Quideau, D. Deffieux, C. Douat-Casassus, and L. Pouységu, "Plant Polyphenols: Chemical Properties, Biological Activities, and Synthesis," Angew. Chem. Int. Ed., vol. 50, no. 3, pp. 586–621, Jan. 2011, doi: 10.1002/anie.201000044.

[29] C. Wang, “Selenium minerals and the recovery of selenium from copper refinery anode slimes,” J. South. Afr. Inst. Min. Metall., vol. 116, no. 6, pp. 593–600, 2016, doi: 10.17159/2411-9717/2016/v116n6a16.

[30] R. Vanholme, B. Demedts, K. Morreel, J. Ralph, and W. Boerjan, “Lignin Biosynthesis and Structure,” Plant Physiol., vol. 153, no. 3, pp. 895–905, Jul. 2010, doi: 10.1104/pp.110.155119.

[31] E. Sjöström, Wood chemistry: fundamentals and applications. New York: Academic Press, 1981.

[32] W. Boerjan, J. Ralph, and M. Baucher, “Lignin Biosynthesis,” Annual. Review. Plant Biol., vol. 54, no. 1, pp. 519–546, Jun. 2003, doi: 10.1146/annurev.arplant.54.031902.134938.

[33] K. Arms and P. S. Camp, Biology, 4th ed. Fort Worth: Saunders College Pub, 1995.

[34] O. V. Voitkevich, G. J. Kabo, A. V. Blokhin, Y. U. Paulechka, and M. V. Shishonok, “Thermodynamic Properties of Plant Biomass Components. Heat Capacity, Combustion Energy, and Gasification Equilibria of Lignin,” J. Chem. Eng. Data, vol. 57, no. 7, pp. 1903–1909, Jul. 2012, doi: 10.1021/je2012814.

[35] H. Erdtman, “Lignins: Occurrence, formation, structure and reactions," Eds. K. V. Sarkanen and C. H. Ludwig, John Wiley & Sons, Inc., New York, 1971.

[36] Ullmann’s Encyclopedia of Industrial Chemistry: Electronic Release. CD. Weinheim: Wiley-vch, 2003.

[37] C. J. Biermann, Essentials of pulping and papermaking. San Diego: Academic Press, 1993.

[38] A. Klash, E. Ncube, B. du Toit, and M. Meincken, “Determination of the cellulose and lignin content on wood fibre surfaces of eucalypts as a function of genotype and site,” Eur. J. For. Res., vol. 129, no. 4, pp. 741–748, Jul. 2010, doi: 10.1007/s10342-010-0380-5.

[39] N. Terry, A. M. Zayed, M. P. de Souza, and A. S. Tarun, “Selenium in higher plants,” Annu. Rev. Plant Physiol. Plant Mol. Biol., vol. 51, no. 1, pp. 401–432, Jun. 2000, doi: 10.1146/annurev.arplant.51.1.401.

[40] G. L. Dilworth and R. S. Bandurski, “Activation of selenate by adenosine 5′-triphosphate sulphurylase from Saccharomyces cerevisiae,” Biochem. J., vol. 163, no. 3, pp. 521–529, Jun. 1977, doi: 10.1042/bj1630521.

[41] Åke Olin, Bengt Nolang, Evgeniy G. Osadchill "Chemical thermodynamics of selenium," OECD Nucl. Energy Agency NEA, vol. 7, 2004, [Online]. Available: https://www.oecd-nea.org/jcms/pl_37421/chemical-thermodynamics-of-selenium?details=true

[42] J. E. House, Inorganic chemistry, 2. ed. Amsterdam: Elsevier [u.a.], 2013.

[43] Greenwood, N N, and A Earnshaw. *Chemistry of the Elements*. Oxford: Butterworth-Heinemann, 1997.

[44] J. Saghaei, A. Fallahzadeh, and T. Saghaei, "Vapor treatment as a new method for photocurrent enhancement of UV photodetectors based on ZnO nanorods," Sens. Actuators Phys., vol. 247, pp. 150–155, Aug. 2016, doi: 10.1016/j.sna.2016.05.050.

[45] Johnson C.M. (1976) Selenium in the environment. In: Gunther F.A., Hylin J.W., Westlake W.E. (eds) Residue Reviews. Reviews of Environmental Contamination and Toxicology (Continuation of Residue Reviews), vol 62. Springer, New York, NY. https://doi.org/10.1007/978-1-4613-9404-4_10

[46] S. Potash and S. Rozen, "A General and Efficient Method To Convert Selenides into Selenones by Using HOF·CH $_3$ CN: A General and Efficient Method To Convert Selenides into Selenones," Eur. J. Org. Chem., vol. 2013, no. 25, pp. 5574–5579, Sep. 2013, doi: 10.1002/ejoc.201300694.

[47] G. Erker, R. Hock, C. Krüger, S. Werner, F.-G. Klärner, and U. Artschwager-Perl, "Synthesis and Cycloadditions of Monomeric Selenobenzophenone," Angew. Chem. Int. Ed. Engl., vol. 29, no. 9, pp. 1067–1068, Sep. 1990, doi: 10.1002/anie.199010671.

[48] N. Das, "Recovery of precious metals through biosorption — A review," Hydrometallurgy, vol. 103, no. 1–4, pp. 180–189, Jun. 2010, doi: 10.1016/j.hydromet.2010.03.016.

[49] J. R. Dodson et al., "Bio-derived materials as a green route for precious & critical metal recovery and re-use," Green Chem., vol. 17, no. 4, pp. 1951–1965, 2015, doi: 10.1039/C4GC02483D.

[50] M. Rovira et al., "Sorption of selenium(IV) and selenium(VI) onto natural iron oxides: Goethite and hematite," J. Hazard. Mater., vol. 150, no. 2, pp. 279–284, Jan. 2008, doi: 10.1016/j.jhazmat.2007.04.098.

[51] J. He and J. P. Chen, “A comprehensive review on biosorption of heavy metals by algal biomass: Materials, performances, chemistry, and modeling simulation tools,” Bioresour. Technol., vol. 160, pp. 67–78, May 2014, doi: 10.1016/j.biortech.2014.01.068.

[52] M. Tuzen and A. Sarı, “Biosorption of selenium from aqueous solution by green algae (Cladophora hutchinsiae) biomass: Equilibrium, thermodynamic and kinetic studies,” Chem. Eng. J., vol. 158, no. 2, pp. 200–206, Apr. 2010, doi: 10.1016/j.cej.2009.12.041.

[53] K. Nettem and A. S. Almusallam, “Equilibrium, Kinetic, and Thermodynamic Studies on the Biosorption of Selenium (IV) Ions onto Ganoderma Lucidum Biomass,” Sep. Sci. Technol., vol. 48, no. 15, pp. 2293–2301, Oct. 2013, doi: 10.1080/01496395.2013.791318.

[54] H. Khakpour, H. Younesi, and M. Mohammadhosseini, “Two-stage biosorption of selenium from aqueous solution using dried biomass of the baker’s yeast Saccharomyces cerevisiae,” J. Environ. Chem. Eng., vol. 2, no. 1, pp. 532–542, Mar. 2014, doi: 10.1016/j.jece.2013.10.010.

[55] S. H. Hasan, D. Ranjan, and M. Talat, “Agro-industrial waste ‘wheat bran’ for the biosorptive remediation of selenium through continuous up-flow fixed-bed column,” J. Hazard. Mater., vol. 181, no. 1–3, pp. 1134–1142, Sep. 2010, doi: 10.1016/j.jhazmat.2010.05.133.

[56] L. Lortie, W. D. Gould, S. Rajan, R. G. L. McCready, and K.-J. Cheng, “Reduction of Selenate and Selenite to Elemental Selenium by a Pseudomonas stutzeri Isolate,” Appl. Environ. Microbiol., vol. 58, no. 12, pp. 4042–4044, 1992, doi: 10.1128/AEM.58.12.4042-4044.1992.

[57] A. Tyburska and K. Jankowski, “Preconcentration of selenium by living bacteria immobilized on silica for microwave induced plasma optical emission spectrometry with continuous powder introduction,” Anal. Methods, vol. 3, no. 3, p. 659, 2011, doi: 10.1039/c0ay00721h.

[58] Y. Zhang and W. T. Frankenberger, “Removal of selenium from river water by a microbial community enhanced with Enterobacter taylorae in organic carbon coated sand columns,” Sci. Total Environ., vol. 346, no. 1–3, pp. 280–285, Jun. 2005, doi: 10.1016/j.scitotenv.2005.02.019.

[59] K. Y. Foo and B. H. Hameed, “Insights into the modeling of adsorption isotherm systems,” Chem. Eng. J., vol. 156, no. 1, pp. 2–10, Jan. 2010, doi: 10.1016/j.cej.2009.09.013.

[60] X. Chen, “Modeling of Experimental Adsorption Isotherm Data,” Information, vol. 6, no. 1, pp. 14–22, Jan. 2015, doi: 10.3390/info6010014.

[61] A. S. Thajeel, “Isotherm, Kinetic and Thermodynamic of Adsorption of Heavy Metal Ions onto Local Activated Carbon,” Aquat. Sci. Technol., vol. 1, no. 2, pp. 53–77, May 2013, doi: 10.5296/ast.v1i2.3763.

[62] N. Ayawei, A. N. Ebelegi, and D. Wankasi, “Modelling and Interpretation of Adsorption Isotherms,” J. Chem., vol. 2017, pp. 1–11, 2017, doi: 10.1155/2017/3039817.

[63] K. Fujiwara, A. Ramesh, T. Maki, H. Hasegawa, and K. Ueda, “Adsorption of platinum (IV), palladium (II) and gold (III) from aqueous solutions onto l-lysine modified crosslinked chitosan resin,” J. Hazard. Mater., vol. 146, no. 1–2, pp. 39–50, Jul. 2007, doi: 10.1016/j.jhazmat.2006.11.049.

[64] T. Rubcumintara, “Adsorptive Recovery of Au(III) from Aqueous Solution Using Modified Bagasse Biosorbent,” Int. J. Chem. Eng. Appl., vol. 6, no. 2, pp. 95–100, Apr. 2015, doi: 10.7763/IJCEA.2015.V6.459.

[65] M. Funaoka, K. Mikame, and M. Aoyagi, “Lignin-Based Polymers (Lignophenol, Pyronedicarboxylic Acid),” in Encyclopedia of Polymeric Nanomaterials, S. Kobayashi and K. Müllen, Eds. Berlin, Heidelberg: Springer Berlin Heidelberg, 2015, pp. 1080–1098. doi: 10.1007/978-3-642-29648-2_401.

[66] P. T. Martone et al., “Discovery of Lignin in Seaweed Reveals Convergent Evolution of Cell-Wall Architecture,” Curr. Biol., vol. 19, no. 2, pp. 169–175, Jan. 2009, doi: 10.1016/j.cub.2008.12.031.

[67] D.I.S. Goldstein, “Organic Chemicals from Biomass,” p. 26, Jan, 2021, https://www.osti.gov/biblio/5249999

[68] C. P. Schulthess and Z. Hu, “Impact of Chloride Anions on Proton and Selenium Adsorption by an Aluminum Oxide,” Soil Sci. Soc. Am. J., vol. 65, no. 3, pp. 710–718, May 2001, doi: 10.2136/sssaj2001.653710x.

[69] Yen Ning Lee, “The Biosorption of Platinum and Palladium in Chloride Real Leach Solution by Modified Biomass,” p. 58, 2018.

PERMISSIONS

Appendix A

Dear Mr. Mohamed Ayman,

We hereby grant you permission to reproduce the material detailed below in print and electronic format at no charge subject to the following conditions:

1. If any part of the material to be used (for example, figures) has appeared in our publication with credit or acknowledgement to another source, permission must also be sought from that source. If such permission is not obtained then that material may not be included in your publication/copies.

2. Suitable acknowledgement to the source must be made, either as a footnote or in a reference list at the end of your publication as follows:

"This article was published in Publication title, Vol number, Author(s), Title of article, Page Nos, Copyright Elsevier (or appropriate Society name) (Year)."

3. This permission is granted for non-exclusive world rights in all languages.

4. Reproduction of this material is granted for the purpose for which permission is hereby given, and includes use in any future editions.

Regards,

Kaveri
ELSEVIER | Permissions Granting Team

Submission ID: 1157059
Date: 09 Apr 2021 5:37am

Name: Mr. Mohamed Ayman Mohamed Aly Abdallah
Institute/company: university of Saskatchewan
Address: 6-2157 Rae street
Post/Zip Code: S4T2E8
City: Regina
State/Territory: Saskatchewan
Country: Canada
Telephone: 6399944652
Email: mam345@usask.ca

Type of Publication: Journal

Title: Ecotoxicology and Environmental Safety
Auhtors: A.DennisLemly
Year: 2004
From page: 45
To page: 45
ISSN: https://doi.org/10.1016/S0147-6513(03)00095-2
Volume: 59
Issue: 1
Article title: Aquatic selenium pollution is a global environmental safety issue

I would like to use: Figure(s)

Quantity of material: 1
I am the author of the Elsevier material: No
Elsevier author is involved in my project: No

In what format will you use the material: Print and Electronic
Translation: No

Proposed use: Reuse in a thesis/dissertation

Material can be extracted: No

Additional Comments / Information: I would appreciate it if he permission is available before April 13th, Thank you

Appendix B

Dear Mr. Mohamed Ayman,

We hereby grant you permission to reproduce the material detailed below in print and electronic format at no charge subject to the following conditions:

1. If any part of the material to be used (for example, figures) has appeared in our publication with credit or acknowledgement to another source, permission must also be sought from that source. If such permission is not obtained then that material may not be included in your publication/copies.

2. Suitable acknowledgement to the source must be made, either as a footnote or in a reference list at the end of your publication as follows:

"This article was published in Publication title, Vol number, Author(s), Title of article, Page Nos, Copyright Elsevier (or appropriate Society name) (Year)."

3. This permission is granted for non-exclusive world rights in all languages.

4. Reproduction of this material is granted for the purpose for which permission is hereby given, and includes use in any future editions.

Regards,

Kaveri
ELSEVIER | Permissions Granting Team

Submission ID: 1157060
Date: 09 Apr 2021 6:05am

Name: Mr. Mohamed Ayman Mohamed Aly Abdallah
Institute/company: University of Saskatchewan
Address: 6-2157 rae street
Post/Zip Code: s4t2e8
City: Regina
State/Territory: Saskatchewan
Country: Canada
Telephone: 6399944652
Email: mam345@usask.ca

Type of Publication: Journal

Title: Energy Procedia
Auhtors: Adam HughmanickBergerAbhoyjit S.Bhown
Year: 2011
From page: 563
To page: 563
ISSN: 1876-6102
Volume: 4
Article title: Comparing physisorption and chemisorption solid sorbents for use separating CO2 from flue gas using temperature swing adsorption

I would like to use: Figure(s)

Quantity of material: 1
I am the author of the Elsevier material: No

In what format will you use the material: Print and Electronic
Translation: No

Proposed use: Reuse in a thesis/dissertation

Material can be extracted: No

Additional Comments / Information:

Appendix C

Dear Mr. Mohammed Ayman,

We hereby grant you permission to reproduce the material detailed below in print and electronic format at no charge subject to the following conditions:

1. If any part of the material to be used (for example, figures) has appeared in our publication with credit or acknowledgement to another source, permission must also be sought from that source. If such permission is not obtained then that material may not be included in your publication/copies.

2. Suitable acknowledgement to the source must be made, either as a footnote or in a reference list at the end of your publication as follows:

"This article was published in Publication title, Vol number, Author(s), Title of article, Page Nos, Copyright Elsevier (or appropriate Society name) (Year)."

3. This permission is granted for non-exclusive world rights in all languages.

4. Reproduction of this material is granted for the purpose for which permission is hereby given, and includes use in any future editions.

Regards,

Kaveri
ELSEVIER | Permissions Granting Team

Date: 16 Apr 2021 10:40pm

Name: Mr. Mohammed Ayman Mohamed Aly Abdallah
Institute/company: university of saskatchewan
Address: 6-2157 rae street
Post/Zip Code: s4t2e8
City: regina
State/Territory: saskatchewan
Country: Canada
Telephone: 6399944652
Email: mam345@usask.ca

Type of Publication: Journal

Title: Biosorption of selenium from aqueous solution by green algae (Cladophora hutchinsiae) biomass: Equilibrium, thermodynamic and kinetic studie
Auhtors: Mustafa Tuzen & Ahmet Sarı
Year: 2009
From page: 202
To page: 203
ISSN: 1385-8947
Volume: 158
Issue: 2
Article title: Biosorption of selenium from aqueous solution by green algae (Cladophora hutchinsiae) biomass: Equilibrium, thermodynamic and kinetic studie

I would like to use: Figure(s)

Quantity of material: 3
I am the author of the Elsevier material: No
Elsevier author is involved in my project: No

In what format will you use the material: Print and Electronic
Translation: No
Language(s): english

Proposed use: Reuse in a thesis/dissertation

Material can be extracted: No

Additional Comments / Information:

Appendix D

License Details

This Agreement between university of saskatchewan -- Mohammed Ayman Mohamed Aly Abdallah ("You") and Springer Nature ("Springer Nature") consists of your license details and the terms and conditions provided by Springer Nature and Copyright Clearance Center.

Print Copy

License Number	5063690418820
License date	May 07, 2021
Licensed Content Publisher	Springer Nature
Licensed Content Publication	Springer eBook
Licensed Content Title	Lignin
Licensed Content Author	Yasumitsu Uraki, Keiichi Koda
Licensed Content Date	Jan 1, 2014
Type of Use	Thesis/Dissertation
Requestor type	academic/university or research institute
Format	print and electronic
Portion	figures/tables/illustrations
Number of figures/tables/illustrations	1
Will you be translating?	no
Circulation/distribution	1 - 29
Author of this Springer Nature content	no
Title	Recovey of selenium on lignin from PLS using biosorption
Institution name	university of saskatchewan
Expected presentation date	Aug 2021
Portions	figure 1
Requestor Location	university of saskatchewan 2157 Rae street unit 6 Regina, SK S4T2E8 Canada Attn: university of saskatchewan
Total	**0.00 CAD**

BACK